FOG

Freiberg Online Geology

FOG is an electronic journal registered under **ISSN 1434-7512**

2010, VOL 25

Maike Hamel

Investigation and modelling of the geochemical processes in the hydrothermal system of Panarea, Italy

115 pages, 21 figures, 5 tables, 104 references

Diploma thesis

Investigation and modelling of the geochemical processes in the hydrothermal system of Panarea, Italy

Maike Hamel

Technische Universität Bergakdemie Freiberg
Faculty of Geoscience, Geo-Engeneering and Mining
Department of Geology
Chair for Hydrogeology

Supervisors: Prof. Dr. Broder J. Merkel (TU Freiberg)
Dipl.-Geoökol. Mandy Schipek (TU Freiberg)
Dr. Francesco Italiano (INGV Palermo)

Freiberg, 22.12.2009

Statutory declaration

Herewith I assure that I wrote the present work without inadmissible assistance and without the use of any aids than those declared in the thesis; thought directly or indirectly taken over from other sources are indicated as such.

Freiberg, 22.12.2009

.....

Maike Hamel

Acknowledgements

First of all, I thank my supervisors Prof. Broder Merkel and Dipl.-Geoökol. Mandy Schipek for providing the theme and for realising the field investigations. A special gratitude also for the theoretical preparation and the helpful tips and discussions concerning the difficulties during experimental work.

Sincere thanks to Dr. Francesco Italiano and his colleagues for the offer of and the kind and exciting mentoring during the stay at the INGV in Palermo and the unforgettable trip to Mt. Etna.

Furthermore, I want to thank Dr. Roland Haseneder for placing the autoclaves to disposal.

I am deeply grateful to Dipl.-Ing. Volker Herdegen for the support and the helpful tips and discussions on accomplishing the autoclave experiments.

Acknowledge also to Thurit Tschöpe for the assistance during the laboratory work on the total digestions.

Many thanks are adressed to Dr. Nicolai-Alexeji Kummer for the help and support during water analysis and for being a reliable address for open questions to be answered.

Thank you Daniel Steinbrückner and Robert Sieland for the conjoint work in Italy and in Freiberg as well as the numerous constructive discussions, proposals and motivations and thank you Anja Bretzler, for the English improvements as well as your mental encouragements during arduous times.

Thank you Michael Schierack for your friendship and your support and motivation.

Finally, a very broad ‘thank you’ goes to my family and my friends in Freiberg for continual support, encouragement and good company.

Index of Contents

List of Figures ..... **IV**
List of Tables ..... **VI**
Symbols and Abbreviations ..... **VII**
Abstract ..... **VIII**

1 Introduction **1**
1.1 Fundamentals on submarine hydrothermal systems 1
1.2 State of research 3
1.3 Objectives and concepts 7

2 Description of the investigation area **8**
2.1 Geological settings of the Aeolian Arc 8
2.2 The Panarea hydrothermal system 10
2.2.1 Panarea 10
2.2.2 Investigation Area 11

3 Methods **19**
3.1 Sampling Procedure 19
3.1.1 Water Sampling 19
3.1.2 Rock Sampling 20
3.2 Treatment and Field Analyses of the Water Samples 21
3.2.1 On-Site and In-Situ Parameters 22
3.2.2 Field Analysis of the Water Samples 24
3.3 Laboratory Analysis of the Water Samples 25
3.3.1 Ion chromatography (IC) 25
3.3.2 Inductively coupled plasma mass spectrometry (ICP-MS) 25
3.3.3 Total inorganic carbon (TIC) 26
3.4 Preparation of the Rock Samples 27
3.4.1 Cleaning of the Rock Samples 27
3.4.2 Grinding of the Rock Samples 27
3.5 Total Digestion 28
3.6 Leaching Experiments 29
3.6.1 Experiments in the Autoclave 29
3.6.2 Experiments in the Overhead Rotator 32
3.7 Evaluation of the Data 35
3.7.1 Data processing 35
3.7.2 Hierarchical Cluster analysis 36
3.7.3 Standardization 37

4 Results and Evaluation **38**
4.1 Results of the Time Series performed in Autoclave and Overhead Rotator 39
4.2 The blank samples 41
4.2.1 The blank samples of the autoclave pre-test 42
4.2.2 The blank samples of time series and some real experiments 44

4.3 Hierarchical Cluster analysis 49
4.4 Total digestions 53
4.5 Critical evaluation of the autoclave technique 55
4.5.1 General considerations 55
4.5.2 Corrosion 57
4.5.3 Contamination of the samples 58
4.5.4 Recommendations - Rocking autoclaves for hydrothermal experiments 63
4.6 Characterization of the Panarea water samples 64
4.7 Experiments in the Autoclave 67
4.8 Experiments in the Overhead rotator 69
4.9 Efficiency of the leaching experiments - Comparison of the experimental samples and the total digestions 70
4.10 Results of the leaching experiments in the context of general hydrothermal water-rock-interactions and processes 74
4.10.1 Physico-chemical conditions inside the autoclave 74
4.10.2 Comparison of the experimental samples and the Panarea reference samples 77
4.10.3 Hydrothermal water-rock-interactions – the leaching of rock material 81
4.11 Modelling 85

5 Conclusions 93

6 References 98

Appendix 107

Content of Digital Appendix 115

List of Figures

Figure 1: Schematic model of the hydrothermal system of Panarea (modified by Sieland [2009] from Italiano & Nuccio [1991]). For further descriptions see text. 4
Figure 2: Structural sketch map of the Southern Tyrrhenian Sea and Aeolian Islands, taken from ESPOSITO [2006], indicating the location and chronology of eruptions and earthquakes in the late 2002. 5
Figure 3: The volcanic complex of Panarea, showing the main island and its adjacent islets [modified from CHIODINI et al. 2006]. The investigation area lies within the crater rim sketched by the dotted circular line. 11
Figure 4: Map of the investigation area east of Panarea [taken from STEINBRÜCKNER 2009], showing the location of the different diving sites (marked with triangles). Grey fields indicate the position of the surrounding islets. 12
Figure 5: Location of rock sampling (dotted circle) at the southern coast of Panarea [modified from CHIODINI et al. 2006; LUCCHI et al. 2007b] 17
Figure 6: Diving sites at the investigation area. A) Black Point site and its characteristic black sinter body. B) Black "smoke" of colloids appearing at Black Point during gas sampling. C) Gravel field with wave ripples and some single gas discharges near Black Point site. D) Large fumaroles at Point 21 with strong gas outputs. E) The depression of Hot Lake with some white sulphur and bacteria coatings at lateral walls and a cover of dead *Posidonia* on the bottom. F) Diffuse gas discharges at the crater of Bottaro West. All pictures belong to WISTAU [2007; 2008]. 18
Figure 7: Experimental equipment. a) Autoclave vessels and closures. b) Autoclave vessels embedded in the aluminium heating block and fixed with half-cells. c) Aluminium block on shaking trestle, with inserted vessels and connected pressure tubes. d) Waldner-Apparatus, consisting of a heater, a suction device and glassy-carbon beakers. e) A piece of the metal wire mesh and a bended wire pocket. 34
Figure 8: Chemical composition of the time series samples (24, 48 and 84 hours), performed in the autoclave at 150°C temperature and 250 bar pressure. Concentrations are given in µg/L on a logarithmic scale. The empty bar (secondary axis) represents the mean of all three durations, together with the standard deviation. 39
Figure 9: Chemical composition of the time series samples (24, 48 and 84 hours), performed in the overhead rotator at normal temperature and pressure conditions. Concentrations are given in µg/L on a logarithmic scale. The empty bar (secondary axis) represents the mean of all three durations, together with the standard deviation. 41
Figure 10: Element concentration in the blank samples of the autoclave pre-test. Both the two red and the two blue plotted concentrations each belong to duplicates of the same sample. The connecting line between the samples does not indicate a correlation between the single elements, but should clarify the data points belonging to one sample. 43

Figure 11: Mean element concentration and standard deviation of some autoclave samples (I.03, I.04, II.4, II.4, VII.1, VII.4, VIII, XI) in comparison to the concentration of the deionised water that was applied as leaching fluid. The concentrations are given in µg/L on a logarithmic scale. 45
Figure 12: Examination of the concentration development of the elements Pb, Fe, Zn, Ni, Mn, Cd, Al, Sn, Ag and Mo in the blanks with and without solder. Within the two groups (with solder (left) and without solder (right)) the blank samples are sorted after their chronology of execution. Concentrations are given in µg/L on a logarithmic scale. 46
Figure 13: Mean value and standard deviation of all blanks from the rotation experiments (blanks exist only for the time series samples, which were performed in wire pockets like the corresponding autoclave samples). 48
Figure 14: Blank values, averaged for each of the experiment category (autoclave unsoldered, autoclave soldered and overhead rotator). Concentrations are given in µg/L on a logarithmic scale. 48
Figure 15: Dendrogram of the hierarchical cluster analysis B using Wards algorithm, representing the classification of the samples into five groups having the most significant differences among each other. Further explanations are given in the text. 53
Figure 16: Element concentration in the total digestions of the four rock samples (R1, R2, R3, R4) and the reference sample (GBW). Note: the connecting line between the samples does not indicate a correlation between the single elements, but should clarify the data points belonging to one sample. 54
Figure 17: Percentaged enrichment or depletion for a selection of elements measured in the reference samples from Black Point and Hot Lake in relation to normal seawater [data from BROWN et al. 1995]. The calculation basis has been concentrations in µmol/L (see Appendix 2 and Appendix 3). 65
Figure 18: Comparison of the concentrations leached from the four different rock samples during the autoclave experiments. The concentrations are given in µmol/L on a logarithmic scale. For the rock samples R2, R3, and R4, the concentrations are mean values of two samples from different experiment runs 68
Figure 19: Extraction efficiency [%] achieved during the leaching experiments in autoclave and overhead rotator. The data represent the respective concentration of species released into solution (during the different extraction experiments) in relation to their amount in the starting rock sample. These relations are separately depicted for each rock material (Figure 19a: R1, 19b: R2, 19c: R3, 19d: R4). Note: the connecting line between the samples does not indicate a correlation between the single elements, but should clarify the data points belonging to one sample 72
Figure 20: Comparison of the experimentally performed leaching samples and the Panarea reference samples, separated after (a) major, (b) minor and (c) trace elements. To the experimental concentrations a standard seawater composition (from BROWN et al [1995]) has been added. The concentrations are given in µmol/L on a logarithmic scale. Note: the connecting line between the samples does not indicate a correlation between the single elements, but should clarify the data points belonging to one sample 78
Figure 21: Results of the modelling scenario (C_80-20): Enrichment (%) of modelled and measured concentrations in relation to standard seawater (taken and modified after BROWN et al, [1995]) 89

List of Tables

Table 1: Geographical coordinates of the seven investigation sites [WISTAU 2008]. The notation is given as follows: degree° arc minute' arc second' related to the reference system WGS 84. 13

Table 2: Classification of the measured elements into the groups major, minor and trace elements, according to their mean concentrations. 36

Table 3: Overview about all experiments and their associated samples accomplished for this thesis (s+p: sample includes solder and wire pocket) 38

Table 4: Results of the on-site Parameters for the Black Point (BP) and Hot Lake (HL) reference sample. Ehm means the original measurements in the field laboratory; Eh25°C are the corrected redox values, regarding to 25°C temperature and the standard hydrogen electrode potential; rH is an indicator for the redox power of a system independent from the prevailing pH value. 66

Table 5: Electrical conductivity (EC) and pH value of the experimental leaching samples as well as for deoinised water. All solutions have previously been aerated with CO_2 75

Symbols and Abbreviations

b.s.l.	below sea level
CA	Calc-alkaline
CA(-filter)	Cellulose-acetate
EC	Electrical conductivity
e.g.	exempli gratia (for example)
E_h	standard redox potential
GPS	Global Positioning System
h	hours
HKCA	High-potassium calc-alkaline
HPLC	High pressure liquid chromatography
IC	Ion Chromatography
ICP-MS	Inductively coupled plasma mass spectrometry
INGV	Istituto Nazionale di Geofisica e Vulcanologia
ISE	Ion-selective electrode
L	Liter
M	Molar (mol/L)
Ma	Million years
ml	milliliter
µl	microliter
mM	millimolar (mmol/L)
n.d.	not determined
PE	Polyethylene
PTFE	Polytetra-Flourethylene (Teflon®)
ppm	parts per million
ppb	parts per billion
rpm	revolutions per minute
SI	Saturation index
Std.-dev.	standard deviation
T	Temperature
Temp.	Temperature
TIC	Total inorganic carbon
TUBA Freiberg	Technische Univesität Bergakademie Freiberg
WISTAU	Wissenschaftliches Tauchen (Scientific Diving Group at the TU Bergakademie Freiberg)
WTW	Wissenschaftlich-Technische Werkstätten GmbH

Sample Notation:

PAN	Panarea
BP	Black Point
HL	Hot Lake
BW	Bottaro West
R1, R2, R3, R4	rock samples (1-4)
soldered + pocket	sample treated in autoclave vessel with soldering
Rotator	samples treated in the overhead rotator

Abstract

Experiments were performed in order to investigate hydrothermal water-rock interaction that may take place within the hydrothermal system of Panarea Island (Aeolian Arc, Italy).
Four different rock materials sampled at Panarea have been reacted under both, normal (overhead rotator) and elevated temperature and pressure conditions of 150°C and 250 bars (autoclave). Due to the risk of severe damage to the autoclave equipment, only CO_2-aerated deionized water could be used as leaching fluid.
Reaction times of 24, 48 and 84 hours have been applied, which show no distinct influence on the resulting chemical composition of the leaching fluids.
From each of the four rock samples, a total digestion was prepared, showing the total amount of elements that is present in a distinct quantity of rock material. Comparing the leaching results to the total amounts potentially provided by the rock material, only extraction efficiency between 0.1 and 10 % (and even lower for the experiments under normal conditions) could be reached for most of the measured elements. This was attributed to the only moderate temperatures together with the lack of seawater, which is responsible for a stabilised low pH under hydrothermal conditions.
Although no seawater was included to the autoclave experiments, corrosion took place and caused serious contamination of the leaching fluids.
The experimental fluids have been compared with two fluid reference sample from Panarea (from the diving sites Black Point and Hot Lake), that showed comparably low rate of seawater dilution as well as a typical hydrothermally influenced character, including low pH and E_h, a depletion in Mg^{2+} and SO_4^{2-} and a substantial enrichment of many major, minor and trace elements (like Mn, Al, Fe, Cu, Zn, Pb, Ba, Li, Rb, I...) of several orders of magnitude compared to the ambient seawater. This enrichment was assessed to being the result of intensive water-rock interactions within the hydrothermal system.
The comparison depicted a considerable discrepancy in the way of much lower elemental enrichment for the experimental samples. Reasons are presumed to be mostly the lack of seawater as leaching fluid as well as probably to low temperature and too short reaction time. In a simplified modelling approach with the computer program PhreeqC, the effect of phase separation and remix with seawater (which were both determined to have influenced the Panarea samples) on the experiment samples was calculated. The results well agreed with the natural samples in an overall view, providing indications for both processes as well as a magmatic input to take place and to mainly control the generation of the Panarea hydrothermal fluid.

1 Introduction

1.1 Fundamentals on submarine hydrothermal systems

Geothermal fields are found throughout the world in a variety of geological settings like e.g. spreading centres, orogenic uplift or subduction zones, typically related to tectonic activity. Although they have very different characteristics in chemistry, behaviour and structural aspects, they have in common a heat source at a few kilometres depth, which sets water present inside the earth's crust into convection [NICHOLSON 1993]. High-temperature systems are always related to heat provision by a magmatic intrusion and are termed as volcanogenic [NICHOLSON 1993].

Submarine hydrothermal activity is mostly associated with the formation of new oceanic crust at mid-ocean ridges (MOR) or the submarine parts of subduction zones, both situated in deep-sea environments. PICHLER [2005] defined another type of hydrothermal system, that is found also in marine environments but in shallow water depth and near-shore position or on top of seamounts. Concerning the processes that determine their fluid chemistry, these shallow-water hydrothermal systems significantly differ from both deep-sea hydrothermal vents as well as sub-aerial geothermal systems [SEDWICK & STÜBEN 1996].

General processes taking place in (submarine) hydrothermal systems comprise convectively circulating water that is heated by the hot surrounding host rock (which in turn is heated by the respective heat source). Its flow paths are defined by fractures and fissures in the rock basement. Thereby, the water is converted into a highly corrosive hydrothermal fluid with high temperature, low pH value and low E_h, being capable of leaching large amounts of metals and other elements from the rock [HERZIG & HANNINGTON 2006]. Consequently, water-rock-interactions are thought to represent the major contribution to the chemical character of hydrothermal fluids [HERZIG & HANNINGTON 2006]. Nevertheless, during the ascent to the seafloor, the chemistry of the generated hydrothermal fluid may be drastically modified by processes such as subsequent mixing of different fluids, brine or seawater, the interaction with sediments, incorporation of magmatic degassing as well as phase separation [HERZIG & HANNINGTON 2006].

The process of phase separation in hydrothermal systems is related to the ascent of the hot fluids induced by a buoyancy effect. Thereby, the hydrostatic pressure decreases and at a distinct depth (depending on the actual p-t-conditions defined by the two-phase curve of seawater), the fluid separates into a low-density vapour phase, containing gases and other volatile species, and into a high-density, high saline and metal-rich liquid phase (brine) [BISCHOFF & ROSENBAUER 1984]. This process can be divided into subcritical ("boiling") and supercritical ("condensation") phase separation respectively, depending on if the fluid intersects the two-phase curve below or above its critical point (that is at 407°C and 298 bars for seawater) [FOUSTOUKOS & SEYFRIED 2007a]. These two phases can now move separately and independently from each other towards the seafloor, but eventually remix again during ascent.

At the seafloor, the gases mainly exhale as fumaroles, typically consisting of a mixture of mostly water vapour together with carbon dioxide (CO_2), hydrogen sulphur (H_2S), ammonia (NH_3) nitrogen (N_2), hydrogen (H_2) and methane (CH_4) [NICHOLSON 1993]. The separated gases, as well as previously the hydrothermal fluid, can also contain a contribution of primary magmatic gasses like mainly CO_2, sulphur dioxide (SO_2) and hydrogen chloride (HCl) [HERZIG & HANNINGTON 2006]. When escaping at the seafloor, the strongly enriched hydrothermal fluids come in contact with the ambient cold and oxygen-rich seawater and consequently undergo rapid cooling together with an increase in pH and E_h, which may lead to mineral precipitation as metal sulphides.

On a global scale, submarine thermal fluid discharges are thought to significantly affect the composition of seawater and marine sediments [HERZIG & HANNINGTON 2006; TASSI et al. 2009].

The known shallow type hydrothermal systems have their own characteristic that can be denoted as having transitional attributes between deep-sea hydrothermal vents and terrestrial hot springs [PICHLER 2005]. Their fluid chemistry is likely to be stronger influenced by magmatic degassing and phase separation due to much lower pressure conditions compared to the deep-sea systems [SEDWICK & STÜBEN 1996]. From the sub-aerial systems they differ with respect to a seawater solution rather than groundwater plus a magmatic component.

1.2 State of research

The island Panarea belongs to the Aeolian Islands (Italy), an archipelago located in the southern Tyrrhenian Sea in the Mediterranean. The Aeolian arc is part of an active back-arc volcanic system, generated by the subduction of the African oceanic crust below the Eurasian plate. Volcanic arc and back-arc hydrothermalism, associated with subdution zones, is characterized by extensive tectonics and complex magma production that is generated from diverse parent rock materials [SCHMINCKE 2000]. Additionally, likely higher fluxes of gases occur because of both degassing from the mantel as well as from the subducting slab, which contains carbonates and marine sediments that are decomposed, forming CO_2 [DANDO et al. 1999; MILLERO 2006].

Volcanic activity, both submarine and terrestric, is related to the seismo-tectonic processes as well as induced magmatic inputs due to subduction and is observed throughout the Mediterranean. Thereby, most of the known hydrothermal systems are found in shallow coastal waters less than 200 m deep [DANDO et al. 1999].

The hydrothermal system of Panarea is characterized by discharges of hydrothermal water and gas in a shallow depth (up to 150) m from the seafloor. Investigations by GUGLIANDOLO et al [2006] inferred, that these emissions are the most active among all hydrothermal vents of the Aeolian arc found at shallow depth.

This hydrothermal system has already been known since historical times [ESPOSITO et al. 2006], nevertheless systematic and detailed investigations of the hydrothermal discharges have been carried out only in the last decades [e.g. ITALIANO & NUCCIO 1991]. These authors reported numerous submarine fumaroles exhaling CO_2 (-H_2S) – dominated gases and several low-pH hydrothermal water emissions with temperatures of up to 130°C.

Based on the chemical and isotopic composition of hydrothermal fluids and gases, as well as geothermometrically calculated reservoir equilibrium temperatures, a semi-quantitative model of the circulation scheme beneath the seafloor has been developed by ITALIANO & NUCCIO [1991] (compare Figure 1). They assumed that several distinct and stratified geothermal aquifers exist at different depth, all fed by a deep geothermal heat source of > 350 °C temperature, which is probably a cooling magmatic body with an estimated volume of 1 km^3 [CARACAUSI et al. 2005a]. Intruding seawater gets heated by this underlying geothermal body, generating a relatively large geothermal aquifer of about 240 °C. Fluids from this deeper aquifer ascend towards shallow depth, where they feed two different thermal aquifers with an estimated temperature of 170 – 210 °C. Thereby the deeper aquifer is recharged by seawater circulating at depth. One of these aquifers is

assumed to be only recharged by seawater, whereas clues are identified that indicate a meteoric component probably from Panarea Island, contributing to the second shallow aquifer (compare Figure 1). Both shallow thermal aquifers are feeding the hydrothermal discharges observed at the seafloor.

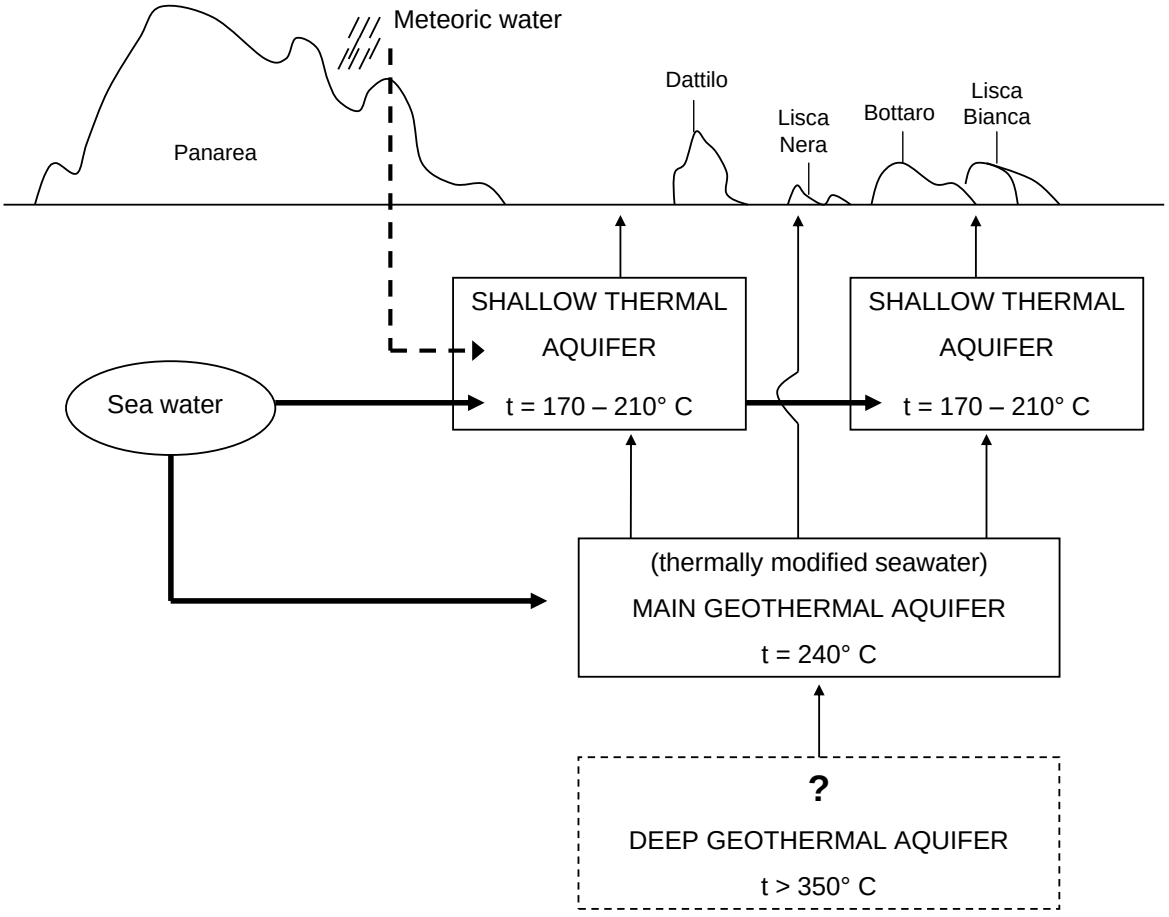

Figure 1: Schematic model of the hydrothermal system of Panarea (modified by Sieland [2009] from Italiano & Nuccio [1991]). For further descriptions see text.

As reported, the hydrothermal activity at Panarea was limited to only light gas bubbling in the years of first investigations (mid-80's) and the system was considered almost static and interpreted as the waning activity of a still cooling and extinct volcano [CARACAUSI et al. 2005b; TASSI et al. 2009].

During September 2002 and January 2003, a series of seismo-tectonic and volcanic events have been registered in the southern Tyrrhenian Sea. Starting (**i**) with an earthquake on September 6th (magnitude = 5.6) affecting the entire southern part of the Tyrrhenian Sea and followed by (**ii**) the onset of the strongest eruptions at Mt Etna on Sicily in the last decade on October 27th, (**iii**) in the night to the 3rd of November 2002, a sudden and massive increase in gas emission issued from the shallow seafloor has been observed near

the islet of Bottaro off the eastern coast of Panarea [DOLFI et al. 2007; ESPOSITO et al. 2006; TASSI et al. 2009] (compare Figure 2). This gas burst was attended by a swarm of low intensity micro-earthquakes (magnitudes generally <1) until November 13th; the intensiveness of gas releases rested until January [CARACAUSI et al. 2005b; CHIODINI et al. 2006]. One month later, on December 28th, (**iv**) Stromboli volcano had its strongest eruption since 1930, and since then remained highly active showing lava flows and explosive activity until May 2003 [CAPASSO et al. 2005; TASSI et al. 2009]. Induced by this eruption and lava release into lateral fractures some hundred meters below the summit, the north-western flank of Stromboli volcano collapsed into a landslide, that skidded into the sea, generating two subsequent tsunamis with a run-up of ~ 11 m [CAPASSO et al. 2005; TINTI et al. 2005]. Implications have been damage on the surrounding islands, severely at Stromboli.

An overview about locations and chronology of the described series of events is shown in the map in Figure 2.

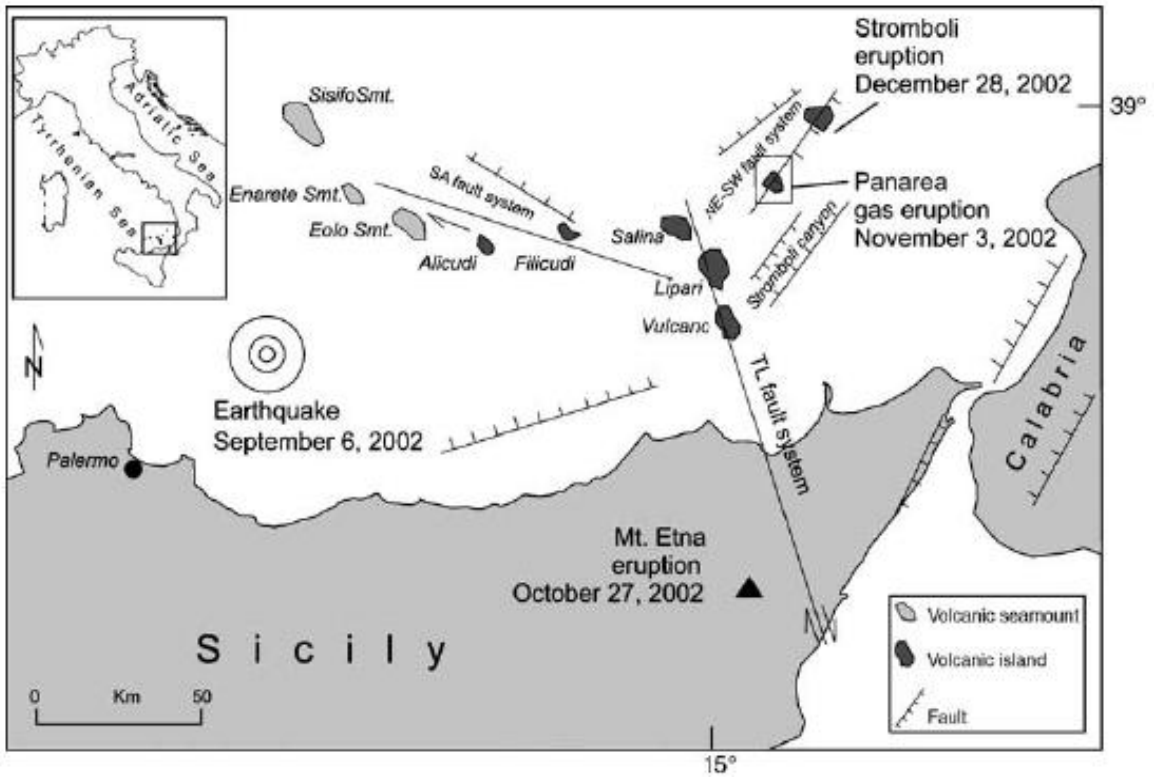

Figure 2: Structural sketch map of the Southern Tyrrhenian Sea and Aeolian Islands, taken from ESPOSITO [2006], indicating the location and chronology of eruptions and earthquakes in the late 2002.

The crisis at the submarine site near Panarea is suggested to be reasoned by a renewed and local input of mass and heat probably derived from a magma body at depth [CARACAUSI et al. 2005b; TASSI et al. 2009]. Such a magmatic source would fully explain the observed

increases in temperature, pressure and gas flux, as the heat would result in higher temperatures and thus higher vaporisation that finally lead to the increased pressure and the intensive gas release. Contribution of a magma-related source was identified by the presence of fluids like HCl, HF, SO_2 and He-isotopic ratios [CARACAUSI et al. 2005a].
As reported by GABBIANELLI [1990], the common NE-SW-trending tectonic structures of Panarea and Stromboli have controlled the evolution of both volcanic edifices throughout the history and thus, the assumption is obvious that recent activity of both systems is still controlled by this connecting structures.
After the crisis, the investigations about Panarea hydrothermal system have been intensified [e.g. CARACAUSI et al. 2005b; CHIODINI et al. 2006; GUGLIANDOLO et al. 2006], with the ambitions of developing a monitoring program that may indicate intensive gas eruptions and changes in fluid chemistry as precursors to volcanic eruptions within the southern Tyrrhenian Sea. By this means, hazardous scenarios as occurred at Stromboli in 2002 could be curtailed.

As already mentioned, the interaction between fluid and host rock is mainly responsible for the initial chemistry of the hydrothermal solution which consequently is sensitive to the composition of this source rock. At Panarea, magmas of a high potassium calc-alkaline composition (HKCA) forming mainly andesitic to dacitic rocks constitute the emerged lava domes and islets (section 2.1). However, Panarea is part of an active back-arc volcanic system associated to an active subduction zone. During subduction, different parts of both continental and oceanic crust as well as overlaying sediments are involved in magma generation and partial melting, leading to diverse magmatic compositions [MARKL 2004]. This means a considerable difference to hydrothermal systems associated with mid-ocean ridges (MOR), which are typically made up of basaltic rocks. But even at MOR settings, the bulk composition of emitted hydrothermal fluids appears to be quite sensitive to the chemistry of the source rock. The bedrock of the Panarea hydrothermal system may be constituted by rocks, derived from magma portions of time-related strongly varying composition.
Because its composition is generated by water-rock interactions, hydrothermal fluids are suggested to be strongly dependant on the type of rock that is present along the flow path. Consequently, at Panarea (and also other subduction-related hydrothermal systems), at which depth a fluid is established and through which way and direction the fluid intersects through the bedrock during ascent may be an important factor influencing fluid chemistry.

1.3 Objectives and concepts

The aim of this thesis is to investigate the interactions between rock and fluids taking place inside the hydrothermal system of Panarea. Thereby the impact of different aspects (like physico-chemical conditions, water-to-rock ratio, reaction duration, phase separation and mixing) on the final composition of the hydrothermal fluids that escape from the system should be elaborated. The investigative focus lies on explaining the minor and trace elemental composition of these fluids and to investigate to which extend their dissolution from rock is determinant.

By the approach of experimental water-rock interactions at elevated temperatures and pressures, the effect of both parameters on rock leaching processes should be examined.

Subsequent modelling with the experimentally derived fluids should give insight to how processes like phase separation and (re)mixing affect the chemical composition of the hydrothermal fluids.

Doing so, the investigative focus lies on hydrothermal fluids from two distinct sampling points (Black Point and Hot Lake) that both show typical hydrothermal but considerably different chemical composition – indications for the determining processes should be discovered by applying defined conditions.

The overall ambition of these experiments on rock leaching and simulations is the question how the Panarea hydrothermal fluids were formed and which processes and conditions have dominant impact.

The conceptual idea was, to react rock samples from Panarea with seawater under elevated temperature and pressure conditions for simulating the hydrothermal modification of both, the rock material under dissolution attack and the seawater as leaching fluid.

For the reason of insufficient equipment, reactions using seawater were not realisable and hence, only deionised water should be utilised instead. For including the effect of hydrothermal gases dissolving in the fluid, the experimental starting solution should be aerated with CO_2 until saturation previous to the experiments. Reasoned by the investigative focus of mainly explaining the composition and source of minor and trace elements, no complete water analyses have been performed but only measurements using ICP-MS.

2 Description of the investigation area

2.1 Geological settings of the Aeolian Arc

The island Panarea belongs to the Aeolian arc, a volcanic structure extending for about 200 km through the southern Tyrrhenian, bordered by the Marsili back-arc basin to the north and the Sicilian and Calabrian continental margin to the south-east [CALANCHI et al. 2002unpublished; FAVALLIM et al. 2005]. Seven main islands (Alicudi, Filicudi, Salina, Lipari, Vulcano, Panarea and Stromboli), some minor islets and several seamounts belong to the Aoelian archipelago, representing the emerged parts of former submarine volcanoes belonging to a complex quaternary volcanic structure [GUGLIANDOLO et al. 2006; MARAMAI et al. 2005a; 2005b].

The formation of the Aeolian Arc and the Tyrrhenian Sea is (as most authors agree) related to the active subduction of the Ionian foreland (African plate) beneath the Eurasian continental plate [ANZIDEI et al. 2005; CALANCHI et al. 2002; TASSI et al. 2009]. Still in debate is an alternative origin which is related to a short phase of intensive spreading, confined to the Marsili Basin, and stagnating magmatism [DOLFI et al. 2007; FAVALLIM et al. 2005]. This phase was dominated by vertical tectonic processes causing rapid foundering of the oceanic crust and an uplift of the Calabrian arc and the adjacent Aeolian Islands in the last 0.5 – 0.7 Ma [DEKOV & SAVELLI 2004].

However, volcanism entirely took place during the quaternary, probably from about 400 ka to the present, as detected from the exposed volcanic products above sea level [CALANCHI et al. 2002; GAMBERI et al. 1997; PECCERILLO 2005].

Convergence of African and European plates has resulted in complex tectonics in the Mediterranean and is attended by the formation a number of microplates [DANDO et al. 1999]. Such, a regional fault system has evolved controlling the distribution of the seamounts and islands of the Aeolian Arc [LUCCHI et al. 2007b]. The arc can be divided into three segments, which show distinct magmatic, volcanic and structural features [PECCERILLO 2005; SAVELLI et al. 1999]:

The **western sector** extends along a W-E trending fault system and includes the islands Alicudi, Filicudi and Salina. Their volcanic rocks show a typically calc-alkaline composition with mainly mafic to intermediate rocks.

The **central sector** comprises the islands Lipari and Vulcano, which is oriented from NNW to SSO and continues until Mt. Etna on mainland Sicily. The rocks present a mafic to silicic calc-alcaline, shoshonitic and potassic composition.

The **eastern sector** includes Panarea and Stromboli which are made of rocks with a composition similar to those of the central sector. The segment develops along NE-SW running faults.

The current volcanic activity is more related to the central and eastern sectors, where the active volcanoes Stromboli and Vulcano are located. Stromboli shows continuous moderately explosive strombolian eruptions [PECCERILLO 2005], Vulcano is in a state of solphataric activity and on Lipari and Panarea, low temperature vents are found [GUGLIANDOLO et al. 2006]. Submarine hydrothermal exhalations, both deep and shallow, exist in the vicinity of all Aeolian islands, whereas those found off the eastern coast of Panarea showed the most active hydrothermal system at shallow depth [GUGLIANDOLO et al. 2006].

The petrochemistry of the Aeolian Islands show compositions varying from calc-alkaline (CA) to high potassic-calc-alkaline (HKCA) and shoshonitic composition [PANZA et al. 2007]. Thereby a diversity between rocks from western and the eastern Aeolian arc has been recognized, showing a trend from CA (Alicudi, Filicudi, Salina) in the west to a combination of CA, HKCA shoshonitic composition in the central and eastern part (Vulcano, Lipari, Panarea, Stromboli), whereas potassic-alkaline rocks occur only in at Stromboli (compare Figure 1) [CALANCHI et al. 2002].

These variations are interpreted as a result from mantle processes where a source of MORB (mid oceanic ridge basalts) is metasomatised by components derived from the subducted slab [FRANCALANCI et al. 1993]. Thereby the amount of metasomatising agent increases from west to east, producing variable melt compositions.

These geochemical and geophysical (fault system) conditions have led to the conclusion that the Aeolian Arc can be divided into two distinct branches (west and east), differing in structural and compositional features [CALANCHI et al. 2002]. As suggested from geochemical and isotopic data, Panarea owes its composition of volcanic products to its particular position between western and eastern tectonic structures of the Aeolian Arc, resulting in a mixing of two types of mantle source that produce calc-alkaline (west) and high-K to shoshonitic calc-alkaline (east) respectively [PECCERILLO 2005].

Exposed rocks within the Panarea volcanic complex (described in the following section) consist predominantly of andesitic to dacitic lava domes, but also basalts and rhyolites and

minor flows of pyroclastics were found, all dated to an age between 150 and 45 ka [GABBIANELLI et al. 1990; PECCERILLO 2005]. However, the most intensive volcanism that almost entirely built up the Panarea volcanic edifice is thought to have proceeded from 150 to 105 ka [LUCCHI et al. 2007b]. Many of the Panarea rocks and lavas enclose up to 20% igneous and metamorphic xenolithes [PECCERILLO 2005]. Thereby the geochemical compositional trend of an increasing SiO_2-amount during fractionation leads to the sequence of basaltic – andesitic – dacitic – rhyolitic magmas [WIMMENAUER 1985]. A typical calc-alkaline magma for example undergo these changes, whereas in accordance to its content of potassium (K_2O), a calc-alkaline melt can be further divided into low-K, intermediate-K, high-K or shoshonitic series [MARKL 2004].

2.2 The Panarea hydrothermal system

2.2.1 Panarea

The Panarea volcanic complex consists of the main island Panarea as well as several small islets to its east (Basiluzzo, Bottaro, Lisca Bianca, Lisca Nera, Panarelli, Formiche and Dattilo) (Figure 3). They represent the emerged remnants of a former submarine stratovolcano, measuring 2000 m in height and 23 km in diameter by covering an area of about 460 km^2 [ESPOSITO et al. 2006; GABBIANELLI et al. 1990]. Thereby only the uppermost part (maximal 421 m of the main island) is exposed above sea-level [CHIODINI et al. 2006].

Concerning the evolution of the Panarea volcanic complex, different stages of activity could be distinguished [GUGLIANDOLO et al. 2006]: In the first period, a central volcano rose in the western end of the structure, forming the main island Panarea. In the second step, the volcanic complex was enlarged to the east, building the lobed eastern structure [ITALIANO & NUCCIO 1991]. Thereby, the activity was regulated by the regional NE-SW trending fault system, which continues until Stromboli volcano, indicating a geochemical affinity and a temporal relationship in the volcanism of Panarea and Stromboli [GABBIANELLI et al. 1990]. The evolution was terminated by the collapse of the central part forming a large caldera associated with a high gravimetric anomaly due to a magmatic intrusion [BONASIA et al. 1973; ITALIANO & NUCCIO 1991].

Presently, volcanic activity at Panarea is characterized by still continuing subsidence as well as continuous degassing from several, mostly submarine, fumarolic areas, also associated with escaping hydrothermal fluids [ESPOSITO et al. 2006; ITALIANO & NUCCIO 1991].

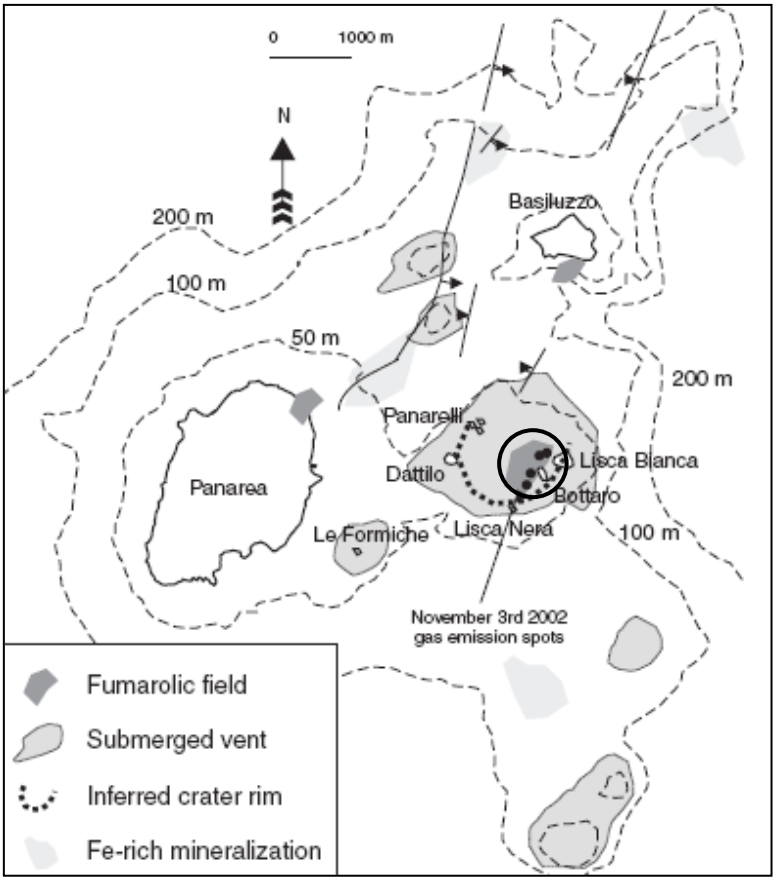

Figure 3: The volcanic complex of Panarea, showing the main island and its adjacent islets [modified from CHIODINI et al. 2006]. The investigation area lies within the crater rim sketched by the dotted circular line.

2.2.2 Investigation Area

About 2.5 km east off the coast of Panarea Island, a subcircular submerged depression with a maximum depth of 30 m is located, enclosed by the islets Lisca Nera, Bottaro, Panarelli, Lisca Bianca and Dattilo. This structure covers an area of about 2.3 km^2 and is thought to be a former crater, with the islets representing the relicts of the crater rim [ESPOSITO et al. 2006; GABBIANELLI et al. 1990]. Within this depression, the seafloor consists of loosely- to partly-consolidated Holocene sands and conglomerates that mainly originate from oceanic erosion of the emerged domes around [TASSI et al. 2009]. They were partly covered by dead *Posidonia* mats – flora and fauna is generally sparse due to the acid discharges.

Numerous sites of escaping thermal water and exhalating gases are found at the seafloor associated with the active hydrothermal system. Their distribution is determined by the NE-SW oriented fault system [GUGLIANDOLO et al. 2006]. The fluids escape from fissures and gaps in the rock or in form of diffuse discharges through the seafloor sediments. Gas emissions are mostly marked with white deposits of colloidal sulphur, owing to bacterial activity.

During two investigation periods in May and September 2008, seven locations of particular interesting conditions have been investigated, which were named Black Point, Hot Lake, Fumarolic Field, Bottaro North, Bottaro West, Point 21 and Area 26d and are described in detail in the following. The specific positions of the diving sites are shown in Figure 4. Also geographic coordinates have been measured with GPS and are given in Table 1.

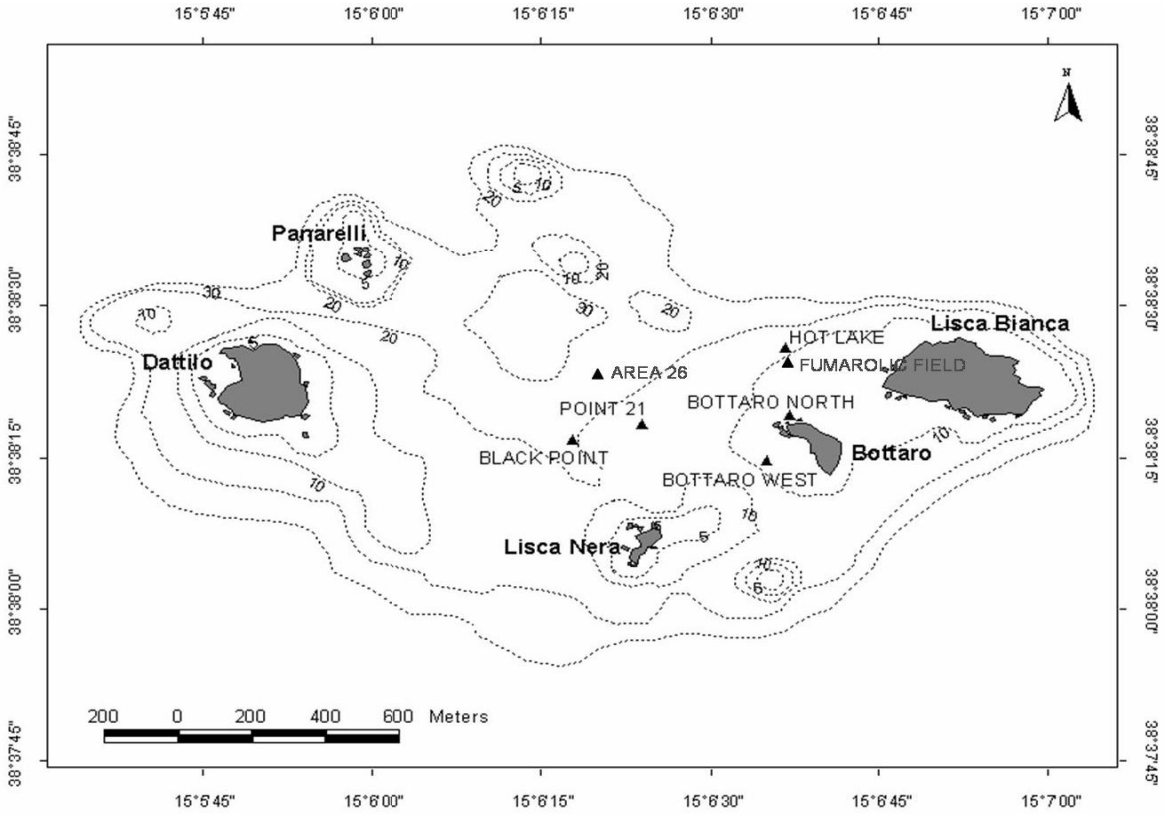

Figure 4: Map of the investigation area east of Panarea [taken from STEINBRÜCKNER 2009], showing the location of the different diving sites (marked with triangles). Grey fields indicate the position of the surrounding islets.

Table 1: Geographical coordinates of the seven investigation sites [WISTAU 2008]. The notation is given as follows: degree° arc minute' arc second'' related to the reference system WGS 84.

Location	Northing	Easting
Black Point	38°38'16.7''	15°06'17.1''
Hot Lake	38°38'24.5''	15°06'35.0''
Fumarolic Field	38°38'24.1''	15°06'35.8''
Bottaro North	38°38'19.2''	15°06'36.4''
Bottaro West	38°38'14.4''	15°06'34.1''
Point 21	38°38'18.1''	15°06'24.4''
Area 26	38°38'21.2''	15°06'18.5''

Black Point

The diving site Black Point is wide and flat crater in the seafloor, having an extension of about 25 m in N-S and about 20 in W-E direction and an average depth of 23.5 m. Its geographic coordinates are given in Table 1. The sea bottom is covered with sand and gravel forming a rippled structure from wave action (Figure 6c), whereas the flanks are overgrown with *Posidonia*. Many fumaroles of low intensity are distributed over the area, and also some hydrothermal water discharges were found in the north-west of the depression.

The location is named after a greyish-black sinter body situated to the south-east of the crater. This body has a size of ~ 2.7 m length (N-S), 1 m wide and 0.5 m high and is made up of fine-layered, porous mineral crusts intermingled with the original conglomerate block [BECKE 2009] (see Figure 6a). These encrustations are associated with escaping hydrothermal fluids – the most intensive exhalation being positioned in the NE-part of the body. When the fluids are released from the body into the surrounding seawater, a greyish "smoke" of metallic precipitation particles evolve due to rapid cooling of the fluid that is then no longer capable of carrying the minerals in dissolved form (Figure 6b). This grey precipitate was also observed by other investigators in the period from 2002 till 2005 [e.g. TASSI et al. 2009]. During the scientific diving excursions previous to September 2008, the grey smoke was only observable when the gas-sampling funnel was attached on the emission point, which probably affected the pressure conditions inside the vent, leading to precipitations. However, in September 2008, this phenomenon took place without any intervention of divers.

Investigating the sinter body, several boreholes were drilled, realising both, the gaining of core samples and taking fluid samples from as deep as possible out of the emitting vent. The highest temperature measured in a ~ 50 cm deep drill hole at Black Point was 135°C [WISTAU 2008]. The cores, as well as several sample of the precipitated mineral crusts, have been analysed and described in detail by BECKE [2009]. Shortly summarised, they consist mainly of Zn, Pb, Ba, Sr, Mn, Fe and As, forming metal sulphides like pyrite/marcasite (FeS_2), galena (PbS), sphalerite ((Zn,Fe)S) and strontium-baryte ($(Sr,Ba)SO_4$).

Hot Lake

The investigation point Hot Lake lies about 250 m to the north of Bottaro (geographic coordinates see Table 1) at a depth of about 18 m b.s.l. It is named after a deepening in the seabed (like a small lake), where hot hydrothermal fluids escape diffusely from the sediment, leading to higher temperatures near the bottom of the deepening (see Figure 6e). The lake measures about 10 m in length (NE-SW orientated) and about 6.5 m in width, showing an irregular oval shape. The enclosing walls of the basin consist of consolidated and partly cemented sediments and sinter materials, having a height of ~ 0.5 m in the north-eastern edge and 2 m in the south-west. Partly overhanging walls form cave like structures, which are covered with whitish bacteria mats. The bottom of the basin is filled with a thick layer of dead *Posidonia*, also partly covered with the white bacteria deposits and fine sands and particles. The mentioned hot hydrothermal water leaking diffusely from the sediment is retained among the *Posidonia* layer - their temperatures have been measured to range about 96°C [WISTAU 2008]. Stronger gas vents do not occur.

Fumarolic Field

About 50 m to the south-west of Hot Lake (geographic coordinated are given in Table 1), a plain gravel- and boulder-covered field is found where numerous fumaroles of varying but moderate intensity are accumulated. The field lies at a depth of 15-17 m and reaches over an estimated length of 30 m (W-E) and a width of 20 m (N-S). Most of the gas exhalations are scattered randomly, probably indicating diffuse leaking, but some vents also show an aligned structure, highlighted by white deposits of sulphur and bacteria. Inside the fumaroles temperatures of 39.7° C up to 59.1° C have been measured [WISTAU 2008].

Bottaro North

The diving site Bottaro North is located in shallow depth of about 7.5 to 9 m close to the NW-end of the islet Bottaro. The particularity of this site is the assemblage of large boulders, arranged in a stacked manner, which strongly differ from the seafloor character of the other sites. The point of interest is a central gravel field of some meters in diameter, surrounded by boulders and southwardly rising towards the steep rocky islet Bottaro. On the gravel field, five extensively exhalating fumaroles are found in the southern part, describing a circular shape. Some smaller gas vents are also found, arranged as lined structure or separately distributed between the boulders. Measured in-situ temperatures of the vents varied between 27.9 and 56°C [WISTAU 2008].
Due to the shallow depth, the escaping gases of the main vents are recognizable at the sea surface during calm days by means of their bubbling and smell of hydrogen sulphur. Geographic coordinates are given in Table 1.

Bottaro West

Approximately 30 m off the western margin of Bottaro, a submarine crater with a diameter of about 11 m is found, defined as Bottaro West (for geographic coordinates see Table 1). During the crisis in November 2002 (described in section 1.2), the most intensive gas exhalations were observed at this site and it is suggested that the crater-like structure was opened by the explosive character of the gas burst, extracting an estimated mass of nearly 4000 m^3 rock material [ANZIDEI et al. 2005; ESPOSITO et al. 2006]. After this explosive release, the crater showed an ellipsoidal form of much larger size (about 40 m length (NW-SE orientated), 25 m width) and a depth of 7 m reaching from -8 to -15 m b.s.l. [ANZIDEI et al. 2005]. But until September 2008, the crater size has decreased due to refill with erosive debris and sediment, presenting now a moderate depression at a depth of ~ 12 m. Within the crater structure many fumaroles of various but moderate intensity are located, as well as a circular shaped plane of diffuse discharges (Figure 6f), escaping from the gravel-covered bottom.
The crater is enclosed by relatively steep walls of large boulders embedded in a cemented mixture of conglomerates and sediments. In the south-western edge, a conglomerate wall of approximately 7 m length and 1.5 m height is exposed, following a SE direction.
Water temperatures measured inside some fumaroles at Bottaro West lie in the range of 28.4 and 43.6° C [WISTAU 2008].

Point 21

The Point 21 investigation site is situated approximately 200 m west of to Black Point (Figure 4); its geographical coordinates are given in Table 1. Characteristic for this location is a submarine depression that is flanked by a vertical rock face tending NW-SE direction. This wall is about 10 m long and reaches from 17 to 22 m depth. In front of the wall five large fumaroles discharge large amounts of gas (Figure 6d). Thereby, two of the vents are located at the northern and two at the southern part of the depression. The fifth escape directly from a cavity inside the rock wall. Around and inside all five outlets including parts of the rock wall, thick white to yellowish coatings of sulphur and bacteria mats have deposited. The temperature inside these large fumaroles was determined to be between 25 and 71 °C [WISTAU 2008]. Beside these five big fumaroles, also some smaller ones are distributed around this location.

Area 26

The position of this site lies about 100 m north-east of point 21, continuing the direction of the rocky wall orientation (for coordinates see Table 1). At a water depth of 26 m two distinct sediment fields are found, covering an area of about 50 times 50 m [WISTAU 2008]. Beside the cover of sand and gravel sediments, also some conglomerate bodies overgrown by vegetation are exposed [BECKE 2009]. Fumaroles of varying intensity are scattered over the area, partly aligned or with white sulphur coverage. The escaping fluids are described as hot and aggressive [WISTAU 2008].

Lava domes (Panarelli, Bottaro)

Panarelli is one of the emerged islets representing the relicts of the north-eastern part of the crater rim around the investigation area (Figure 3 and Figure 4). Actually, it is a elevation with only some single parts being exposed above surface and leading to the impression of several single boulders sticking out of the water. Between these exposed parts, a small basin exists, covered with algae and mussel-incrustations. At this site, a lithostratigraphic unit outcrops – one of three for the investigation area that have been distinguished and described by ESPOSITO et al [2006]. This unit is suggested to have basaltic-andesitic composition, consisting of a microcrystalline groundmass with dispersed phenocrusts of plagioclase, clinopyroxene, boitite and olivine [ESPOSITO et al. 2006]. Xenolithes of the

underlying unit made of highly porphyritic lava of plagioclase and amphiboles and suggested to have a hypabyssal origin have also been identified. Varied degrees of alteration has been observed. The rock material of this units strongly resemble in texture and mineralogy the lavas that constitute the other circumjacent islets, leading to the interpretation that the islets are grouped together, owing to a possible common genesis [ESPOSITO et al. 2006; LUCCHI et al. 2007a].

The islet Bottaro emerges at the south-east of the former crater rim (Figure 4). As mentioned, it consists of the same lithostratigraphic unit as Panarealli. Around the islet, the covering unit made of partly cemented sediments and eroded conglomerate material is outspread and only the exposed dome of Bottaro protrudes out of this overlying unit.

From both islets Panarelli and Bottaro, a rock sample was taken.

Panarea South Coast

A rock sample has also been taken from the southern coast of Panarea (Figure 5). Due to several eruptive stages constituting to its formation, different stratigraphic units are identified at Panarea [CALANCHI et al. 2002]. The rock material sampled for this thesis derives from the so called "Caletta dei Zimmari synthem", constituting amongst others the southern coast of Panarea. This unit consists of HKCA andesite and dacite lava flows and are dated to an age of 132.5 ± 8.0 ka [CALANCHI et al. 2002].

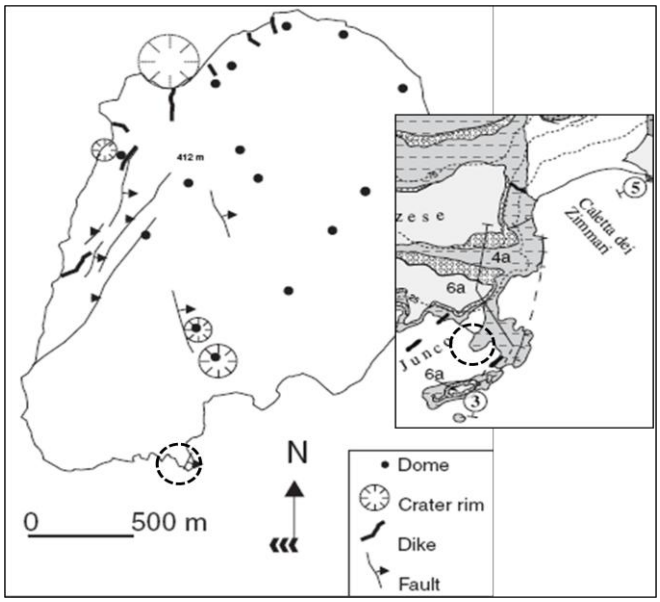

Figure 5: Location of rock sampling (dotted circle) at the southern coast of Panarea [modified from CHIODINI et al. 2006; LUCCHI et al. 2007b]

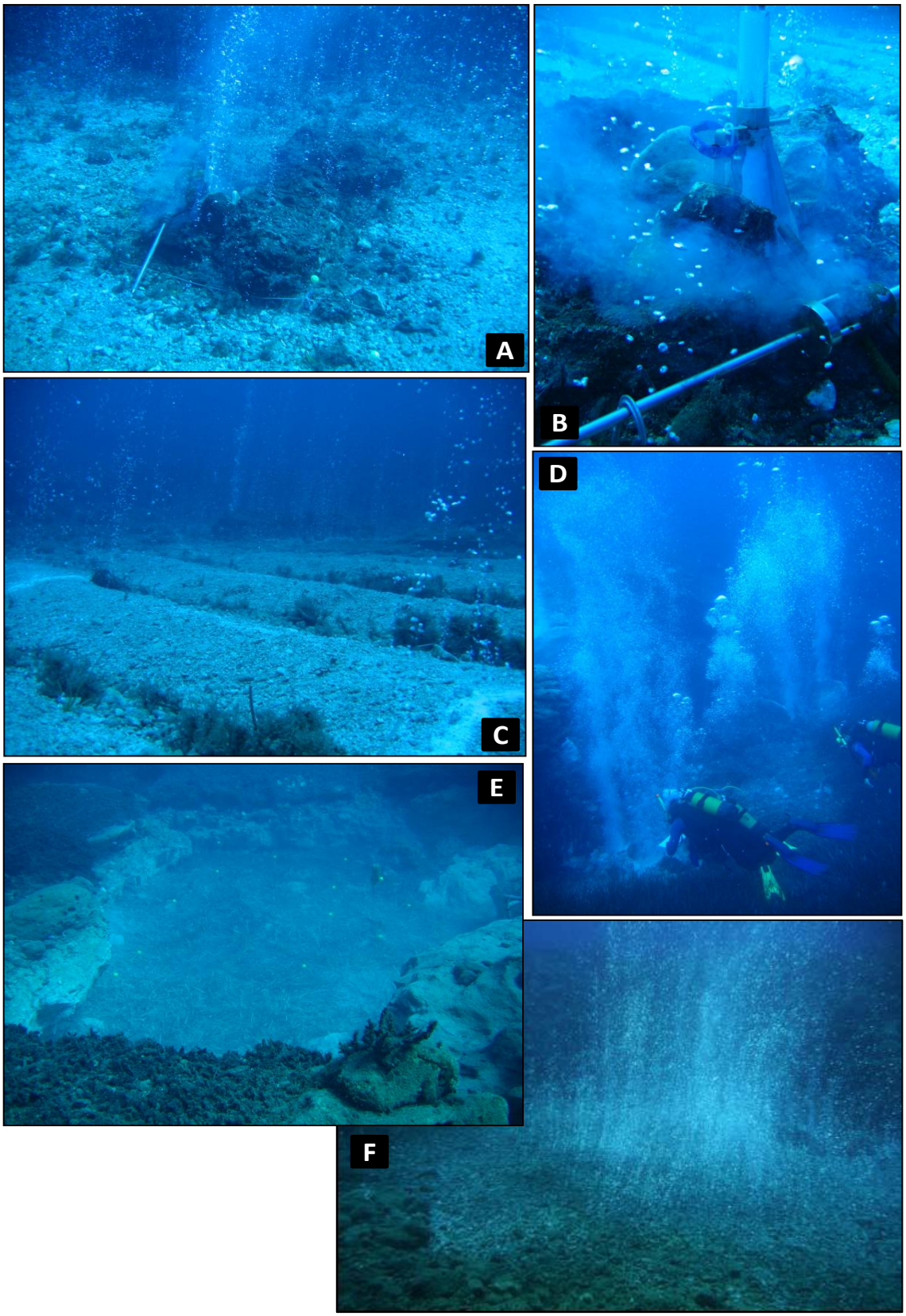

Figure 6: **Diving sites at the investigation area. A) Black Point site and its characteristic black sinter body. B) Black "smoke" of colloids appearing at Black Point during gas sampling. C) Gravel field with wave ripples and some single gas discharges near Black Point site. D) Large fumaroles at Point 21 with strong gas outputs. E) The depression of Hot Lake with some white sulphur and bacteria coatings at lateral walls and a cover of dead *Posidonia* on the bottom. F) Diffuse gas discharges at the crater of Bottaro West. All pictures belong to WISTAU [2007; 2008].**

3 Methods

3.1 Sampling Procedure

Investigations on the hydrothermal system of Panarea were performed during two field campaigns in 2008. The first period lasted from May 12th till May 18th 2008 and the second from August 30th till September 10th 2008 within the scope of the annual diving excursion of the scientific diving research group at the TU Bergakademie Freiberg. Most investigations were carried out by scuba diving, taking samples of the discharging fluids (gas and water) directly over the location of discharge at the seafloor and measuring physico-chemical parameters preferably inside the emission point. Moreover, rock samples of some geological formations within and around the investigation area were taken as well, bothbelow and above sea level.

The scientific work under water implicates some difficulties concerning the applied techniques and equipment which had to be adapted for the prevailing conditions. Some general problems, for example the portability and functionality of devices under water and the time limits for each dive, had to be taken into account, as well as the particular problems sampling a hydrothermal system (e.g. contact with acid fluids, being aggressive towards metallic devices and even rustproof materials).

Since the gas samples are not evaluated in this thesis, their sampling procedure will not be described here. Further description of the sampling and analysing as well as the properties of the Panarea hydrothermal gas emissions are given by STEINBRÜCKNER [2009] and SIELAND [2009].

3.1.1 Water Sampling

Samples of the hydrothermal waters were taken during both campaigns, in May and September 2008.

The water sampling in general was done by using a syringe which was connected to a flexible Teflon hose with an included three-way valve. In order to avoid mixing with the surrounding seawater as much as possible, the ~30 cm long hose was inserted as deep as possible into the sampling location, which is a fracture or an opening in the sediment

where the sampling fluid escapes. In preparations for the actual sampling, syringe and hose were flushed three times by taken up the hydrothermal water from the emission point through the hose into the syringe and deflating them through the three-way valve into the surrounding water. After the sampling the syringes were sealed with (self-made) rubber caps. Syringes with 100 ml and 450 ml volume were applied.
At the sampling points Black Point and Hot Lake, particular effort was made to obtain hydrothermal water as pure as possible.

At the diving site **Black Point** the sinter block was penetrated by using a customary drilling machine, driven by compressed air (compressed air drill 4200/4300, RodCraft Pneumatic Tools GmbH & Co. Kg (Mühlheim, Germany), with 2000 rpm and 6.3 bar operating pressure). With this technique it was possible, to drill some 50 cm deep into the sinter material, permitting sampling of hydrothermal water from inside the rock as described above.

At the **Hot Lake** site, a 1 m Teflon lance was installed in May 2008 in order to extract hydrothermal water from the underground. In September 2008, the lance had to be removed and reinstalled, as it was obstructed or broken, so that no more water could be extracted. This new lance reached down to a depth of 2 m into the sediment.
The installation was accomplished by the application of a drop hammer device, which drove a special rod into the seafloor. The rod consisted of an inner and an outer tube, which were telescoped. After the desired depth was reached, the inner rod was pulled and replaced by the Teflon lance. Subsequently, the outer rod was withdrawn from the sediment, while the Teflon lance remained in the ground.
For the sampling of hydrothermal fluid through the lance, syringes could be connected to the lance via a Teflon hose and a self-sealing coupling. After flushing the syringe, the actual sample was taken out of the deep sediment.

3.1.2 Rock Sampling

Rock samples were taken in May 2008 from four different sites in and around the investigation area. One of these sites was submarine, at the small conglomerate rock face to the south-west of Bottaro West diving site in about 17 m depth (see description in section 2.2.2). The others were above the sea-surface at some of the surrounding islets

(Panarelli and Bottaro, the remnants of the former crater rim, Figure 4) as well as at the southern coast of Panarea, Figure 5).

These sites were chosen based on the geological map and Digital Terrain Model, developed by Esposito et al. [2006] in which the geological and morphological features of the Panarea volcanic complex are described (see section 2.2.2).

The hand-sized rock samples were taken from the cliff using hammer and chisel. The four collected rock samples were all solid rocks and it was tried to obtain preferably unweathered material. However, the samples from the Bottaro dome were already highly weathered showing strong discolouring along the fracture faces. By using the described method, it was not possible to obtain unweathered material from the accessible area of the cliff. Therefore it was tried to eliminate the weathered parts of the sample during the crushing process in which the rock material was ground to granulate for further experiments (section 3.4.2).

3.2 Treatment and Field Analyses of the Water Samples

After each dive, the collected water samples were prepared for some analyses in the field laboratory arranged at Panarea, as well as for the storage and transport until further analyses.

The hydrothermal water was filtered through a cellulose-acetate filter with 200 nm pore-size (Sartorius Biolab Products) in order to eliminate suspended particles, colloids and biota. For the filtration, a filter-container with hand pump was used (Nalgene/Mityrac).

One portion of each filtered sample was analysed by Photometry; another portion was acidified with nitric acid (HNO_3, 65% ultrapure) and stored in PE vials for trace element analyses with Inductively Coupled Plasma Mass Spectrometry (ICP-MS). For ion chromatography (IC), the samples were filtered but not acidified and stored in PE-bottles. Samples for the determination of the total inorganic carbon (TIC) remained unfiltered and non-acidified and were filled into glass bottles directly from the sample syringes, with care being taken that they have as little contact with air as possible.

3.2.1 On-Site and In-Situ Parameters

The on-site parameters of the hydrothermal waters like temperature, pH-value, electric conductivity, redox potential and oxygen content were measured in the collected and untreated fluid samples directly after the dive.
In some cases, the parameters pH, temperature and electric conductivity were also measured in-situ, directly at the sampling point under water by means of a multiple parameter sensor in a water-tight casing.

Temperature

The temperature of the escaping hydrothermal waters at the moment of sampling was measured with a thermocouple in water-proof casing, which was taken on the dive. At the chosen sampling points, the thermocouple was inserted into the outlet and the temperature was received at the display and documented on a writing board. Often, the measuring of the temperature in connection with the electric conductivity at a given point was used for choosing a spot of special interest for sampling.

pH-value

For measuring the pH-value a pH-meter from HACH was utilized. In May 2008, the device type HQ20 was used; the inner electrolyte in the electrodes was a 4 M KCl solution. In September 2008, a HQ40d model was applied, which had an inner electrolyte of 3 M KCl. Both devices were calibrated using a multipoint method with calibration standards from MERCK. The calibration steps were of one pH unit from pH 2 to pH 10. This led to the following calibration lines:

$$pH = -0.0179 * [mV] + 7.1007; \quad R^2 = 0.9984 \quad \text{(May 2008)}$$
$$pH = -0.0175 * [mV] + 7.1783; \quad R^2 = 0.999 \quad \text{(September 2008)}$$

Simultaneously with the pH-value, the current temperature of the sample was measured again with the same device.

Specified electrical conductivity (EC)

The specific electrical conductivity of the water samples was measured with a WTW LF 320 conductivity meter and with a WinLab Data Line Conductivity-Meter from WINDAUS Labortechnik respectively. Reference temperatures were set to 25 °C and a linear temperature correction of 2% per K. For checking the device, the EC of a 0.5 M KCL standard solution was measured, which resulted in a value of 55.0 mS/cm (May 2008) and 59.2 mS/cm (at 28.3°C, September 2008) respectively. These values differed slightly from the exact value of 54.6 mS/cm.

Oxygen content

The content of dissolved oxygen in the samples was measured with optical sensors from HACH. In May 2008, the system O2 LDO HQ20 was used and in September 2008 an O2 LDO HQ40d.

Redox Potential

For the determination of the redox potential, a pH-meter from WinLab Data Line (WINDAUS LABORTECHNIK) was used together with a combined Ag/AgCl-electrode from PCE containing a 3 M KCl solution as inner electrolyte. Calibration was done using a redox standard solution.

The measurements of the redox potentials were performed directly after sampling, whereby the contact with atmospheric oxygen was avoided as far as possible. Therefore, the sample was filled into a closed titration vessel, where the electrodes could be inserted through holes in the cap. These holes were additionally sealed with Parafilm®.

Because the redox potential is dependent on temperature, pH and the potential of the measuring electrode, the readings on the display (E_m) had to be corrected in several steps.

The temperature correction includes the conversion of E_m to the potential at standard temperature ($E_{25°C}$) using the equation below, with T – temperature of the sample solution.

$$E_{25°C} = E_m - 0.198 * (T - 25°C)$$

The resulting redox potential was then referred to the potential of a standard hydrogen electrode (E_h) by adding the correction factor of the applied electrode (Ag/AgCl) which accounts for 207 mV [HÖLTING & COLDEWEY 2005].

$$E_h = E_m + 2.07\ mV$$

Furthermore, the so called rH-value was computed, which is independent of the prevailing pH conditions in solution and thus provides a more expedient comparison of samples with different pH. Applied was the following with E_N being the Nernst voltage accounting for 59.16 mV at 25°C [HÖLTING & COLDEWEY 2005].

$$rH = 2 * (E_h / E_N) + 2 * pH$$

3.2.2 Field Analysis of the Water Samples

Photometry

Photometric measurements were performed with a colorimeter DR/890 from HACH. They comprised all filtered water samples for which concentrations of the following species were determined: iron (Fe_{total}, Fe^{2+}), manganese (Mn_{total}), nitrite (NO_2), ammonia (NH_4), phosphate (PO_4^{3-}) and sulphide ($H_2S_{(aq)}$, HS^-, S_2). The measurement instructions were given by HACH and declared a specific method, concentration range and precision for every substance. In case of high concentrations above the detection range, the sample was diluted adequately and measured again.

Ion-sensitive electrodes (ISE)

The activities of **Iodide**, **Fluoride** and **Bromide** were determined from the untreated samples in the field laboratory by using ion-sensitive electrodes. Because these values were not included in the evaluation of this thesis, the measuring procedure is not further described here, but can be read in SIELAND [2009].

3.3 Laboratory Analysis of the Water Samples

3.3.1 Ion chromatography (IC)

The major anions and cations in the hydrothermal water samples were determined by means of an ion chromatograph at the department of Hydrogeology of the TU Bergakademie Freiberg.

The concentrations of the **major cations** lithium (Li^+), sodium (Na^+), potassium (K^+), calcium (Ca^{2+}), magnesium (Mg^{2+}), manganese (Mn^{2+}) and strontium (Sr^{2+}) were determined using an ion chromatograph 6000 from MERCK/HITACHI, consisting of the following components: Column Thermostat (L-5025), Interface (D-6000A), HPLC pump (L-6200A Intelligent Pump), conductivity detector (L-3720), a pre-column Metrosep Guard and a 250 mm separation column Metrosep C2 (250/4) from METROHM. As mobile phase for transporting the cations across the column, an eluent consisting of 2 mM HNO_3 and 0.25 mM crown ether was used, as well as 1 mM dipicolinic acid (Pyridin-2,6-dicarboxylic acid) which is needed for coordinating the element manganese. Eluation tooks place with a flow rate of 1 ml/minute. Previously to the analysis, all samples were diluted with 2 mM HNO_2 in different amounts: 1:150 for sodium, 1:50 for lithium and the remaining species (calcium, potassium, magnesium and manganese) could be detected in both dilutions.

The **major anions** fluoride (F^-), chloride (Cl^-), sulphate (SO_4^{2-}) and bromide (Br^-) were analysed in an ion chromatograph IC 2001 from EPPENDORF/BIOTRONIK combined with an anion suppressor column (FGC 1AG-P). As anions eluent a 2 mM $NaCO_3$ and 4 mM $NaHCO_3$ with a flow rate of 2 ml/minute was applied. The samples were measured in different dilutions, 1:300 for Cl, and 1:20 for bromide. Sulphate was detectable in both dilutions.

3.3.2 Inductively coupled plasma mass spectrometry (ICP-MS)

For determining the trace element composition of the Panarea hydrothermal water samples, portions of the filtered and acidified samples were sent to ACTLABS[1], where they were analysed by ICP-MS, using a High Resolution Magnetic Sector (Finnegan Mat ELEMENT 2).

[1] Activation Laboratories Ltd., 1336 Sandhill Drive, Ancaster, Ontario, Canada; http://www.actlabs.com (22/11/2009)

The samples taken in May were analysed with the protocol Code 6 MB (marine water, brines or other aqueous solutions with TDS > 0.05 %). The samples from September were diluted in different proportions (HL: 1+61; BP: 1+51; others: 1+41) before measurement and therefore analysed with the protocol Code 6 (natural waters with low TDS < 0.05 %).
A total of 68 elements were analysed at ACTLABS (Appendix F).

The water samples achieved from the **leaching experiments** as well as the solutions from the **total digestions of the rock material** were all analysed with ICP-MS in the laboratory of the department of Hydrogeology at the TU Bergakademie Freiberg. All together, 38 elements were measured in the experiment samples (see Table 2), but not for every measurements run, all 38 elements have been included.
Some dilutions prior to the analyses have been conducted using deionised water in varying proportions: The total digestions have been diluted 1:1000 for the major ions Na, Ca, K, Mg, Al, Fe and 1:20 for all other detected elements. Some other samples of the first analysis-run with ICP-MS have also been diluted (1:20) due to the uncertainty about the overall amounts that could be expected to be extracted from the rock material during the leaching experiments. Afterwards all samples in deionised water were analysed without dilution. The samples performed in NaCl-solution were diluted in parts of 1:10. For preparing the samples for ICP-MS analysis, 10 ml of the pure or diluted sample was filled into a vial and 100 µl of internal standard (Merck, internal standard containing a defined concentration of the elements Ge, Rh and Re) were added for evaluating the performance and recognizing potential errors of the system. Additionally, multi-element standards (Merck) were included in different concentration steps for conditioning the measurement towards the broad range of elemental concentrations being present in the samples. To these standards, the 100 µl of internal standard were added as well.

3.3.3 Total inorganic carbon (TIC)

Contents of total inorganic carbon were also determined for the Panarea water samples in the laboratories of Hydrogeology at the TU Bergakademie Freiberg using a LiquiTOC elemental analyser (elementar Analysensysteme GmbH). Further details on these measurements are given by STEINBRÜCKNER [2009].

3.4 Preparation of the Rock Samples

3.4.1 Cleaning of the Rock Samples

Before using the rock samples from Panarea geological formations for experiments, they were first cleaned with a scrubber and water in order to take off adherent sea water and dirt and dust. Afterwards they were flushed with plenty of deionised water [according to JAMES et al. 2003]. For some other leaching experiments, the rock material was also cleaned with acidic solutions (e.g. 0.1% HF and 5% H_2SO_4 [MOORE et al. 1985] or HCl [UEDA et al. 2005]) in order to eliminate not only adherent dust but also the surface layer of the basalt, whose structure has been disrupted during the grinding process. However, such acid-washing was not applied on the rock samples used for this thesis.
After the grinding of the rock material, the resulting granules were again flushed with distilled water and air-dried afterwards, for removing the dust, which was produced during the milling process.

3.4.2 Grinding of the Rock Samples

For the intended experiments, the rock samples needed to be in a grain size of a few millimetres in diameter, providing a larger surface and thus allowing a better contact between leaching fluid and rock material during the simulated hydrothermal interaction. Hence, the rock pieces of every sampling point were each crushed repeatedly in a jaw-breaker until a mm-grain-size was achieved for most of the rock. The desired fraction of between 0.8 and 2.5 mm was then sieved out and preserved in sealable plastic bags until the following experiments.
It was tried to remove the rock pieces with intensely altered surfaces from the already roughly crushed material. Complete removal of weathered parts however, was not possible.
The grain fraction smaller than 0.8 mm was further milled in a vibrating cup mill ("Pulverisette 9" from Fritsch) into a pulverized form of a grain size of < 0.63 µm. The mill consisted of three rings of agate in an agate-coated pot. The obtained rock powder was used for the total digestion.

3.5 Total Digestion

The pulverized rock material with a grain size < 0.63 µm was used for a total digestion of the samples. This was done using a so called **Waldner-Apparatus**, consisting of several 50 ml-beakers of glassy carbon. The cap of these beakers contains a Teflon-sealing and long Teflon-tubes which can, when placed into their heater, be connected to a suction device, taking off the acid fumes emerging during the digestion process (Figure 7d).

The procedure of a wet total digestion in this equipment is described in the following.

Of each of the four rock samples 0.100 g was weighed. Furthermore, the same amount of an industrially produced basalt-reference material (*GWR-07105*) from China with a known composition was included. A sixth beaker with no sample material was subjected to the same procedure in order to get a blank sample indicating contaminations delivered via the digesting agents.

The rock powder of the five samples was filled into the digestion beakers and all six beakers (including the empty one without rock material) were moisturised with a small amount of ultrapure water followed by adding 2.5 ml HNO_3 (ultrapure). For a uniform distribution of water, acid and rock powder, the vessels were carefully rotated and then allowed to stand overnight. The next day, 5 ml HF (ultrapure) were added to each sample and mixed by carful rotation. The vessels were then locked, embedded into the heater and connected to the suction device. The substances were at first heated to 50°C and allowed to react for one hour without suction. Afterwards the temperature was raised to 100°C for simmering over half an hour again without suction. Now under continued heating, the suction was activated so that all liquid could evaporate.

After the digestions had completely dried, the same amounts of acid (2.5 ml HNO_3 and 5 ml HF) were added again and the procedure of heating and simmering was repeated as described previously. When the solution had dried the second time, the residue was first spiked with 5 ml of concentrated HNO_3 (ultrapure) and shortly boiled, then spiked with 10 ml of ultrapure water and boiled again for some minutes. The digestions were decanted into 50 ml volumetric flasks, cooled down and filled up with ultrapure water to the total 50 ml volume.

3.6 Leaching Experiments

3.6.1 Experiments in the Autoclave

The aim of the leaching experiments was, to investigate the way and amount in which the chemical constituents of the rock samples were dissolved during alteration under hydrothermal conditions. To achieve comparable conditions as in the hydrothermal system of Panarea (in which the energy source is thought to be located deep beneath the seafloor, providing energy for heating the intruding fluids to temperatures > 240 °C [ITALIANO & NUCCIO 1991]), the rock samples were treated in autoclave-pressure-vessels under elevated temperature and pressure conditions.

Configuration of the Autoclaves

The autoclave apparatus consists of four pressure containers, which can be inserted into a heating block and can each be connected to a pressure pipe.

The autoclave containers have a size of about 25 cm height, an outer diameter of 7 cm and an inside diameter of 3.5 cm (Figure 7a). The inner volume is about 100 ml. The vessels consist of stainless steel with the material number 1.4542, which is a martensitic alloy of chromium, molybdenum, nickel, copper and niobium [DIN EN 10088-1; 2005] (the composition in detail is listed in Appendix 6). Producer of the autoclave containers is NWA (New Ways of Analytics, Maximator GmbH).

The containers were inserted into a heating block of aluminium, which is heated via two heating sleeves. With a temperature controller, the desired temperature can be regulated. Beside the temperature measurement of this controller (which measures directly at the heating sleeves), a thermocouple is inserted into a small bore into the inner of the aluminium block, receiving the temperature there. A difference of circa 15 °C was observed and thus, the temperature of the controller was enhanced to 165.5°C, providing a temperature of 150 °C (± 0.5) inside the block.

The pressure tubes coming from each autoclave container are combined via three-way-valves in two steps to one pipe leading to the pressure pump. The pressure is generated by a high pressure pump from ‘Maximator’ (Type: MAF 111 (L)), and by means of gaseous CO_2, which is pumped into the vessels until the desired pressure is reached. The pressure is

controlled by the valves in two pressure steps. Each container can be pressurized separately.
For safety considerations, two half-shells were screwed on top of the aluminium block and across the inserted autoclaves (Figure 7c). This should curtail the risk of explosive damage due to over-pressurization and bursting closures.

The heating block together with the inserted autoclave containers is installed on an engine-driven trestle (Figure 7c) which can slowly shake the whole system. This is needed to force a better distribution of the leached elements and to avoid a distribution only by molecular diffusion.
Before the experiments, the insulation of the aluminium block incorporating the four autoclave vessels had to be renewed and advanced. Therefore, the old insulation was removed and a new and thicker enveloping was attached. As isolation material a ceramic fibre fleece was applied. This fleece matting was cut into a suitable form, including notches and gaps for the trestle-seating and heating cables etc. Enclosing the insulation, technical aluminium foil was installed in several layers, carefully covering all parts of the insulation and fastened with heat-resistant aluminium adhesive tape (Figure 7c).

Procedure of the leaching experiments

For each leaching experiment, 2.00 g of rock sample with a grain size of 0.8 – 2.5 mm were used. Instead of a sample splitter and for getting a homogeneous and representative rock sample, all crushed rock material with the appropriate grain size was filled into a petri-dish and divided into four quarters. From each quarter, a similar amount of material was picked with a spatula. When weighting the material, care was taken that only unweathered material and grains from the whole size range were chosen for the experiments.
To avoid plugging in the pressure tubes of the autoclaves, whose inner diameters of about 2 mm are in the same order of magnitude as the grain size, the weighted rock material was filled into a pocket of metal wire mesh. The use of a larger grain size was no option due to the mechanical and thermal load of the rock material during the experiment, which can lead to abrasion and breakup of larger grains.
These wire pockets were formed of metal wire cloth with the following product designation: *mesh number: 107/59, material number 1.4401, wire thickness 0.16 mm* and

was produced by PACO (Paul GmbH & Co)[2]. The wire mesh was cut into pieces of about 40 cm^2 and bent to small oblong pockets (see Figure 7e). The material 1.4401 is an austenitic alloy, consisting of chromium, molybdenum, nickel, and manganese [DIN 10088-1; 2005] (the composition in detail is listed in Appendix 6).

Instead of the metal wire pockets, it was also tested with one of the four autoclave containers to solder a piece of the metal wire mesh across the inlet of the pressure pipe in the middle of the sealing cap. This method would have the advantage that the rock material is more mobile in the autoclave and thus more exposed to the leaching fluid.

As solvent in the leaching experiments, deionised water was used, aerated with CO_2 over approximately 30 minutes directly before loading of the autoclaves.

Filling the autoclaves was done by putting one sample-filled wire pocket into each container and adding 75 ml of the CO_2-aerated water. Thereby care was taken, that no water contacts or remains on the copper gasket, which seals vessel and cap. The vessels were closed with the sealing caps, screwed tightly with 6 bolts and inserted into the aluminium heating-block, which was already pre-heated to circa 65 °C. The autoclaves were connected to their pressure pipes and all valves were closed, so that the system is completely closed and no gas and vapour could escape. Then the system was heated until an inner temperature of 150 °C was reached. Following, the pressure inside the autoclaves was raised by means of the pressure pump, which pumped CO_2-gas into the vessels. Due to the low accuracy of automatic control, the pressure was adjusted manually by opening the valves.

All leaching experiments in the autoclaves were performed at 250 bars. The pressurizing was executed in two, sometimes three steps with some minutes of disruption for allowing the system to equilibrate concerning temperature and CO_2 dissolution in water. The first step was approximately 200 bar, the second the aimed 250 bar. Every time after the full pressurization, the pressure decreased in the following minutes by approximately 20-30 bar, which is due to the dissolution of CO_2 in the water. Therefore the pressure needed to be readjusted after circa 15 minutes. Afterwards, the shaking mechanism was activated and the experiment time started.

For leaching experiments of hydrothermal character in general, different testing times ranging from a few hours (10-24h) to several thousands (3000-4000h) were applied [e.g.

[2] http://www.paco-filter.de/index.php?id=63 (22/11/2009)

ALLEN & SEYFRIED 2003; ELLIS & MAHON 1964; ELLIS & MAHON 1967; GHIARA et al. 1993; HENNET et al. 1988].

To evaluate the varieties between different leaching times being in an applicable range, some pre-tests with the different reaction times of 24, 48 and 84 hours were performed. For these time series, only one of the four different rock samples, the sample *R2* (Bottaro North) was used. For assessing the leaching of the metal of autoclave vessel and wire pocket, a blank sample was included with every run as well.

On the basis of these results (see section 4.1), a test duration of 24 hours was chosen for the following experiments with all four rock samples.

After the particular reaction time of each run, the shaking and heating mechanism were turned off and the whole system needed several hours (mostly over night) for cooling down.

When the temperature had cooled down to about 30-40 °C, the pressure could be released. The pressure pipes were disconnected and the autoclave vessels could be removed. In order to dissolve all element sorption from the vessel walls, the autoclaves were shaken again before opening. Immediately after opening, the wire pockets with the rock material were removed and pH and electric conductivity of the solution was measured in a separated portion of the sample using a pH-meter pH320 (WTW, 2-point calibrated using buffer solutions) and an EC-meter LF320 (WTW, tested with a conductivity standard solution) respectively.

Afterwards the solution was filtered through a cellulose acetate filter with 200 nm pore size (SARTORIUS) into acid-cleaned PE-bottles. The filtered samples were acidified to a pH of 1-2 with 20-30 µl of HNO_3 (MERCK, 65% ultrapure) and stored at 4 °C until the analyses with ICP-MS.

3.6.2 Experiments in the Overhead Rotator

Beside the experiments in the autoclave, a series of leaching experiments in an overhead rotator at normal atmospheric pressure and room temperature were accomplished. These experiments were also conducted as a time series in three runs over 24, 48 and 84 hours and with the same amounts of rock material (*R2*) and CO_2-aerated water. For a better comparability, the rock material was also wrapped in the wire pockets.

Beside these time series experiments, also two experiment runs with material of all four rock samples were undertaken using deionised water and NaCl-solution (0.5 M) respectively as leaching fluid. Both have been aerated with CO_2 previously to the experiments. For these two experiments, the loose rock granules without a wire mesh were used.

Preparing the rotation experiments, the samples (with or without a wire pocket) together with 75 ml leaching fluid were filled into 100 ml PE-Bottles, capped tightly and clamped into the overhead rotator. The rotation was activated for the respective reaction time with 5 revolutions per minute (rpm). Again a blank was included for every run.

Directly after the reaction time, the solutions were measured with respect to pH-value and EC, filtered, stabilized with HNO_3 and stored in a refrigerator as described above.

Using NaCl-solution in the autoclaves at elevated temperatures was not possible due to the danger of intense corrosion of the materials and valves (see section 4.5).

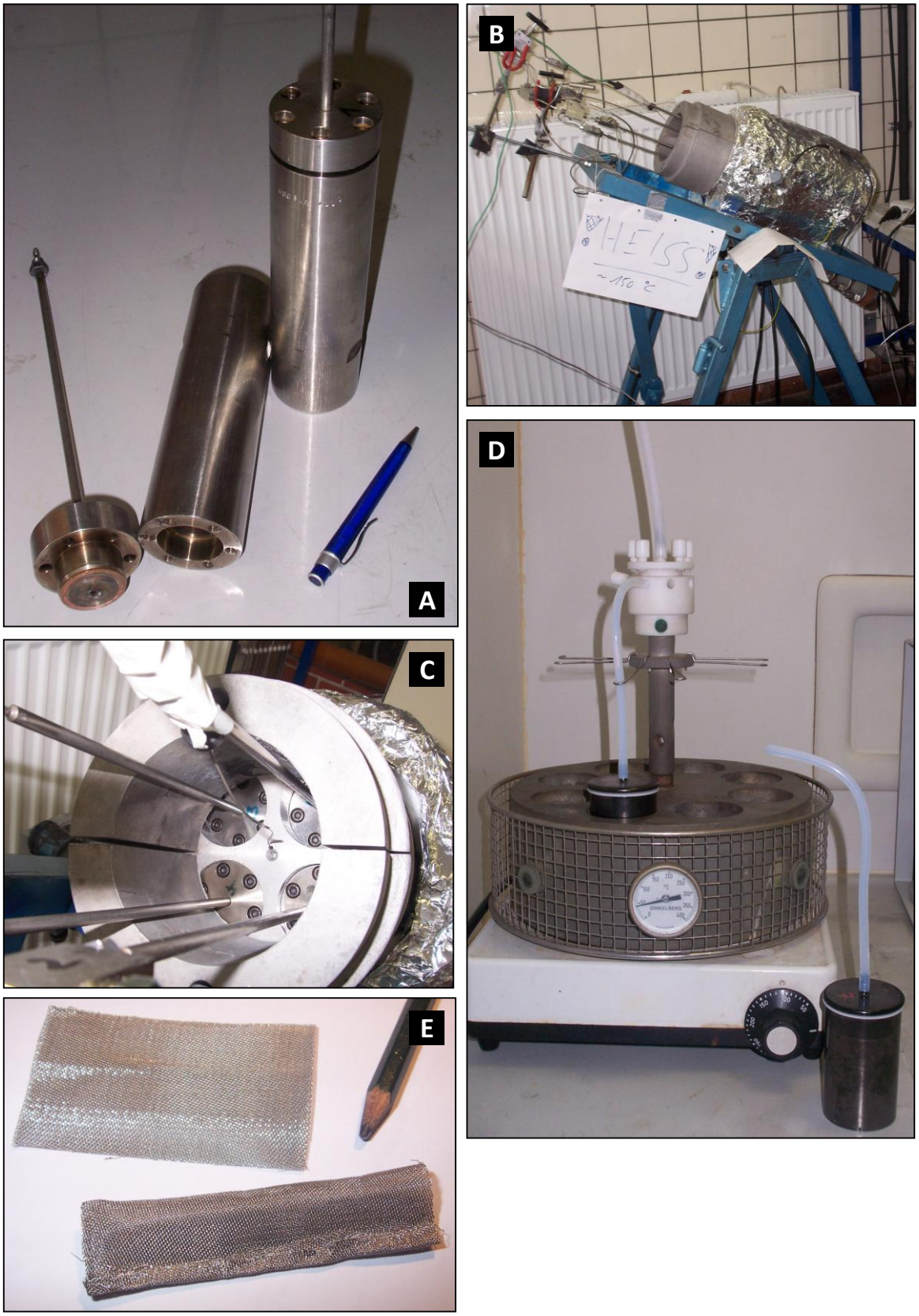

Figure 7: Experimental equipment. a) Autoclave vessels and closures. b) Autoclave vessels embedded in the aluminium heating block and fixed with half-cells. c) Aluminium block on shaking trestle, with inserted vessels and connected pressure tubes. d) Waldner-Apparatus, consisting of a heater, a suction device and glassy-carbon beakers. e) A piece of the metal wire mesh and a bended wire pocket.

3.7 Evaluation of the Data

3.7.1 Data processing

Before evaluating the chemical measurements of the samples, the raw data were checked concerning concentrations below or above detection limit as well as for missing values.
Measured **concentrations lower than the detection limit** of the respective element, were replaced by half of the value of their detection limit. The particular detection limit of an element was calculated from its calibration data of the ICP-MS-measurement (see digital Appendix B.8). Thereby, a value clearly above the background level (measured value of the blank) was demanded. A value of three times the background level was supposed to be significantly higher. Accordingly, for the computation of the detection limit, the rate of counts produced by the blank sample (deionised water) was multiplied by three and then converted to a ppb-concentration via the calibration line. This calculation was done for every individual element in every measurement run. Related to several measurement runs, different detection limits can be found, for the reason of a varying performance of the ICP-MS or slightly different element concentrations in the applied blank solution.
The upper detection limit was reached by the element Sr in the two reference water samples from Panarea, measured with ICP-MS. For these samples, the value of the upper detection limit was applied. To prevent element concentrations exceeding the upper detection limit, some experiment samples were diluted previously to the measurement.
For the performance of a cluster analysis (see section 3.7.2) missing values can cause calculation problems. Hence, missing data were replaced by a mean value of other samples of the same experiment category. If this was not possible (because no other samples of this category were available), the parameter in total was excluded from the calculation.

For the sake of clarity in the presentation of the results, the elements were classified into the classes major, minor and trace elements, according to their frequency. The assignment of the elements was calculated using the average concentration of an element, calculated from 17 relevant samples. With the arbitrarily established concentration limits for each class [referring to Aiuppa et al. 2000], the elements have been classified as follows (see Table 2):

Table 2: Classification of the measured elements into the groups major, minor and trace elements, according to their mean concentrations.

Major elements	> 1 mg/L	Na, Ca, K , Mg, Si, S, Mn, Al, Fe, B, Sr, Li, Rb, Cu
Minor elements	10 µg/L – 1 mg/L	Ni, Zn, I, Cs, Ba, P, Br As, Cr, Pb, V, Se, Co, Tl, Cd
Trace elements	< 10 µg/L	Ga, Mo, Be, U, Ag, Bi, Sn, Te, Sb

3.7.2 Hierarchical Cluster analysis

The term *cluster analysis* comprises a series of statistical methods for identifying homogeneous groups out of a set of multivariable data [CHEN et al. 2007]. Thereby, the objects within one class have similar parameter values, whereas the single classes show high dissimilarity [HANDL 2002]. The application of a hierarchical clustering algorithm calculates the classification iteratively by a stepwise combination of the most similar observations [CHEN et al. 2007].

In this thesis, a hierarchical cluster analysis was performed with the aqueous samples in order to identify if there exist sample groups having similar chemical structures within the collectivity of all samples. The calculation was carried out with the statistics program SPSS version 11.0 for windows (SPSS Inc., Chicago, USA). To compute the degree of similarity between two objects, different algorithms can be applied as well as different methods for calculating the distance between two objects. Here, the Wards Algorithm was used, in combination with squared Euclidean distances. This leads to relatively homogeneous clusters with small distances between the objects and their cluster centre [STOYAN et al. 1997].

For input data, two different combinations of the aqueous samples were listed in matrices where the samples represent the individual objects and the element concentrations indicate the variables (input data are listed in Tables C.1 and C.3 in the digital Appendix C). All missing values were replaced if possible (see section 3.7.1) or the parameter in total was excluded from the calculation. Previous to the cluster analysis, all data were standardized by variables (also in SPPS) to adjust scaling differences. For a cluster analysis, a Z-Transformation is advised [STOYAN et al. 1997].

For each data matrix, a cluster analysis was run for the cases of 2 till 8 clusters and with the methods described above.

After the performance, it was tested, if the newly classified groups differ significantly from each other with regard to all variables. Therefore, a Kruskal-Wallis test was applied to each

of the seven classifications (into 2 till 8 clusters) with the classifications after Ward being the grouping variable.

A Kruskal-Wallis test is based on ranks, which were allocated to the data, so a normal distribution is not required [HANDL 2002].

Using the test, it is tried to reject the null hypothesis that the median for all variables are equal. A level of significance of $\alpha = 0.01$ was chosen to be acceptable, so the right decision is made with a security of 99%. The alternative hypothesis therefore is that the median of all variables differ significantly on the confidence interval.

3.7.3 Standardization

The chemical data of the aqueous samples show concentration varieties over several orders of magnitude between individual elements, this means the scale of concentration is very large (from ng/L to mg/L). For better clarity in some graphical evaluations and for statistical purposes, the data has to be standardized to provide a consistent scaling of all parameters.

For statistical evaluation, a **Z-Transformation** was performed with the statistics program SPSS:

$$Z = \frac{x - \bar{x}}{s}$$

[STOYAN et al. 1997]

with: Z – standardized value; x – original value; $\bar{x}$ - mean value of the parameter; s – standard deviation value of the parameter

4 Results and Evaluation

As an overview, Table 3 lists all experiments that have been performed within the scope of this thesis and that will be evaluated in the following.

Table 3: Overview about all experiments and their associated samples accomplished for this thesis (s+p: sample includes solder and wire pocket)

Experiment Type	Sample Series	Included Samples	Notes
Pre-Test	I	I.01_Blank_soldered I.02_Blank_soldered I.03_Blank_Pocket I.04_Blank_Pocket	PTFE-Filter
Time Series Autoclave	II	II.1_Sample - 24h II.3_Sample - 24h II.2_Blank - 24h (s+p) II.4_Blank - 24h	Slightly pressure release from vessel 4 during experiment
	III	III.1_Blank_84h III.4_Blank_84h III.2_Sample_84h (s+p)	Sample III.3 has been discarded due to a leaky vessel
	VII	VII.1_Blank_48h VII.4_Blank_48h VII.2_Sample_48h (s+p) VII.3_Sample_48h	
Time Series Overhead Rotator	V	V.1_Sample_24h_R V.2_Blank_24h_R	
	IV	IV.1_Sample_84h_R IV.2_Blank_84h_R	
	VI	VI.1_Sample_48h_R VI.2_Blank_48h_R	
Sample Series Autoclave	VIII	VIII-Blank VIII_R1 (s+p) VIII_R3 VIII_R4	
	XI	XI-Blank XI_R2 (s+p) XI_R3	Valve of vessel 4 (R4-sample) was not completely closed
	XII	XII_Blank (s+p) XII-R1 XII-R2 XII-R4	
Sample Series Overhead Rotator	X	X_R1_R X_R2_R X_R3_R X_R4_R	
	IX	IX_R1_R_NaCl IX_R2_R_NaCl IX_R3_R_NaCl IX_R4_R_NaCl	Measured in 1:10 dilution

4.1 Results of the Time Series performed in Autoclave and Overhead Rotator

In order to find out how the time of exposition affects the concentration of rock- leached elements in solution, a time series with reaction durations of 24, 48 and 84 hours was performed, both in the autoclave and in the overhead-rotator.

The chemical analyses of these samples are displayed graphically in Figure 8 (autoclave experiments) and Figure 9 (rotation experiments). The individual elements have concentrations in strongly different orders of magnitude (ng/L till mg/L), therefore a logarithmic concentration scale was chosen.

Concerning the three reaction times of the **autoclave samples** the concentration differences are slight for most of the elements (Figure 8).

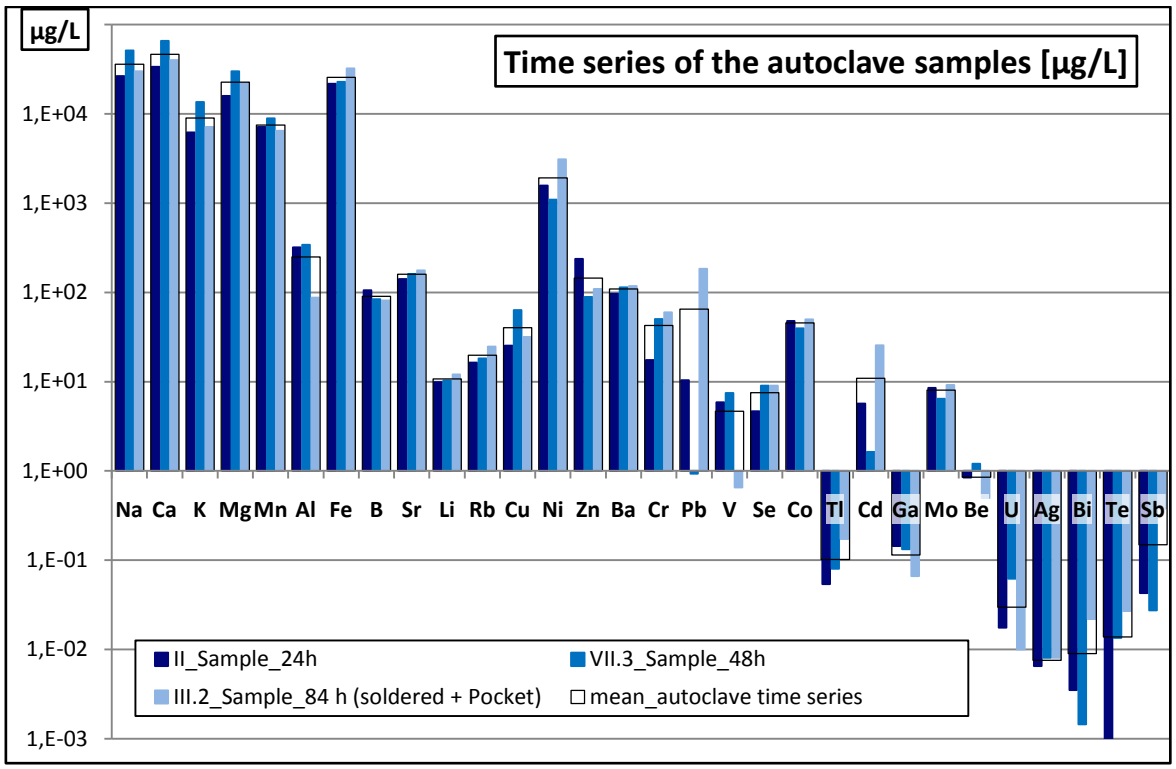

Figure 8: Chemical composition of the time series samples (24, 48 and 84 hours), performed in the autoclave at 150°C temperature and 250 bar pressure. Concentrations are given in µg/L on a logarithmic scale. The empty bar (secondary axis) represents the mean of all three durations, together with the standard deviation.

Only for a few elements (As, Pb, V, Cd, U, Bi, Te, Sb), which all belong to the category of minor or trace elements (compare Table 2), a noticeable difference between the three reaction times exists (compare Figure 8 and Figure 9 and Tables A.1.1 and A.1.2 in the digital Appendix A.1). But these differences do not always show a clear trend in the way

that a longer reaction time results in a higher amount of leached elements (which would have been expected due to slow reaction kinetics for some mineral phases): for some elements this trend is present (Li, Si, Cr, Fe, Se, Rb, Sr, Ag, Te, Ba, Tl) and for other elements the dissolved amount is decreasing with a longer reaction duration (B, Ga). For some of the elements again, the reaction time of 48 hours show the highest (Na, K, Ca, Mg, Be, Al, V, Mn, Cu, U) or the lowest (Co, Ni, Zn, Mo, Cd, I, Cs, Pb) concentration.
In previous leaching experiments by other authors, reaction durations of several days have been applied for providing the possibility of reaching equilibrium conditions [e.g. GHIARA et al. 1993]. For the experiments performed for this thesis, such a long reaction time was not feasible, though the range of 24 – 84 hours reaction time has also been applied in the literature [ELLIS & MAHON 1964].

The results of the **rotator experiments** at normal temperature and pressure conditions have overall a similar appearance: for some elements a positive or negative dependence of reaction time is observable, for other elements this is not the case (Figure 9). Compared with the autoclave samples, the rotation experiments result in clearly lower concentrations for nearly all elements. Only for Na, Zn, Se and Sb, concentrations are more or less equal or even higher than the autoclave samples (Figure 9 and Table A.1.1 in the digital Appendix A.1).
Using a statistical cluster analysis it was tested, if significant differences between the different reaction durations do exist, which was not the case (compare section 4.3).
Based on the results of the different reaction times, which do not show a clear dependency between element concentration and reaction time (and also with regard to time efficiency), a reaction duration of 24 hours was chosen for all the following experiments.
The results of the chemical analysis of all the pre-tests and time series were listed in the tables in the digital Appendix A.1 and A.2.

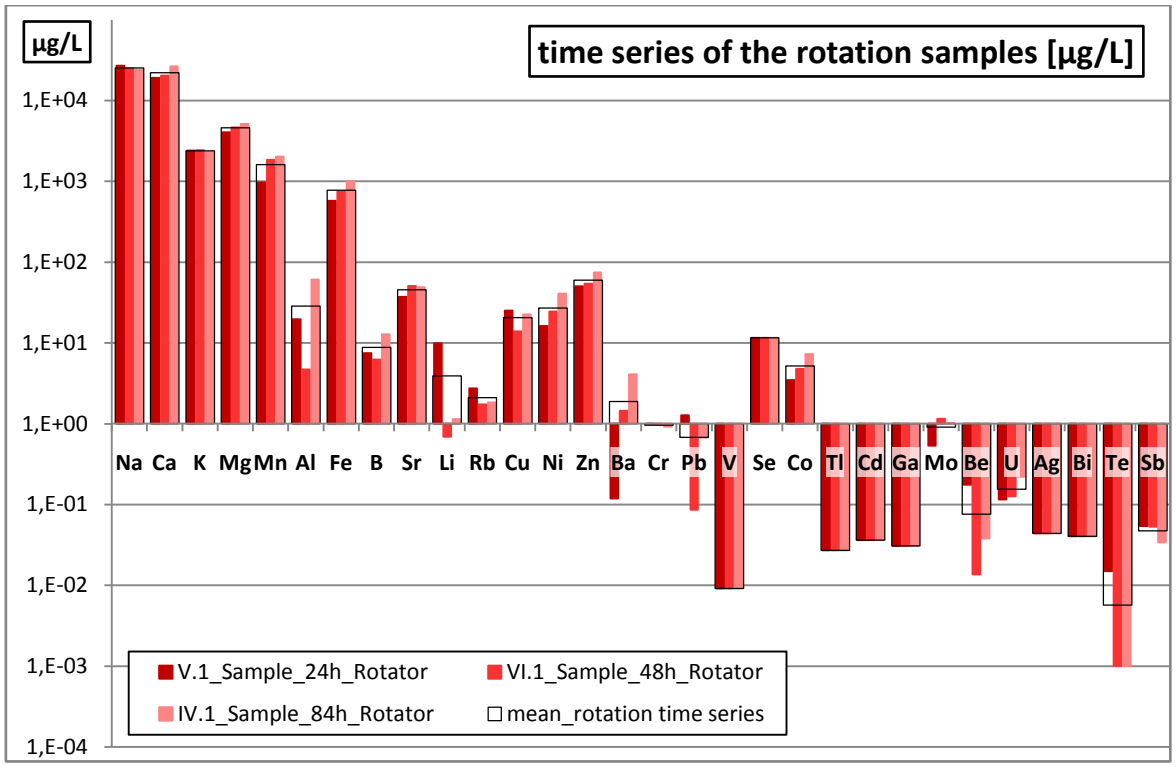

Figure 9: Chemical composition of the time series samples (24, 48 and 84 hours), performed in the overhead rotator at normal temperature and pressure conditions. Concentrations are given in µg/L on a logarithmic scale. The empty bar (secondary axis) represents the mean of all three durations, together with the standard deviation.

4.2 The blank samples

Blank samples exist for each autoclave experiment run as well as for the time series samples performed in the overhead rotator. They were executed in order to correct the influence of leaching from the system materials (autoclave vessels, metal wire pockets and solder).

The autoclave containers and the wire mesh both consist of stainless steel of the **type 1.4542** and the **type 1.4401** respectively. The chemical compositions of both steels are taken from the German version of the European Norm **EN 10088-1 Stainless steels** [DIN EN 10088-1; 2005] and are listed in Appendix 6. The chemical composition of the solder is not known, only some typical elements can be listed according to the German version of the European Norm **EN ISO 9453 soft solder alloys** [DIN EN ISO 9453; 2006] (see Appendix 7).

4.2.1 The blank samples of the autoclave pre-test

In order to investigate how the autoclave system works with an aqueous solution and at the applied temperature and pressure conditions, an initial pre-test was done during the first experiment run (already before the time series). Furthermore the practicability of the wire mesh pocket and the soldering was tested for their resistance towards the experiment conditions.
Therefore, a blank run was accomplished using two of the autoclave containers – one with water and a metal wire pocket, the other one just with water and the soldered sealing.
This test showed that both alternatives were applicable in principle concerning the experiment requirements, nevertheless the wire pockets were chosen for the following experiments, to rule out, that the soldered mesh could peels off in the course of experiments.
Unfortunately, the soldering at the sealing cap of one of the autoclave containers was not removed after this first experiment run but was from now on included in every following run.
The subsequent chemical analyses showed that the leaching of the soldering material has a severe impact on some specific element concentrations. Thus all samples treated in this autoclave vessel were contaminated, strongly affecting the results of the rock leaching experiments.

In Figure 10a comparison of the two samples processed in a wire pocket and the soldered autoclave vessel is shown. Both the two red and blue plotted concentrations are duplicates of the same sample. From the figure it becomes evident that a noticeable discrepancy exists in most of the element concentrations between the blanks exposed to the wire pocket or the soldering inside the autoclave vessel.
The highest difference occurs for the element lead (Pb), where the concentration for the **soldering sample** is more than three orders of magnitude higher than those in the pocket variant. The explanation suggests itself that during the leaching experiment in the soldered autoclave, a high amount of Pb is extracted from the soldering material, which largely consists of Pb (Appendix 7). [DIN EN ISO 9453]. Pb is already slightly soluble in water at normal temperature and pressure conditions and at neutral pH. At more acidic pH-values, the Pb-solubility is significantly increased [PAIS & J. BENTON JONES 1997]. Hence, the acidic pH value predominant inside the autoclave (4.10.1) and the large quantity of Pb available leads to such high Pb-concentrations in the sample. Further components of the

solder are Ag, Al, Bi, Cd, Cu, Sb, Sn, and Zn (Appendix 7), which are (beside Cu) likewise enriched in the blank of the soldered vessel (Figure 10).

The elements Cr and Mo, which are clearly enriched in the **pocket blanks**, are constituents of the pocket material (Appendix 6). Thus, the higher concentrations can be explained by the supplemental exposition of the pocket material to the leaching solution. For the other elements enhanced in the pocket sample (Ba, V, Be, Ag, Te), the author assumes that they are minor constituents of the stainless steel and are similarly dissolved from the pocket material.

Further discussion about the problems concerning the solder, the wire pockets and the utilization of this autoclave system in general as well as the reason for the high Cu concentrations is given in section 4.5.

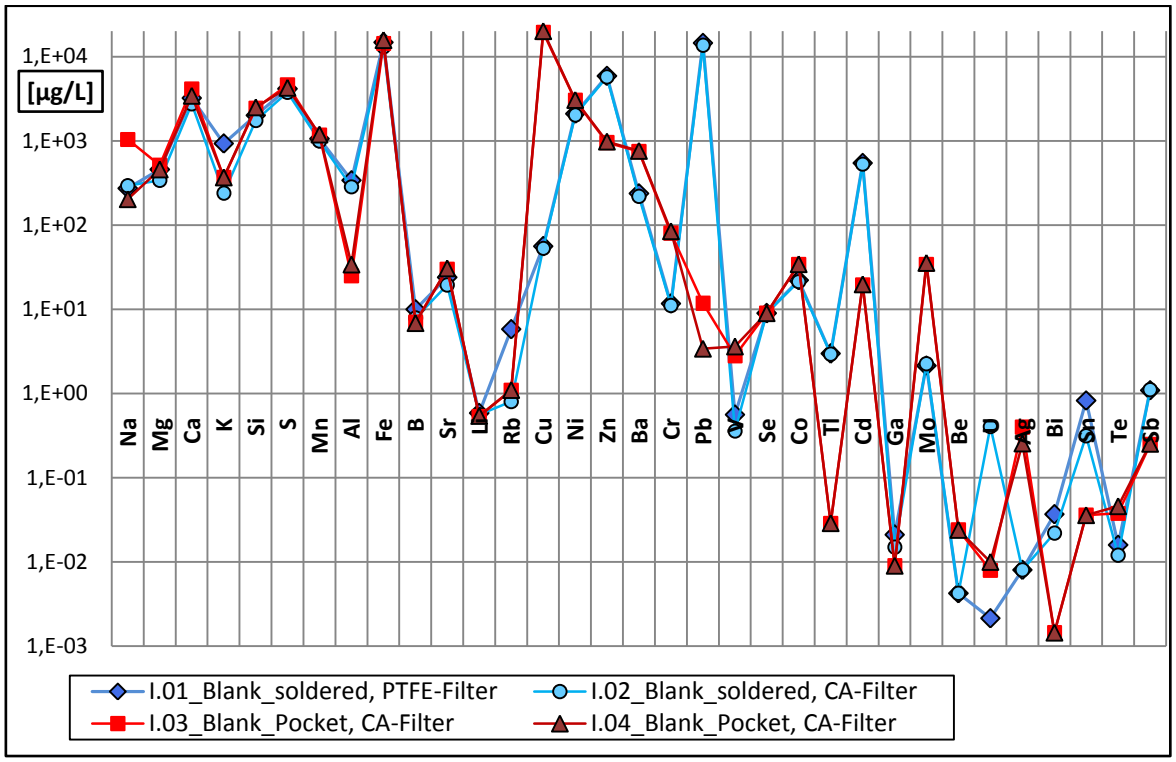

Figure 10: Element concentration in the blank samples of the autoclave pre-test. Both the two red and the two blue plotted concentrations each belong to duplicates of the same sample. The connecting line between the samples does not indicate a correlation between the single elements, but should clarify the data points belonging to one sample.

It should be mentioned, that it was tried to filter a part of the blank from the soldered vessel through a PTFE-filter (pore size 0.45µm) instead of a CA-filter (sample *I.01_Blank_soldered, PTFE-Filter*) in order to avoid any sorption of elements to the CA-filter material. Because the PTFE-filter material is permanently hydrophobic, the filtering of the aqueous sample solution through this medium was hardly possible by using a hand

pump. Hence, for a better handling of the sample preparation, all following samples were filtered through a CA-filter, disregarding an eventually low sorption of the dissolved elements. Nevertheless, the slightly enhanced concentrations of some elements in the PTFE-filtered sample part, compared with the CA-filtered part, are presumably explained by that.

4.2.2 The blank samples of time series and some real experiments

With all blank **samples of the autoclave experiments** which have not been performed in the soldered autoclave container the mean value was calculated as well as the standard deviation. The results together with the background concentrations of the deionised water used for the experiments are displayed in Figure 11. The diagram in general shows relatively high concentrations of 100 – 1000 µg/L for most of the major elements (Na – Cu) and some of the minor elements (Ni – Cd). Most of the trace elements (Ga – Sb) have concentrations between 0.01 and 0.1 µg/L.

The mentioned element classification has been introduced in section 3.7.1. Looking at the deionised water sample, it can be seen that for most of the measured elements (21 of 27), the concentration is < 1 µg/L. For a few elements it is < 10 µg/L and only Si shows a concentration slightly above 100 µg/L. It is suggested, that also for the major elements Na, Mg, Ca and K, which are not measured for this sample, the background concentration lies in the range of 10-100 µg/L due to their natural abundance.

Conspicuous are the amounts of Mn, Al, Fe, Sr, Cu, Ni, Zn, Ba, Cr, Pb, V, Co, Cd, Mo and Ag, which exceed the range of their background concentrations over orders of magnitude. These elements (except Sr, Ba and V) are all constituents of the stainless steels of which the autoclave system as well as the sample pockets are made and are supposed to be extracted from there during the experiment.

Also for all other element the concentration in the blank mean is higher, though to a smaller extent. This enhancement probably results likewise from dissolution of the minor constituent out of the contact materials, or is inserted during the process of sample processing (filtering, filling, acidification).

The concentrations of the main cations Na, Ca, K and Mg in the deionised water have not been detected, and thus the background value of the water could not be compared to the additional element input during the experimental procedure.

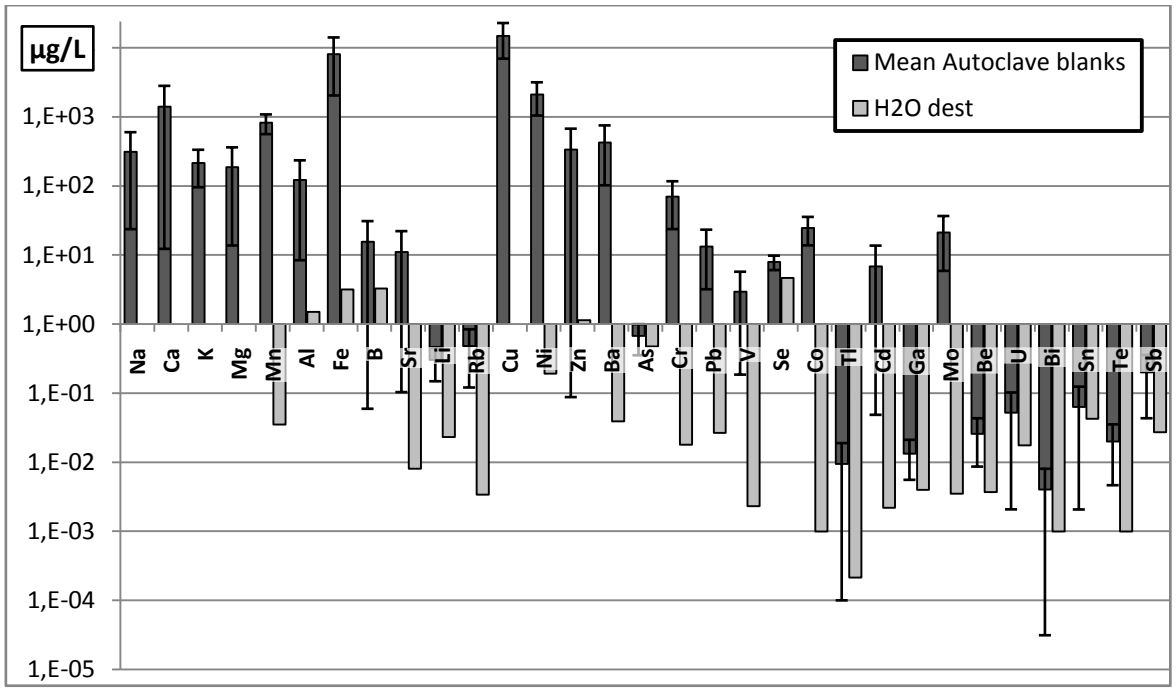

Figure 11: Mean element concentration and standard deviation of some autoclave samples (I.03, I.04, II.4, II.4, VII.1, VII.4, VIII, XI) in comparison to the concentration of the deionised water that was applied as leaching fluid. The concentrations are given in µg/L on a logarithmic scale.

For all blank samples treated in the autoclave, the experimental setup, preconditions and experiment procedure had been equal (see section 3.6). Nevertheless, a look at the standard deviations shows, that for a set of elements (amongst others Na, Mg, Ca, Al, Zn, Ag…) the concentrations in the related samples differ a lot causing standard deviations of 50 – 100% (or even more for B, U, Ag, Bi…). For the exact differences between all blank samples, see Figure 11 (note the logarithmic scale!) as well as Tables A.3.1 and A.3.2 in the digital Appendix A.3.

A discrepancy of up to 10 – 20 % can be explained by the measurement inaccuracy of the analysing method (ICP-MS), but for the higher concentration differences it is hard to find an explicit and convincing explanation.

The hypothesis recommended by the author is, that during the complete experiment procedure (from the preparation of the samples and starting the autoclave system until the processing and measuring of the resulting solution), each sample is exposed to a multitude of internal and external influences. Thus, every sample of every experiment run has to be considered in some respects as an individual and independent system and is only comparable with constraints.

For a more detailed discussion of the problems and influences occurring during the experiment procedure see section 4.5.

Concerning the following quantitative evaluation and interpretation of the experiment results, the chemical concentrations of the samples will be seen as an overall range or rough order of magnitude, not taking into account the eventual error of up to 100% or even more.

Another important aspect probably affecting the changes in the chemical composition of all autoclave samples is the formation of a protection layer of hydroxides, depositing on the vessel walls and other surfaces [e.g. BOUCIER & BARNES 1987] (further details are given in section 4.5). This may yield to a decreasing extent of leaching out of the autoclave system (including the solder) in the course of experimental runs.

In Figure 12, the concentrations of some important alloy constituents in all autoclave blanks is shown, separated into blanks of the soldered and the normal vessel. In both groups the samples are sorted after their temporal succession of performance.

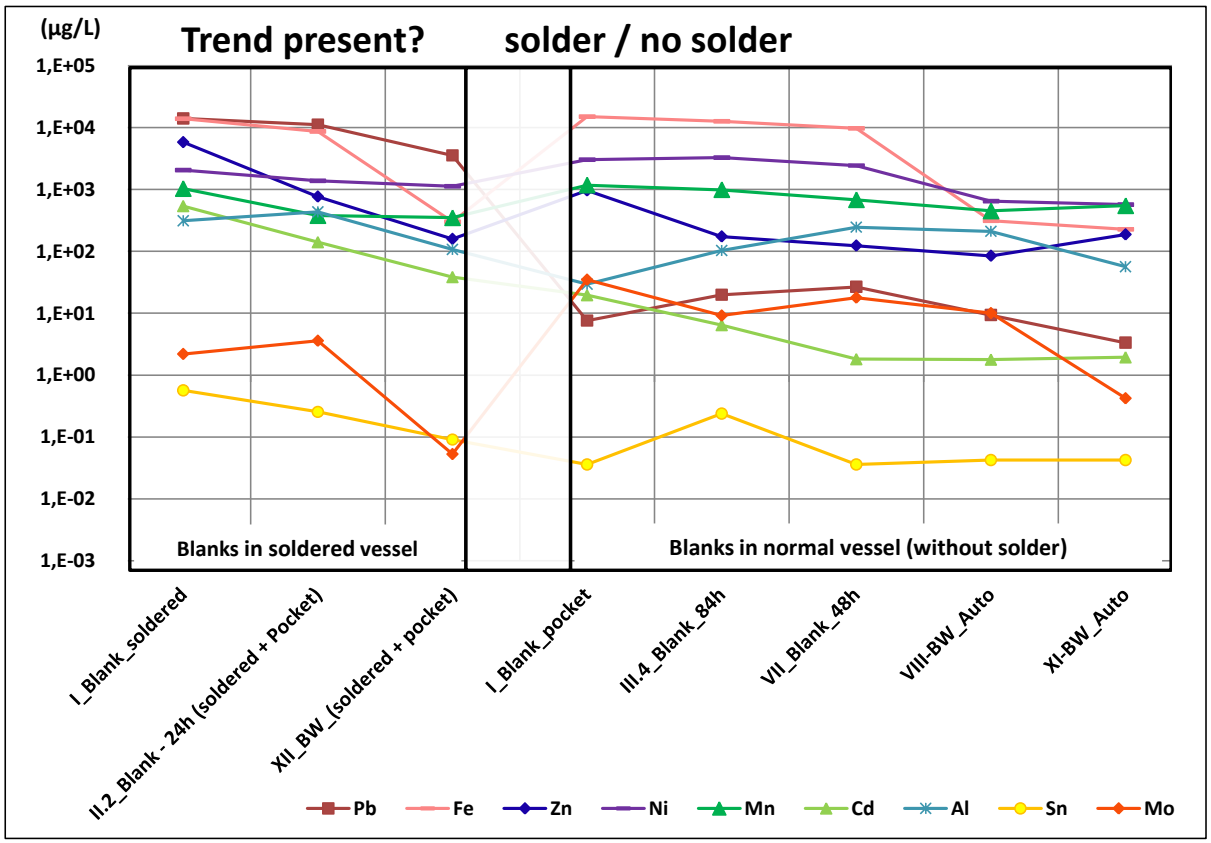

Figure 12: Examination of the concentration development of the elements Pb, Fe, Zn, Ni, Mn, Cd, Al, Sn, Ag and Mo in the blanks with and without solder. Within the two groups (with solder (left) and without solder (right)) the blank samples are sorted after their chronology of execution. Concentrations are given in µg/L on a logarithmic scale.

Looking at the group of **blanks from the soldered vessel** (left window) a clear and strongly decreasing trend is evident for all elements (note the logarithmic scale!), confirming the declaration about an inhibited leaching from the system with time.
In the **blanks without solder-influence** (right window) this decreasing trend is also present for most of the elements, but only to a lower degree.
It occurs also, that the continuous decrease with gradually experiments is interrupted by one or more again higher concentration (Pb, Zn, Al, Sn, Mo). This can be explained by other impact factors (explained in section 4.5), like for example small pieces of the coating layer that spalls from the steel surfaces and promotes further corrosive attack.
In this diagram moreover, the extremely different concentrations of Pb among blanks in the soldered and unsoldered vessels are well identifiable: between the left and the right window, a discrepancy of about 3 orders of magnitude exists.
Blank samples were included for every experiment when executing the **time series in the overhead rotator** at normal temperature and pressure conditions. This was done because the real rock samples have been filled into wire mesh pockets, likewise to those samples of the autoclave time series, to better compare the results of both time series. Consequently, also a blank with just the leaching solution and the wire pocket were performed.
The chemical concentration of the three rotation blanks in general has a similar appearance to the autoclave blanks with a relatively high concentration of the major and some of the minor elements and a very low concentration for all trace elements (except Ag) (Figure 13 and Table, digital Appendix A.1.2). As compared to the deionised water that has been the starting solution, it becomes evident, that already at normal temperature and pressure a small but considerable amount of metals has been contributed from the system.

Interesting is the comparison between the blanks from the overhead rotator and the autoclave samples in both, soldered and normal vessel. For each case the average is depicted in Figure 14 (for exact values see Tables in the digital Appendix A.3). Noticeable is the fact, that the rotation blanks have a clearly lower concentration for nearly all elements, pointing out the lower leaching capacity of the solution at normal temperature and pressure conditions. Exemptions are the elements Na, Se and U which have equal concentrations in both experiment types as well as Se, Tl, Ga, Ag and Bi, where the rotation blanks have a higher concentration. Nevertheless, already at the conditions of the rotation experiment it is observable that the characteristic elements of the stainless steel come into solution in small amounts.

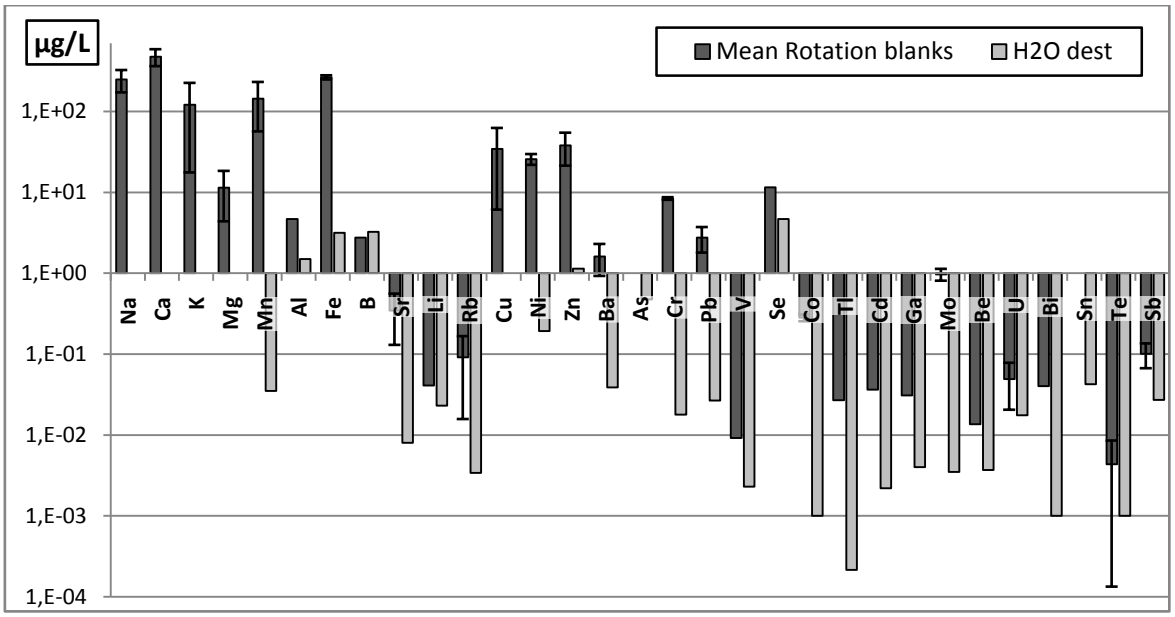

Figure 13: Mean value and standard deviation of all blanks from the rotation experiments (blanks exist only for the time series samples, which were performed in wire pockets like the corresponding autoclave samples).

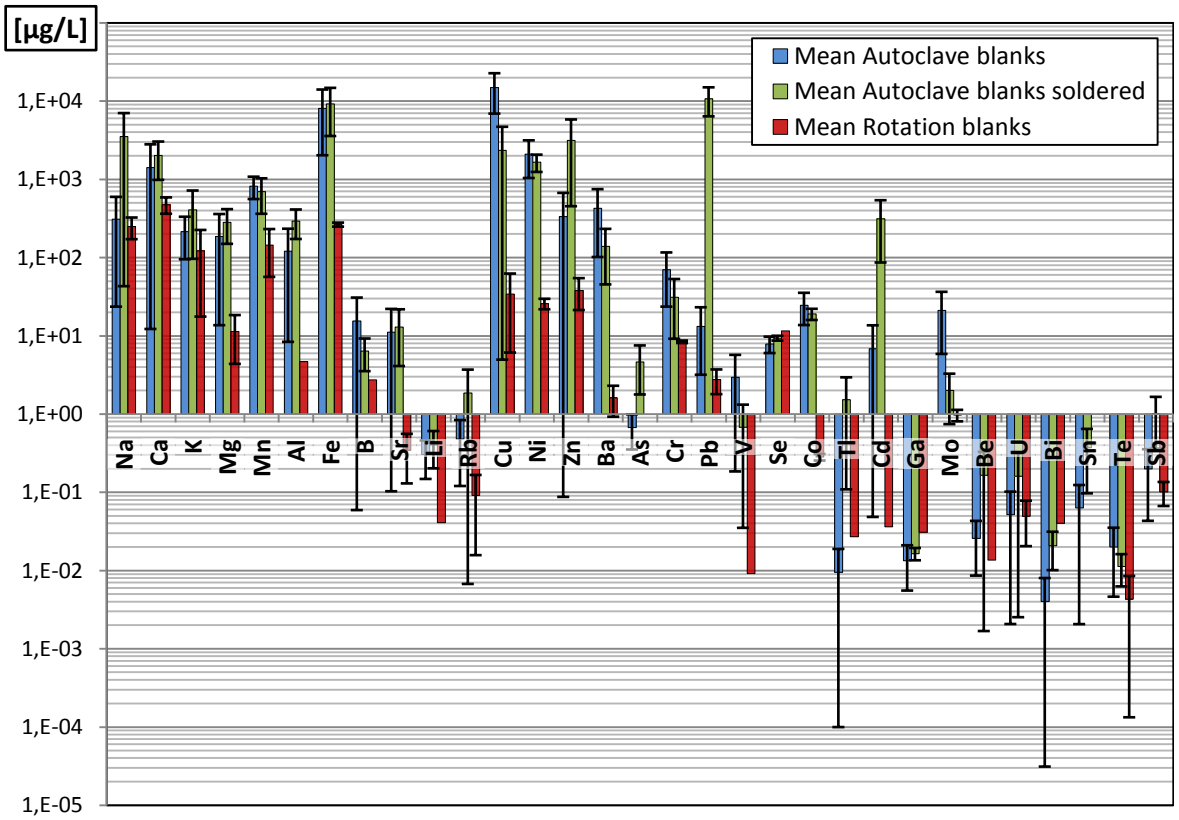

Figure 14: Blank values, averaged for each of the experiment category (autoclave unsoldered, autoclave soldered and overhead rotator). Concentrations are given in µg/L on a logarithmic scale.

Moreover it can be seen, that an (more or less large) extra portion of some elements like Na Al, Zn, Pb, Cd, Bi and Sn is leached from the soldering in one of the autoclave containers, which is already described in section 4.2.1.

The problem with these blank samples is their partially inexplicable differences between every single run (as mentioned earlier in this section), which can be seen from the large standard deviations (see error bars in Figure 14, note logarithmic scale!). Accordingly, a simple subtraction of a blank from its run-related real sample often leads to slightly till massive negative concentrations for several elements, which is of course not possible. In other words, the concentrations generated through the contact of the sample solution with the instrument materials are higher than those arising from both the experiment system plus the rock materials. Reasons for this occurrence are discussed in section 4.5.

Finding a way to avoid those negative concentrations that resulted from the subtraction of blanks from the rock sample, the mean value of all blanks of one category was computed. In such means the extreme concentrations should be more equalized, representing a more reliable concentration. The mean value was then subtracted from every appropriate sample, but for some elements negative concentrations still occur (compare Table A.4.1 in the digital Appendix A.4).

4.3 Hierarchical Cluster analysis

The intention for running a statistical cluster analysis is to ascertain an inner structure of the sample similarity by means of their chemical concentrations. On the basis of these similarities it is hoped to find a classification of the samples displaying the different experiment procedures.

For the first run of a hierarchical cluster analysis (Cluster analysis A), the samples of all experiments were included (total digestions, autoclave samples, rotator samples with and without NaCl-solution and blanks). The input- and evaluation-data are given in Tables C.1 and C.2 in the digital Appendix C, together with the appropriate output-files.

The results are shown in form of a dendrogram in the Appendix (Appendix 1). Pursuant to the Kruskal-Wallis test and on a significance level of $\alpha = 0.01$, the classification into 6 clusters show significantly different medians of the clusters for 26 of the 29 variables (digital Appendix C.2). That means that the classification of all samples into 6 clusters has the highest overall difference between its groups.

A detailed look at the contents of each class shows that all the samples of the total digestions (classes 6) as well as all samples of the rotator experiments performed with NaCl-solution (class 3) each form an individual, easily explainable class (Appendix 1). Also most of the autoclave samples (class 4) and most of the autoclave blanks (class 1) fall in one class. Questionable is the combination of samples in class 2, where mostly samples of the rotator time series and rotator experiments occur, but also some blanks of the rotator time series, some autoclave samples and autoclave blanks. This assembly of samples leads to the assumption, that all these samples (although they come from different experiment types) have a similar structure in their chemical composition. Incomprehensible is, that samples as well as their appending blanks (e.g. series IV, V, VI, series VIII, series XII) should have the same structure in chemical concentrations. An obvious division would have been, if all blanks, all autoclave samples and all rotator samples (without NaCl solution) each had formed an individual class.

Moreover, the clustering resulted in one class with only two samples (class 5). These are actually duplicates of the blank of the autoclave pre-test, performed in the autoclave container with the soldered mesh (compare Table 3). Hence, this is about only one sample. It is remarkable that this one sample was found to be a single class already in the second step of calculation and directly after combining the total digestions to one group, whereas all of the other samples remain in one large group (see schedule “cluster membership” in the Output-File document in digital Appendix C). This indicates that the sample originating from only deionised water in the soldered autoclave container has a strongly individual chemical composition, different to all of the other samples. From this result it can be concluded, that a characteristic concentration of some elements is leached out of the solder, leading to the isolated position in the classification. The momentousness of this result is, that probably all samples, treated in this soldered autoclave vessel are contaminated by elements leached from the solder (amongst others Pb, Zn, Cd).

Some other blank samples treated in the soldered vessel were not classified into class 5, but into class 1 (*II.2_Blank_24h_s+p*) and class 2 (*XII_Blank_s+p*) although they have externally the same experiment conditions. For this allocation other aspects like the processes inside the autoclave seems to be important, which is further discussed in section 4.5)

For samples of the autoclave leaching experiments, treated in the soldering vessel, it is thought that the signature of solder contamination is covered by the leaching of the rock material and therefore these samples are mostly classified into class 4, the group of all

normal autoclave samples. Only the sample *VIII_R1_s+p* apparently has a more similar signature to the blanks and the rotation samples and is therefore "misclassified" in class 2 with respect to the interpretation. Nevertheless, the contamination by the solder is still present, adulterating the results of the rock leaching experiments in the autoclave.

It was tried to achieve a better result of the cluster analysis concerning a better explainable allocation of the samples to the clusters. Therefore, a second run of the cluster analysis was carried out, where beside the element concentrations of the sample also their electrical conductivity was included as a parameter. Since this parameter to a certain extent can be seen as something of a sum parameter for all element concentrations and with great discrepancy among the different sample types (compare Table 5 or Input data in Table C.3 in Appendix C), it is expected, that the inclusion of this parameter will lead to a clustering which better represents the various types of samples. In exchange, all data of the total digestions had to be excluded from the input matrix, because no measurement of the EC was available for these samples. Similarly all samples with probable solder contamination as well as some samples with obvious mistakes in their chemical measurement (e.g. extremely higher concentration for some elements compared with other samples of this type) were excluded, in order to receive a more homogeneous grouping and expecting a guidance of decision which samples are representative for a particular type of experiment. All samples involved in the second run (Cluster analysis B) are listed in Table C.3 in the digital Appendix C.
The resulting classification was again checked for significant differences between all groups using the Kruskal-Wallis test. On a confidence interval of 99%, the division into 5 clusters shows significantly different medians for 5 of 29 parameters (see Table C.4 in the digital Appendix C). Moreover this result equals the one of the first cluster analysis, where 6 classes were found to be significant, but including the discarded samples of the total digestions which on their own form the sixth group.
The result of the second cluster analysis is shown in form of a dendrogamm (Figure 15) and is discussed in the following:

- In **Cluster A** six samples are grouped, which are now only blank samples from the autoclave experiments.

- **Cluster B** comprises all samples (blanks and rock samples) treated in the overhead rotator with deionised water, and furthermore some blanks from the

autoclave experiments, but no autoclave rock samples anymore. The fact, that in this cluster blank and rock samples are grouped together, could be explained by the overall very light mineralization of the blank samples as well as the rotation rock samples. Although the autoclave blanks have also a very light mineralization, they are grouped separately, confirming the supposition, that a characteristic elemental background level is leached from the autoclave system. Nevertheless, three autoclave blanks are classified together with the rotation samples, indicating that the group of autoclave blanks and of all the rotation samples have high similarity. This is affirmed by the fact, that in the next step of calculation the clusters A and B are combined to one big cluster containing all blank samples and all rotation samples in deionised water (Figure 15).

- **Cluster C** is similar to the corresponding third cluster from calculation A and includes all five samples produced in NaCl-solution.

- The pre-test blank, performed in the soldered autoclave vessel, form again one cluster (**Cluster D**) on its own, already from the second step of calculation.

- The last **Cluster E** contains only autoclave rock samples, like its corresponding cluster from run one. But now the samples *XII_R1, XII_R4* and *VIII_R4*, previously misclassified to class 1 and 2, are found in one group together with all other samples of their experiment type. The classification structure within Cluster E, shows further characteristics of the four different rock samples (*R1-4*): in the first step of combination, the two samples of rock type 3 *(VIII_R3, XI_R3)* and of rock type 4 (*VIII_R4, XII_R4*) are each grouped together. In the second step the R2-sample *(XII_R2)* is combined with those of the time series, which are in fact also performed using rock sample R2. The rock sample R1 remains as an individual case until the last step of combination within this group of autoclave samples.

In summary the second run of the cluster analysis, including the electric conductivity as a parameter and eliminating some specific samples, provided a much better classification due to the representation of the different experiment types. Therefore the data of these samples is used as a basis for further evaluation, whereas all other samples which are not comprehended in the second run have to be viewed with caution.

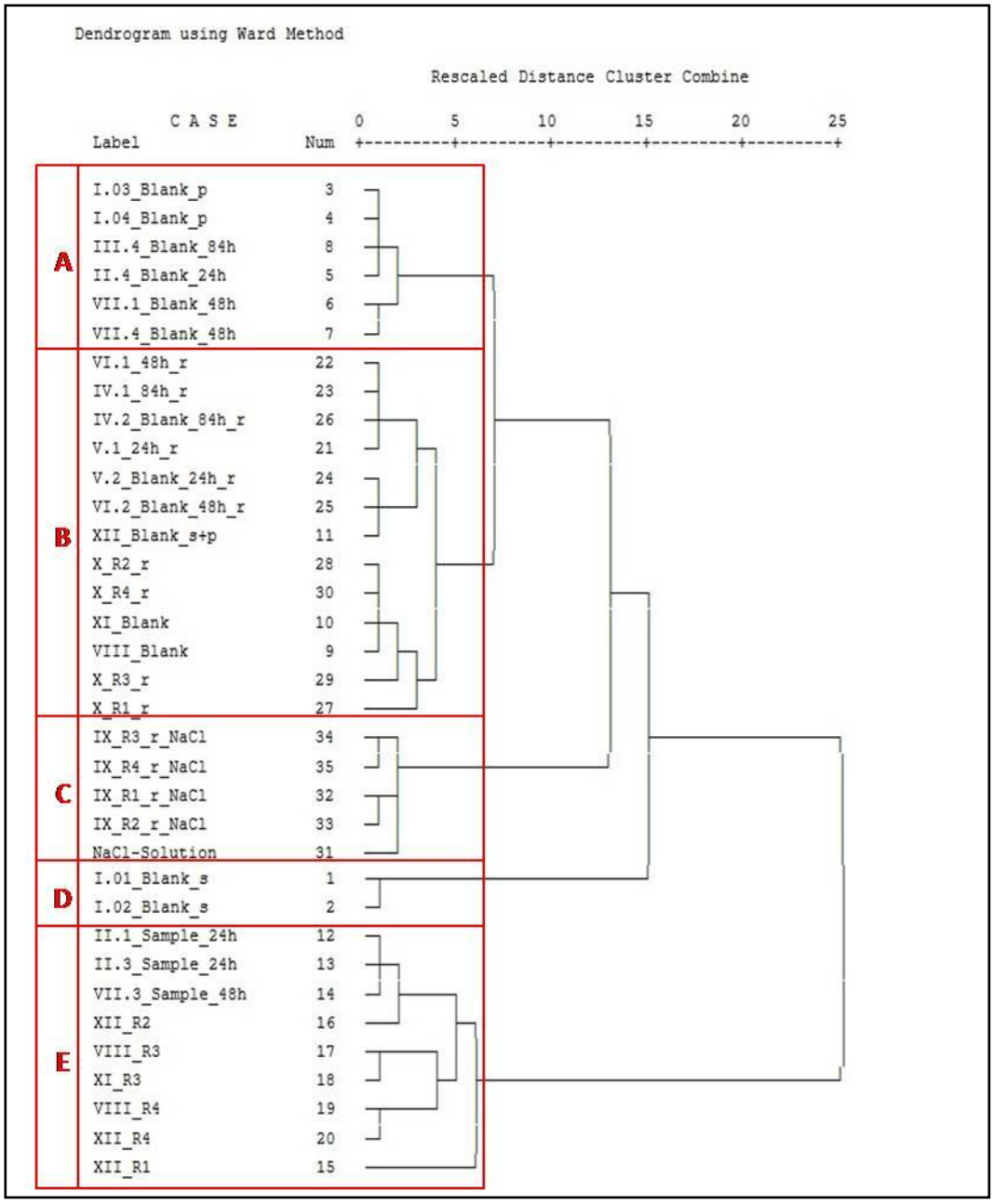

Figure 15: Dendrogram of the hierarchical cluster analysis B using Wards algorithm, representing the classification of the samples into five groups having the most significant differences among each other. Further explanations are given in the text.

4.4 Total digestions

For the total digestions of the four rock samples (*R1, R2, R3, R4*), all together 30 elements were analysed with ICP-MS. The results are shown in the Tables of digital Appendix B.1., sorted after the mean element concentration of all relevant samples (compare Table 2).

In Figure 16 it can be seen, that the concentration in the four rock samples is more or less equal for most of the elements, so that the connecting line of all four rock samples display

a similar pattern. Slightly larger differences in concentration occur for the major elements Mg, Ca, and B as well as the minor element Cr. High deviations exist for the trace element Te. The rock sample *R1* (diving site Bottaro West) furthermore has a significant higher concentration in Tl and Mo.

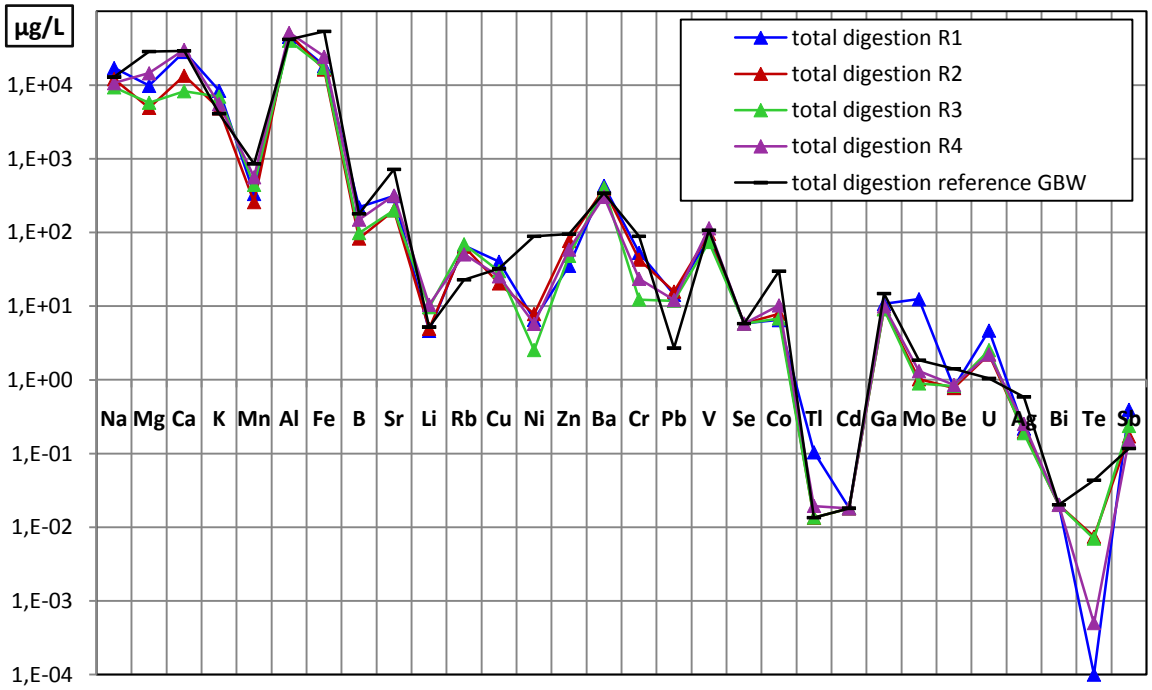

Figure 16: Element concentration in the total digestions of the four rock samples (R1, R2, R3, R4) and the reference sample (GBW). Note: the connecting line between the samples does not indicate a correlation between the single elements, but should clarify the data points belonging to one sample.

The element concentrations in the reference sample (a basalt rock from China with known concentration) show a more different structure compared with those of the Panarea rock samples. This denotes that the Panarea rocks described as andesitic-dacitic type have another chemical composition than a typical basalt rock, as it was presumable. Moreover, the similar element characteristic of the four Panarea rocks may indicate that the mentioned rock types [identified by ESPOSITO et al. 2006] are of similar origin.

Also the results of the cluster analysis (section 4.3) where all total digestions (including also the reference sample) belong to one group approves, that they have an individual elemental character compared to all experiments samples, mainly reasoned by the comparably much higher element concentrations.

4.5 Critical evaluation of the autoclave technique

4.5.1 General considerations

The primary idea of the rock leaching experiments was to subject the four samples of rock material to leaching conditions similar to those assumed for the natural hydrothermal system of Panarea. These are pressures of up to 250-300 bar (and more, according to the depth) and reservoir temperatures of 310-345 °C [SIELAND 2009]. Thus, the leaching conditions the Panarea bedrock is exposed to lie in a conditional range up to 345°C temperature and 250 bar pressure that decreases towards the sea bottom. Moreover the hydrothermal processes under these conditions together with the input of some volcanic gases escaping from the deeper reservoir being probably dissolved in the ascending fluid lead to an acidic pH value of < 3 [SCHULZ & ZABEL 2006].

In a more shallow depth above the geothermal body also seawater is present that infiltrates into the underground. There it is heated up and converted into a hydrothermal fluid by exchange with the surrounding bedrock material. It was thought to carry out leaching experiments with NaCl-solution (as simplified seawater) in the autoclave as well, in order to investigate the special processes in the shallow underground. The problem with NaCl-solution in contact with metal materials is its strong corrosive capacity. Therefore, experiments with NaCl-solution could not be performed using the autoclaves of stainless steel, which have only been available for the leaching experiments.

For the solubility experiments conditions of 300 bars and 350°C were primarily suggested in order to simulate the hydrothermal processes, but with the autoclave system being at disposal, some difficulties concerning these requirements exists. The temperature of 350°C for example was not realizable because of an insufficient heating capacity of the heating sleeves around the embedded autoclave containers the combination with an isolation which is not configured for those high temperatures. Moreover, concern exist about a possible corrosion of the autoclave materials (vessel walls, valves, sealing and pressure tube) due to an aggressive solution, resulting from the leaching fluid (deionised water + CO_2) and the rock material at high temperature, in particular if they come close to the critical point. A too high corrosion rate could damage the entire autoclave system and can cause explosions with property damage and personal injury [BOUCIER & BARNES 1987]. Therefore, a temperature of merely 150°C together with a pressure of 250 bars were chosen to be a

compromise between both, providing elevated conditions for the leaching experiments and a secure utilization of the autoclave system.

The autoclave containers used for these experiments consist of stainless steel of the type 1.4542, a type of noncorrosive martensitic steel which is characterized by high wear resistance, high compressive strength and high carrying capacity [BENEDIX 2008a]. Chemically, this steel is high-alloyed (>5% of alloying components[BENEDIX 2008a]) containing mainly Cr, Ni, Cu and Nb as steel refining components (see Appendix 6) [DIN EN 10088-1; 2005].

Due to their high amount of alloying additives, all stainless steels have a high corrosion resistance. These additive elements have a strong affinity to oxygen (atmospheric or dissolved) and react to metal oxides, which form a microscopic oxide layer on the steel surface that inhibits the electrochemical reactions and thus prevents further corrosion of the stainless steel [ILSCHNER & SINGER 2005]. The quality of this passivation layer depends not only on the hard solubility of the oxides in a corrosive media but also on its permeability, because even if the formed oxides are completely inert in the solution, there is no protection when the solution can penetrate through a permeable layer getting in contact with the underlying metal surface [BOUCIER & BARNES 1987]. However, the martensitic steels contain smaller amounts of Cr, Mo and above all Ni compared to other noncorrosive steels, which leads to a high strength towards elevated temperatures and pressures but are not that corrosion resistant and thus not preferred for hydrothermal experiments [BOUCIER & BARNES 1987].

Furthermore the martensitic steels exsolve carbon and thus become brittle at temperatures above 300°C which is another cause for not heating the system to the primarily desired 350°C.

However, the chosen experiment conditions of 150°C and 250 bars mentioned above are well suitable for the autoclave equipment and should not induce severe damage. A corrosive contamination of the experiment solution could anyhow not be ruled out.

Examining the whole experimental system and -proceeding that comes to operation for this thesis (see section 3.6), various effects and problems may occur both, during the treatment in the autoclaves as well as the preparation and processing of the sample before and after the experiment. These impacts can contaminate the chemical composition of the sample, leading to adulterated results of the experiments. A discussion of those effects and also possible reasons for their varying intensity is adduced in the following.

4.5.2 Corrosion

Although stainless steels in general have a good corrosion resistance, degradation always takes place to a low extent and is intensified under elevated temperature and pressure, such as the experimental conditions of hydrothermal experiments [BOUCIER & BARNES 1987; ROOS & MAILE 2005]. As already mentioned, the alloy composing the autoclaves used in this thesis, has a good strength against the mechanical stress under elevated temperatures and pressures, but a less appropriate corrosive resistance. The electrochemical reactions taking place during the corrosive attack are redox reactions, catalysed by a difference in the electrochemical potential between distinct areas on the metal surface (anode and cathode) which are conjoint through an aqueous electrolyte [BRIEHL 2008]. The potential can arise from several situations inside the system, for example due to the existence of varied noble metals within the microstructure of an alloy, which possess different standard electrode potentials [BENEDIX 2008a]. During the anode reaction, metal atoms are oxidized to metal cations that exist in the solution as hydrated (dissolved) ions or form hardly soluble molecules with constituents of the electrolyte (e.g. oxides or carbonates) [BENEDIX 2008a; ROOS & MAILE 2005]. The excessive electrons remaining in the metal surface and facilitate the reduction of the aggressive media which can be a different agent depending on the corrosive conditions. For the corrosion in acidic solutions for example, this agent are the oxonium-ions which are reduced to pure hydrogen gas [BRIEHL 2008].
Hence, the corrosion process influences both the chemical composition as well as the acidity and the redox state of the solution [BOUCIER & BARNES 1987].

The general corrosion reaction on metallic materials is the oxidation of the respective metal, conforming the follow equation:

$$Me \rightarrow M^{n+} + n\,e^{-} \quad \text{(anodic process)} \quad [\text{BRIEHL 2008}],$$

contemporaneous with the reduction of the aggressive agent:

$$X \rightarrow n\,e^{-} + X^{n-} \quad \text{(cathodic process)} \quad [\text{BRIEHL 2008}].$$

As mentioned above, this agent could be oxonium-ions, reduced to pure hydrogen (under more acidic pH values) or in neutral or slightly alkaline media the reduction of oxygen to hydroxide-ions [ILSCHNER & SINGER 2005].

Using NaCl-solution with concentrations similar to those of seawater for solution experiments inside the autoclave vessel, the danger of severe corrosion of the material strongly increases. The huge amount of dissolved ions turns the solution to an electrolyte

with high electric conductivity. The electrochemical reactions taking place during the corrosion process need a closed circuit, which is provided and even accelerated by a high concentration of ions in solution [BENEDIX 2008a]. The chloride ions their self have an even stronger corroding effect because they catalyze the oxidation of iron [REESE & GRABKE 1993] and form aqueous iron-chloride-complexes (for example [FeCl4]-, [FeCl6]3-). This leads to further iron oxidation due to a shift of equilibrium and moreover inhibits the formation of hardly soluble oxides and oxide-hydrates that deposits as a protective coating on the steel surface. Based on this property of the dissolved chloride, it was not possible to conduct experiments including seawater-solution inside the available autoclaves. Hence, such experiments using a NaCl-solution as simplified seawater were only performed at normal temperature and pressure conditions (see section 4.8).

4.5.3 Contamination of the samples

Due to the described corrosive attack, it is unavoidable that during the rock leaching process in the autoclave, not only the rock material is dissolved, but substances from the contact materials (stainless steels and solder) are extracted as well. These elements are certainly the principal constituents of the solder or the steels and their additives (compare Appendix 6 and Appendix 7). The experiments are actually generated for highlighting the chemical composition that is dissolved from the rock material at the defined conditions, but through the accessory leaching of the equipment materials the samples get contaminated by those metals. To quantify the contamination, a blank sample without any rock material was included in every experiment run. The chemical analysis of the blanks show high amounts of those elements composing the alloys (stainless steels and solder) (see Figure 10, Figure 11 and section 4.2).

Each of the four autoclave vessels has its own **history of usage** and thus an individually stressed material (e.g. due to the previous contact to aggressive media), which provides a larger surface and promotional conditions for corrosive processes. This can result in a dependency of the amount of corroded elements on the specific autoclave vessel where the sample is treated in.

In contrary, the formation process of an inactive and **protecting layer** of metal oxides on the inner vessel walls should lead to a decreasing amount of corroded elements in the course of experiment runs [BOUCIER & BARNES 1987].

In fact, a decreasing trend in the blank concentrations within the temporally ordered samples is noticeable for some of the principal elements of the alloys (among others Fe, Ni, Mn, see Figure 12).

But it is also conceivable, that small pieces of this coating layer spalls from the vessel wall, as a result of the mechanical stress to the material during the experimental heating and cooling [ROOS & MAILE 2005]. This would again reactivate and even intensify the corrosion rate [FLIETHMANN et al. 1992]. Consequently further release of steel metals to the sample solution is exited.

Input of contaminating elements comes also from the contact with the **metal wire mesh**, where the rock material is encased and which is also included in the blank samples. Like the autoclave containers, the wire mesh consists of stainless steel and a similar element contribution is extracted by the sample solution. However, a serious problem of those wire pockets is the **huge quantity of small corners, angles and wholes** that is evolving from the interlaced metal wire. Within these cavities and fissures, the formation of so called concentration or aeration cells takes place, which is a discrepancy of electrolyte- or oxygen-concentration between two parts of the mesh-surface caused by a constricted diffusion [BRIEHL 2008; ROOS & MAILE 2005]. In the case of oxygen, the more aerated part occurs outside the crevice, forming the local cathode, whereas the local anode forms at the less aerated part inside the crevice. Hence, a potential difference occurs between those surface parts, leading to oxidative dissolution of the metallic substance at the anode and reduction of oxygen at the cathode [BENEDIX 2008a].

Additionally to this crevice corrosion, interlacing of the metal wire may have lead to accumulated mechanical defects on the wire surface, which inhibits the formation of a passivation layer and thus provides further contact points where initial corrosion could start [BENEDIX 2008a].

In summary, the corrosion of the wire pockets is supposed to be the most important factor concerning the contamination of the sample solutions (oral information of Dipl.-Nat. M. Mandel, Department of Material Technology, TUBA Freiberg).

The corrosion of the wire pockets is also visible in form of a matt grey to black or a brownish colouring at the employed pockets.

A further source of contamination is potentially supplied via the metal wire cloth. Preparing the experiments, the cloth has been bend to small pockets (Figure 7e) at which

they has contact with tools like scissors and tongs, from which tiny particles in varying amounts could have been abraded and introduced into the sample solution.

A very strong impact on the chemical composition has the leaching out of the **solder**, which was used to affix a cover of wire mesh over the income of the pressure tube. This soldering was unfortunately not removed after testing this protection, thus a characteristic set of elements (most of all Pb, but also Cd, Zn, Al and Sn, see Figure 10 as well as section 4.2.1 and 4.2.2) denotes an extra input to the sample composition. For these elements the trend over the sequence of experiments mentioned above is particularly conspicuous (see Figure 12).

While the sample solution is inside the autoclave vessel, an amount of the already dissolved elements can **adsorb** to the vessel walls and to their oxide coating respectively. Thereby, the chemical composition of the sample solution is differently influenced depending on the degree the material was previously stressed and on the protective coating of each vessel.

During the experimental **shaking** or the concluding pressure release, it is possible, that sample solution attains inside the pressure tube. This small quantity of for example high mineralized sample solution is released at the next experiment run into a potentially low mineralized blank solution resulting in an impurity of the current sample. Only from the experiment run VIII on, not only the sample containers but also the feeding pressure pipes were cleaned carefully.

After the completed experiment, the samples were **filtered** in order to eliminate all suspended particles, caused by the abrasion of the rock material. On several filters a considerable quantity of deposition remained. It is not clarified, if these filter residues are solely abraded particles, precipitated minerals previously dissolved from the rock material, hardly soluble complexes or a combination of them all.

The partially extreme high concentrations of copper found in a lot of samples are presumably explained by a leaching process out of the **copper gasket**. This sealing is situated between the autoclave vessel and its cap, which are screwed tightly during the experiment. However, portions of the leaching fluid are suggested to intrude into fissures between sealing and cap, getting in contact with the copper and generating those high Cu-concentrations. If in general or to which extend this is happening depends on the fissure that is left within the sealing and can vary from vessel to vessel or from run to run. A dependency of the Cu-concentration in a sample from its treatment in a certain autoclave container could not be ascertained. This contamination affects samples as well as blanks

and is observed for all of the four autoclaves. For the reason that the Cu impact could not be deducted from the analysed overall amount, all Cu concentrations are considered to be potentially contaminated and thus, excluded in further data evaluations.

The **rock material** used for these experiments was sampled from the investigation area at sides below and above sea level (section 2.2.2). Anyhow, all rock samples have been in continuous or regular contact with seawater or at least sea spray and are already weathered to a varying degree. When grinding and weighing the rock material, care was taken that preferably only unweathered material was selected. Nevertheless, all of the weighed samples of rock material used for an experiment are subjected to inhomogeneities. These could also contribute to varying chemical concentrations of the samples.

All these aspects mentioned above, have a more or less strong contaminating influence on the chemical composition of a sample, causing inaccurate results of the leaching experiments and can be drawn on as explanation for the inconsistence of the resulting data. This is expressed by the overall very large inhomogeneity of the data, like for example the high standard deviations (of up to 100% or even more, see Table A.4.1, digital Appendix A.4) for the mean values of samples which have in fact undergone the same experiment conditions.

However, actually these contaminations should concern the samples with rock material in the same way than the blanks. But as already pointed out in section 4.2, the result of subtracting the blank from its related sample value shows nearly systematically negative values for (mainly) exactly those elements, which are ingredient of the alloys where the autoclave container, the wire pockets and the solder are made of. This can be assessed as an indication for the hypothesis that under the terms of conditions appearing inside an autoclave container, a noticeable larger amount of elements is leached from the equipment materials if no rock sample is included in the experiment. With other words, the availability of rock material in an experiment changes the chemism that is taking place inside an autoclave vessel and that attacks the equipment materials. In accordance with the **Nernst equation**, the standard electrode potential of a metal is depending on the concentration of its ions in solution in that way, that the lower the concentration of an electrolyte in solution, the more negative is the electrode potential and the greater the reductive power of the metal [BENEDIX 2008b; NICOLICS 2005] (for a more detailed calculation, see Appendix 4). This means, a smaller amount of a metal ions species causes a stronger corrosion of its solid metal.

This can be visualized as equilibrium between solution and metal phase: when the positive charged metal ions pass through the metal-water interface, electrons remain in the solid metal, changing the potential at the interface and (together with the remaining negative charged electrons) counteract the further pass of positive charging. On the other hand, the tendency is present that metal cations (or other oxidant) from the electrolyte solution are discharged at the negative metal surface while precipitating [BENEDIX 2008b]. As a result of these interactions a dynamic equilibrium is established at a defined equilibrium-potential which is dependent on both, the temperature and the concentration of metal-ions in solution [ROOS & MAILE 2005].

When comparing this to the present sample and blank solutions, it explains the fact that higher concentrations of the alloyed metals occur in the blanks rather than in the sample: in the samples including rock material, the high reductive power in the low mineralized starting solution is decelerated more rapidly due to additional dissolution of the specific metal from the rock material. In the blank samples in contrary, the mineralization increase much more slowly only by the corrosive dissolution from the alloy, allowing a more intense corrosion and thus leading to a higher final concentration.

The chemical composition of both, sample and blank solutions are believed to be a result of this fact.

As a consequence of this appearance, the conventional subtraction of the concentration values in the blanks from those in the samples cannot be implemented without changing the truthful concentrations. On the other hand also the actual concentration in the samples is incorrect, because of the supplemental corrosive dissolution from the alloys.

For further evaluation it was decided to use only the samples without blank-subtraction, for the reason that a calculation with negative concentrations is simply not meaningful. Anyhow, the fact of contaminated sample concentrations was always kept in mind during the following evaluations and discussions.

To sum up this discussion, it can be concluded, that the treatment in the autoclave vessels and especially the utilisation of the wire pockets is based on many critical facts that influence the leaching process and hence the chemical composition of the resulting sample solution. Therefore all data have to be considered with care.

For the evaluation of the chemical data, the author suggest to only examine the approximate order of magnitude of the concentrations for compensating the impact of all

sources of error as well as the differences between single samples of the same experimental conditions.

4.5.4 Recommendations - Rocking autoclaves for hydrothermal experiments

For performing hydrothermal leaching experiments, a system is needed that is able to withstand extreme conditions of temperature and pressure and furthermore is inert to corrosion for not influencing the chemical composition of the sample under investigation.
There exist two different facilities that have been used for such approaches, either a **pressure vessel with constant inner volume** or a **flexible reaction-cell system** [SEYFRIED et al. 1987]. The first one should preferably consist of austenitic stainless steel and can furthermore exhibit a lining of chromium, gold, titanium or Teflon®, which are all suitable for a distinct conditional range of temperature and pressure [BOUCIER & BARNES 1987]. The second one is constructed of an inner flexible reaction-cell embedded into an outlying pressure vessel of chromium-vanadium steel [SEYFRIED et al. 1979]. For the inner cell the three different materials gold, titanium and Teflon® have been used until now. Within this system, the fluid and solid reactants are enclosed in the reaction cell, chemically and physically separated from the outlying pressure vessel which contains the pressure fluid [SEYFRIED et al. 1987]. During the experimental run of the system, the pressure fluid inside the outer pressure vessel is pressurized transferring the compression to the inner reaction bag, which adjusts by deformation. Thus, the pressure can be regulated independently of the temperature and without the contact to the sample solution.
All these materials referred here are highly inert and provide a respectable corrosion resistance in a distinct range of temperature and pressure. Teflon for example is almost completely inert to NaCl-solutions and acidic solutions, but above a temperature of about 290°C it becomes weak and permeable and begins to dissociate forming among others toxic fluorine-compounds [SEYFRIED et al. 1987]. For higher temperature applications, a reaction cell of a gold-body in combination with a detachable titanium closure was developed [SEYFRIED et al. 1979], which is well performing in acidic (pH < 3) seawater solution and up to temperatures of 400°C and pressures of 500 bars [BISCHOFF & SEYFRIED 1978].
Both types of rocking autoclaves have another great advantage: they are equipped with an additional high-pressure tube besides the pressure capillary coming from the pressure

pump. Through this outlet, which is directly connected to the inner space of the reactive solution, samples can be withdrawn, regulated by a high-pressure valve. By the reason that the pressure pump works automatically, the inner pressure of the system can be maintained during the sampling process. Further explanations and discussions about the rocking autoclaves are given by [BOUCIER & BARNES 1987; SEYFRIED et al. 1987].

Hydrothermal experiments demand the application of extreme conditions in temperature and pressure and often leading to highly corrosive fluids. Thus, specific requirements need to be fulfilled by the experimental apparatus. The rocking autoclaves described above, well satisfy most of these requirements, at least to a limited conditional range.

Reviewing the experimental method used in this thesis, it can be concluded that in spite of their high costs, the application of a rocking autoclave type can explicitly be recommended in order to achieve uncontaminated and useful results.

4.6 Characterization of the Panarea water samples

During the diving excursions in May and September 2008, all together 20 water samples have been taken from exhalation points of the hydrothermal system of Panarea. Subsequently these samples were analysed regarding their chemical composition as well as their physicochemical parameters.

A detailed evaluation of the hydrothermal water samples is already done in the diploma thesis of Robert SIELAND [2009] and for this thesis only some relevant results are taken over from there.

Within all results, those of the sampling sites Black Point and Hot Lake differ strongly from the samples of other sites [SIELAND 2009] in the way of a much higher concentration for a lot of major, minor and trace elements as well as deviant values for the on-site parameters pH-value, electric conductivity and redox-potential. These significant differences were also confirmed by a statistical cluster analysis. The observed differences probably originate from an intense seawater dilution of all samples except those from Black Point and Hot Lake. These two samples were taken out of a drill holes, that have been drilled some 30-50 cm into the black stone (Black Point) and 2 m into the seafloor (Hot Lake). Hence, the sampled fluids are suggested to be relatively pure and uninfluenced by seawater dilution.

To compare the chemical composition of the hydrothermal fluids with those generated by the leaching experiments, a reference sample from both, the sampling sites Black Point and

Hot Lake was chosen. By mean of the criterion of a possibly low pH and high electrical conductivity, the two samples *PAN-030908-BP-W2* (from Black Point) and *PAN-080908-HL(80cm)-W4* (from Hot Lake) were chosen to have the highest purity being only barely diluted.

Both samples were characterized by high percentage enrichments for most of the measured elements (see Figure 17). The highest enrichment with nearly nine orders of magnitude above the seawater concentration occurs for the element Manganese. But also for most other elements the enrichments are of several orders of magnitude is present. Only the enrichment for Na, K, and Sb is below one order of magnitude and for Mg, Mo and U even a depletion of the sample concentration in comparison to normal seawater is observable.

Beside this general element ranges, a slight till strong concentration difference between the two samples also exists. For the elements Al, Zn, As, Pb, V, and Cd for example, this difference is even larger than one order of magnitude and the higher concentration of these elements always belongs to samples from Black Point.

Also for the major anions Cl^- and Br^- an enrichment for most components occurs by comparing their concentration in the two reference samples to those in normal seawater, whereas at the same time the major anions SO_4^{2-} and HCO_3^- are distinctly depleted in the water samples [SIELAND 2009].

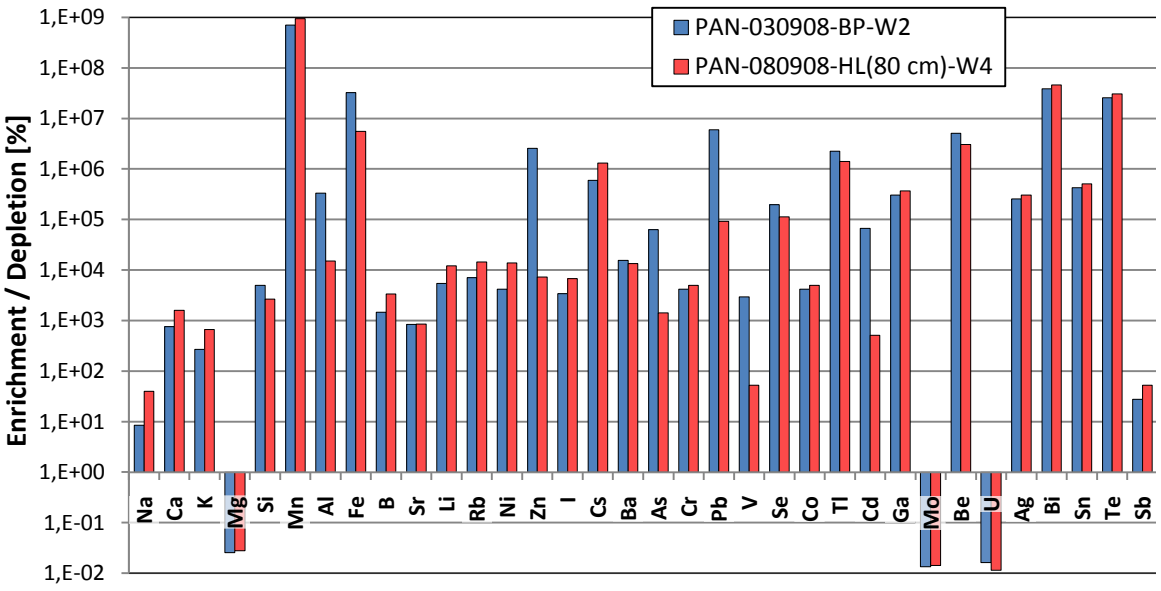

Figure 17: Percentaged enrichment or depletion for a selection of elements measured in the reference samples from Black Point and Hot Lake in relation to normal seawater [data from BROWN et al. 1995]. The calculation basis has been concentrations in µmol/L (see Appendix 2 and Appendix 3).

The measured on-site parameters for the two reference samples are shown in Table 4.

The **pH-value** measured in the reference sample of Black Point was 3.41 and for Hot Lake 4.85, which do also approximately represent the mean values for all water samples taken at these points [SIELAND 2009]. In comparison, the pH-value of normal seawater lies between 8.1-8.3 [BROWN et al. 1989].

For the **specific electric conductivity (EC)** of the hydrothermal reference samples, a value of 75.3 mS/cm for Black Point and 98.6 mS/cm for Hot Lake was measured. The conductivity of normal seawater lies in a range of 45-55 mS/cm [HÖLTING & COLDEWEY 2005], but the local seawater near Panarea is reported to be about 54.0 mS/cm [GUGLIANDOLO et al. 2006]. This means a noticeable higher mineralization of the hydrothermal samples compared to the surrounding seawater due to the interaction of the ascending fluid with the bedrock material and eventually further impact of hydrothermal processes (see section 4.10.3 and 4.11).

Table 4: Results of the on-site Parameters for the Black Point (BP) and Hot Lake (HL) reference sample. Ehm means the original measurements in the field laboratory; Eh25°C are the corrected redox values, regarding to 25°C temperature and the standard hydrogen electrode potential; rH is an indicator for the redox power of a system independent from the prevailing pH value

	pH	EC [mS/cm]	Eh_m [mV]	$Eh_{25°C}$ [mV]	rH [mV]	T [°C]
PAN-030908-BP-W2	3.41	75.3	55	261.4	15.7	26.1
PAN-080908-HL(80 cm)-W4	4.85	98.6	-260	-53.7	7.9	29.2

The water sample from Black Point has a measured **rodox potential** of 260.7 mV which indicates partly reducing conditions, whereas in the sample from Hot Lake with a measured redox potential of -56.7 mV reducing conditions are dominant. The seawater in comparison is normally an oxidizing medium with redox potential of about 800 mV [BROWN et al. 1989].

4.7 Experiments in the Autoclave

Following the pre-test and the time series the actual experiments with the four different rock materials sampled at Panarea were performed in the autoclaves. On the basis of the time series, an experimental duration of 24 hours was chosen for these dissolution experiments.

Because of a blank sample has been included in every run, the altogether six samples (four rock materials and two blanks) had to be divided to the four autoclave vessels implementing two experiment runs (*series VIII* and *XI*). But at the same time, this provides the advantage of attaining a double determination of two rock samples (*R3, R4*).

The results of a first cluster analysis[3] highlighted the strong contaminating influence of the solder material to all samples which were treated inside the soldered autoclave vessel (see section 4.2.1 and section 4.3). It was tried to quantify the contamination using the blank samples and to calculate back to the true concentration (section 4.2.2) but the subtraction failed due to the characteristic of the corrosion process (section 4.5). Based on this results it was decided to exclude all samples with solder-contact from further evaluation. Unfortunately, exactly those rock materials with a single-examination have been performed inside the soldered vessel (*R1, R2*). Hence, a further experiment with those rock materials had to be run (*series XII*).

Finally, for all rock samples despite of *R1*, duplicates in experiment and measurement were available of which the respective mean value was calculated. By reason of the diverse and intense sources of error (section 4.5) also in this case high standard deviations of up to 100% between both related samples occur for several element concentrations (see Table B.2.1 in the digital Appendix B.2).

Due to the immense impact of the experimental procedure (mainly the corrosion of the equipment alloys) and as already mentioned in the discussion of the method, the resulting chemical data of all samples are such diverse, that the evaluation is focused on the rough orders of magnitude whereas the detailed differences between different samples and single elements should be ignored.

The chemical composition of the autoclave rock leaching experiments is graphically presented in Figure 18.

[3] This first cluster analysis is not presented in this thesis, because its result advised to accomplish a further experiment run whose chemical data were certainly not part of this first calculation. Hence, the cluster analysis was repeated including the data of the additional samples. Their results are presented in section 4.3. Nevertheless, the conclusions concerning the solder-contamination have been the same in both calculations.

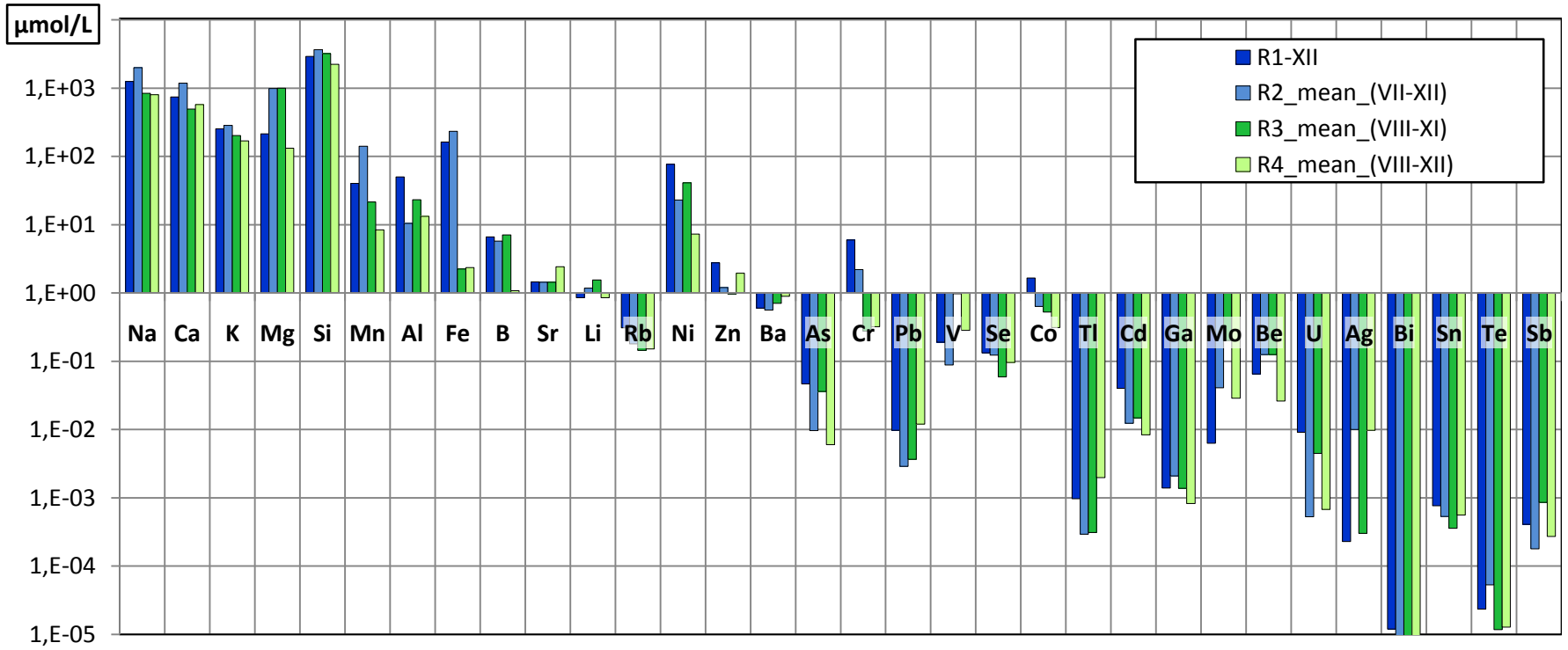

Figure 18: Comparison of the concentrations leached from the four different rock samples during the autoclave experiments. The concentrations are given in µmol/L on a logarithmic scale. For the rock samples R2, R3, and R4, the concentrations are mean values of two samples from different experiment runs.

Examining the approximate magnitudes of the concentrations in the diagram, they appear to be quite similar for all of the four rock samples. This may be an indication, that the four rock materials, which do indeed originate from different rock types, have an overall similar composition of minerals. The leaching process at elevated temperature and pressure conditions should lead to dissolution of the same minerals (if present in the rock sample) according to their solubility constants. Anyhow, the reason for slightly different concentrations might be both, the different constitution of the four kinds of rock or the contaminating interference of the experiment system.
Another factor is the varying alteration state of the rocks that could affect the concentration in the final leaching fluid (for example).
Particularly striking is the extremely different concentration of iron, which accounts for two orders of magnitude between the rock samples *R1*, *R2* (163 µmol/L and 232 µmol/L, respectively) compared with those in the rock samples *R3*, *R4* (2.24 µmol/L and 2.36 µmol/L). This variation seems to be a characteristic of the respective rock material, because it appears to a lesser extent also in the results of the rotation experiments (see section 4.8 as well as Appendix 8 and Appendix 9).

4.8 Experiments in the Overhead rotator

Because no NaCl-solution could be used as leaching fluid for the autoclave experiments (due to the high risk of corrosion damage, compare section 4.5), dissolution experiments were carried out in an overhead rotator at normal temperature and pressure conditions. For these experiments the four rock materials were used together with a 0.5 molar NaCl-solution representing the seawater (*sample series IX*). For comparing the effect of the salinity on the dissolution of the rocks, in a second experiment also deionised water was used as leaching fluid (*sample series X*). Both fluids were previously aerated with CO_2 similarly to all other experiments. In these experiments, the rock granules were applied loosely, that means without an encasement of metal wire mesh.
The chemical composition of the resulting solutions shows, that no clear distinction between the dissolution capacity of NaCl-solution and deionised water under the applied conditions takes place (see Appendix 8 and Appendix 9 and Tables in the digital Appendix B.3). Differences do occur indeed, but without a clear dependency on the salinity; for some elements the concentration in the NaCl-solution is higher and for other elements the concentration in deionised water. Furthermore, this elemental appearance is not similar for

all rock samples. Only for the elements Rb, Pb, Ga, and Ag the results depict a clearly enhanced dissolution in NaCl-solution for all rock samples.

According to the cluster analysis which is performed on the basis of the chemical data (section 4.4), there exists a significant distinction between the samples realized with H_2O or NaCl. The samples in H_2O are grouped together with the other rotation samples (time series) and some blanks, whereas the samples in NaCl-solution form an individual class on their own which is presumably reasoned by their extremely high concentrations in Na^+ and Cl^- (not detected but calculated) as well as the resulting high electric conductivity.
Thus, the classification indicates a characteristic peculiarity of the NaCl-samples but mainly caused by the mentioned parameters.
Looking at the amounts of iron found in the rotation samples, the strong concentrations differences of about two orders of magnitude between the rock materials *R1, R2* (about 60 µmol/L) and *R3, R4* (about 0.2 µmol/L) become obvious. Such high differences were already observed for the iron concentration in the autoclave samples (section 0) and further verify the assumption that this might be due to characteristic content of different iron minerals in the four rock materials.

However, looking at the overall distribution of elements, they seem to be more or less equal in all samples. Differences are probably induced by the characteristics of the single rocks, as well as inhomogeneous element distributions within the rock material due to the naturally occurring variances. The latter one is particularly valid for the minor and trace element.

4.9 Efficiency of the leaching experiments - Comparison of the experimental samples and the total digestions

For evaluating the efficiency of the leaching experiments, the element concentrations in the resulting fluid is compared to their respective amount in the rock material, determined by the total digestions. Since the extraction experiments were conducted with 2g rock material in 75ml deionised water whereas for the total digestion only 0.1g in a final volume of 50ml were used, both concentrations have to be referred to the same amount of rock material for allowing a quantitative comparison. At first, all concentrations were converted to a **[µg/g]-mass ratio** calculating the ratio of µg element per g rock material (see digital

Appendix B.4, Table B.4.1 and Table B.4.2). The percentages of the effectively leached amounts in relation to those potentially provided by the rock material were calculated and are presented in Figure 19 a-d.

Representatively for all four efficiency diagrams, the one presenting the data of rock sample R1 should now be contemplated in more detail. In a basic overview, the general trend of elemental concentration is similar in all three leaching experiments, representing an individual and characteristic composition of the rock material. Thereby, the autoclave samples in comparison to the rotation samples show clearly higher amounts for most of the elements, which denotes the higher leaching capacity of solution at elevated temperature and pressure conditions. Only for Al, Zn, Pb, U and Ag, the autoclave values are equal or even lower than the rotation values. The deviant curve progressions between the three experimental results may have varied reasons: most important as mentioned above, the different experiment conditions like temperature, pressure and leaching solution (including pH-value and redox potential), which determine the solubility of each mineral phases.

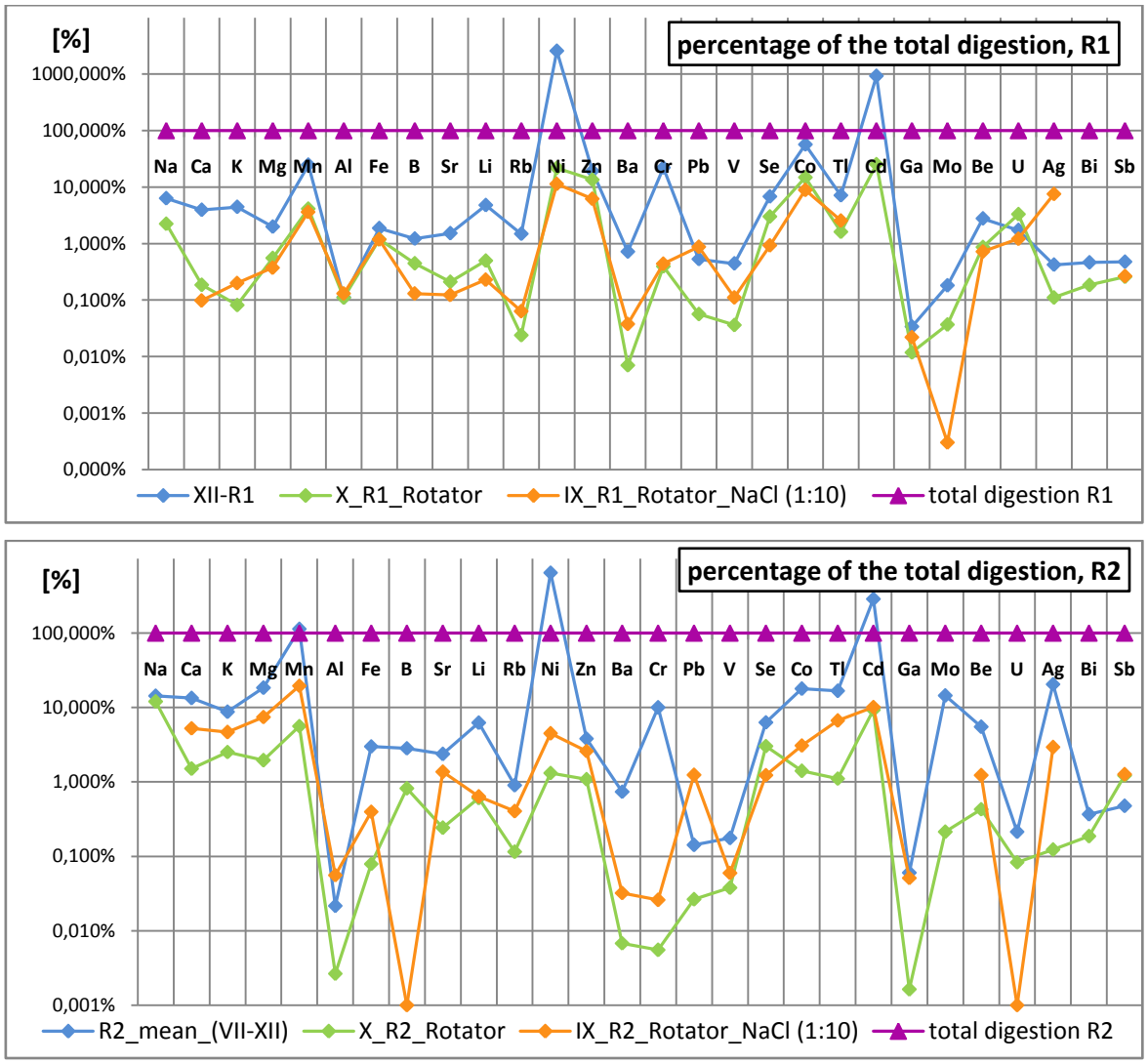

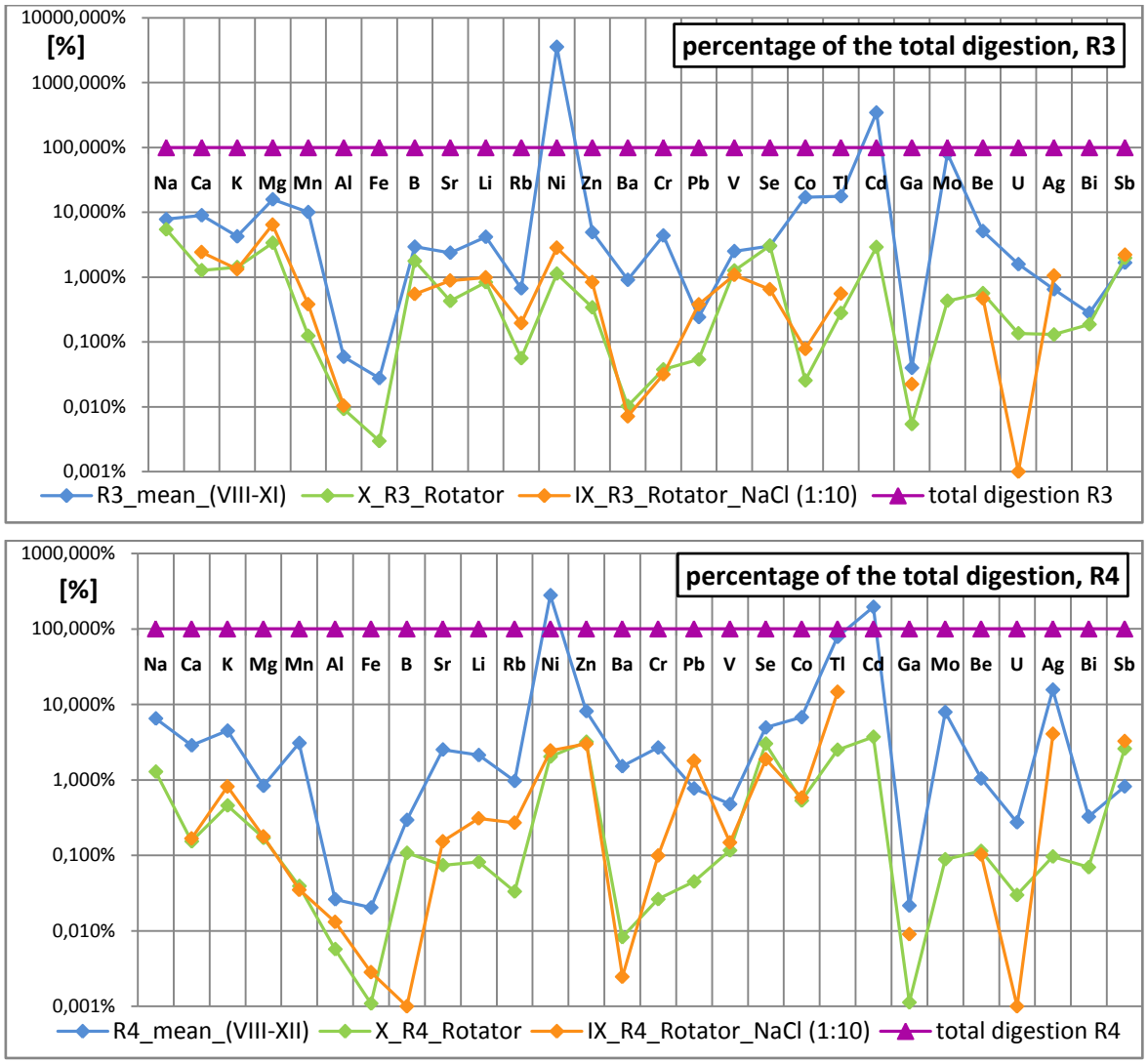

Figure 19: Extraction efficiency [%] achieved during the leaching experiments in autoclave and overhead rotator. The data represent the respective concentration of species released into solution (during the different extraction experiments) in relation to their amount in the starting rock sample. These relations are separately depicted for each rock material (Figure 19a: R1, 19b: R2, 19c: R3, 19d: R4). Note: the connecting line between the samples does not indicate a correlation between the single elements, but should clarify the data points belonging to one sample

Furthermore, inhomogeneities within the rock granules affect the extracted element amounts likewise as the inaccuracies of the measurement by ICP-MS (which can be up to 20%). The amount of species dissolved during the autoclave experiments could also be impacted by contamination caused by corrosive processes as already mentioned earlier (e.g. in section 4.5).

The extraction efficiency for most of the elements and under the applied experiment conditions lies in a range of 0.1-10% or even lower. For R1, only 6 of 36 elements (Mn, Ni, Zn, Cr, Co and Cd) reached efficiency of more than 10% and this only in the autoclave experiment. Furthermore, these elements are all constituent of the system alloys which

suggests that some additional dissolved proportions has arisen from there. This explanation is confirmed by the measured amounts of Ni and Cd in the autoclave samples, which exceed their respective amounts found in the total digestion and leading to the conclusion that a supplemental source must have been present.

4.10 Results of the leaching experiments in the context of general hydrothermal water-rock-interactions and processes

4.10.1 Physico-chemical conditions inside the autoclave

The physico-chemical conditions that adjust inside the autoclaves during the leaching experiments are affected by several interacting factors.
The pressure of 250 bars and the temperature of 150°C are externally adjusted and remain constant over the entire experiment duration.
The **pressure** itself has nearly no influence on the kind of chemical reactions [FLIETHMANN et al. 1992], but has a strong indirect impact. As defined by Henry's law, the concentration of a gaseous species (here particularly CO_2) in the leaching solution is defined by its partial pressure in the gas phase (and eventually consecutive reactions) at a constant temperature [RIEDEL 2008]. The influence of pressure changes on the solubility of solids (mineral phases) only becomes effective for a pressure > 50 bar [MERKEL & PLANER-FRIEDRICH 2002]. Moreover, high pressures can lead to mechanical degradation of mineral structures.

The **temperature** is thought to be a parameter of strong effectiveness for the dissolution of minerals. Temperatures occurring within a hydrothermal system are typically > 300°C [HERZIG & HANNINGTON 2006]. For water in liquid phase, these temperatures can only be reached when the system is pressurised. If the mineral solubility is increased or decreased under a temperature rise, depends on if the chemical reaction is endothermic or exothermic. The dissolution of silicates, sulphides and oxides, for example, are endothermic reactions and thus are enhanced under heat supply, whereas carbonates and sulphates release heat when dissolving and thus additional heat decelerate the dissolution reaction [MERKEL & PLANER-FRIEDRICH 2002].

The **pH value** is considered to be a master variable in chemical systems, controlling chemical reactions and equilibrium distribution of species [DOMENICO & SCHWARTZ 1998]. Especially the dissolution of metals extremely depends on the pH in the way of a higher metal mobility in acidic solution [MERKEL & PLANER-FRIEDRICH 2002].
In the leaching fluid a slightly acidic pH of ~ 4.4 (Table 5) is initially defined through the previous aeration with CO_2 at which the amount of dissolved CO_2 is controlled by its

partial pressure and the consecutive reaction to carbonic acid [MERKEL & PLANER-FRIEDRICH 2002].

In the course of the leaching experiment, this initial pH value is mainly affected by reactions of mineral dissolution from the rock material together with complexation, where metal-carbonates or metal-hydrocarbonates are formed. Eventually also mineral precipitation takes place (predominately during the cooling phase and pressure release), that can have an impact on pH. Furthermore the electrochemical corrosion reactions can influence the pH inside the autoclaves, as the products of corrosion (such as $FeCO_3$, FeOOH...) have a buffering effect on the solution or acid is consumed under the corrosion process [BRIEHL 2008; FLIETHMANN et al. 1992].

Table 5: Electrical conductivity (EC) and pH value of the experimental leaching samples as well as for deoinised water. All solutions have previously been aerated with CO_2

	Sample lable	EC [µS/cm]	pH
Autoclave	*VIII-Blank*	*88.80*	*4.79*
	VIII_R1 (s + p)	284.00	5.07
	VIII_R3	377.00	5.48
	VIII_R4	281.00	5.18
	XI-Blank	*54.20*	*4.40*
	XI_R2 (s + p)	492.00	5.34
	XI_R3	382.00	5.48
	XII_Blank (s + p)	*55.30*	*4.46*
	XII-R1	554.00	4.75
	XII-R2	453.00	5.33
	XII-R4	215.00	5.17
	H2O dest	*0.07*	*4.40*
Rotation	X_R1_Rotator	165.60	3.93
	X_R2_Rotator	245.00	4.63
	X_R3_Rotator	120.00	4.94
	X_R4_Rotator	50.20	4.34
	NaCl-Solution (1:10)	44500	5.60
	IX_R1_Rotator_NaCl (1:10)	45200	3.99
	IX_R2_Rotator_NaCl (1:10)	45000	4.31
	IX_R3_Rotator_NaCl (1:10)	45300	4.76
	IX_R4_Rotator_NaCl (1:10)	44900	4.05

The exact pH inside the autoclave at which the leaching took place could not be determined because no "online"-sampling during the experiment was possible. Only after the system was shut down the leaching samples could be withdrawn and the pH could be measured. This offered pH values around 5.2 (± 0.3) which is at least higher than the initial pH of 4.4 (Table 5). This validates the supposed process of acid consumption inside the

autoclave during water-rock (and -alloy) interaction. Further evidence is given through the autoclave blanks and the rotation samples, which all have a slightly lower pH (around 4.5) than their related autoclave sample, due to an overall lesser exchange with rock material or alloy (compare Table 5). Also in the samples of the rotation time series, a successive increase of pH in accordance with longer durations is present.

Beside its partial pressure dependency, the **CO_2-solubility** is furthermore strongly dependant on the temperature in the way of decreasing solubility with increasing temperature. Thus, the dissolution of CO_2 in the leaching fluid during the autoclave experiments is on the one hand lowered by the high temperature but simultaneously enhanced by the increasing partial pressure caused by the pressurisation with gaseous CO_2.
Executing thermodynamic experiments and simulations of the binary system CO_2-H_2O it was found that the solubility of CO_2 in water at low pressures (<100 bar) gradually decrease with increasing temperature, but at higher pressures (>100 bar), the solubility first decreases with temperature and then increases again with further temperature rise, describing a kind of parabolic curve [DUAN & SUN 2003; SPYCHER & PRUESS ; TAKENOUCHI & KENNEDY 1964]. Thereby the respective minimum solubility is again depending on the combination of temperature and pressure values. Examining a 150°C isothermal curve for example, the minimum solubility is related to a pressure of ~180 bar [TAKENOUCHI & KENNEDY 1964]. Comparing this to the experiments performed here, it means that during pressurisation of the autoclaves at 150°C, the CO_2 solubility first increases until 180 bar und than again decreases with higher pressures. At the experimental t-p-conditions applied in this thesis (150°C, 250 bar), a solubility of ~1.28 mol CO_2/ kg water is given by DUAN & SUN [2003].
Because the sample-filled autoclave vessels contained a remaining volume of air (~25%) as they were closed and pressurised, the gas phase do not only consists of pure CO_2 and water vapour but also small amounts of the other atmospheric components (O_2, N_2, Ar). Compared to the added 249 bar of CO_2 pressure, these amounts of other gases are supposed to be negligible.

4.10.2 Comparison of the experimental samples and the Panarea reference samples

In this section, a comparison should be drawn between the experimental hydrothermal samples achieved from the leaching simulations, the Panarea-reference fluids from the two diving sites Black Point and Hot Lake and general processes taking place during hydrothermal water-rock-interactions.
Doing so, the measured concentrations are considered to be purely leached from the rock material, disregarding all sources of contamination, discussed previously (section 4.5).

In the diagrams of Figure 20, the concentrations attained by experimental leaching at 150°C and 250 bars pressure are compared to those that have been found in the Panarea hydrothermal water samples. The Panarea samples consist of seawater that has been hydrothermally modified, whereas the experiments have been carried out with deionised water. Hence, the experimental samples have been adapted to the seawater characteristic by adding the respective element concentration of typical seawater (taken from BROWN et al [1995], compare Appendix 3).
Regarding the graphs (Figure 20), it has to be considered, that the amount of leaching fluid used for the experiments is somewhat arbitrary. Thus, the concentrations in both sample types (experiment and Panarea) potentially refer to different amounts of solvent and are not quantitatively comparable. Only the relations of element distribution instead of the total amounts could be compared between both sample types.
For the major elements (Figure 20a) the previous slightly differences between the four experiment samples are equalized by the addition of seawater concentrations for all elements (except of Mn, Al, and Fe). This means, that the concentration of the respective element is dominated by its amount in the seawater (where they are present in mg/L or g/L-concentrations (compare Appendix 3) and the contribution in mg/L till µg/L-range by the rock-leaching (Table B.2.1) is marginal. In contrast, the concentrations of Mn, Al and Fe in seawater are in a µg/L-range and hence, the contribution by the rock-leaching is more dominant.
Comparing the experiment samples to those from Panarea, the concentrations of Na, Mg, Si, and fractional also Fe match very well, whereas for all other major elements there is a significant lack of concentration in the experimental samples.

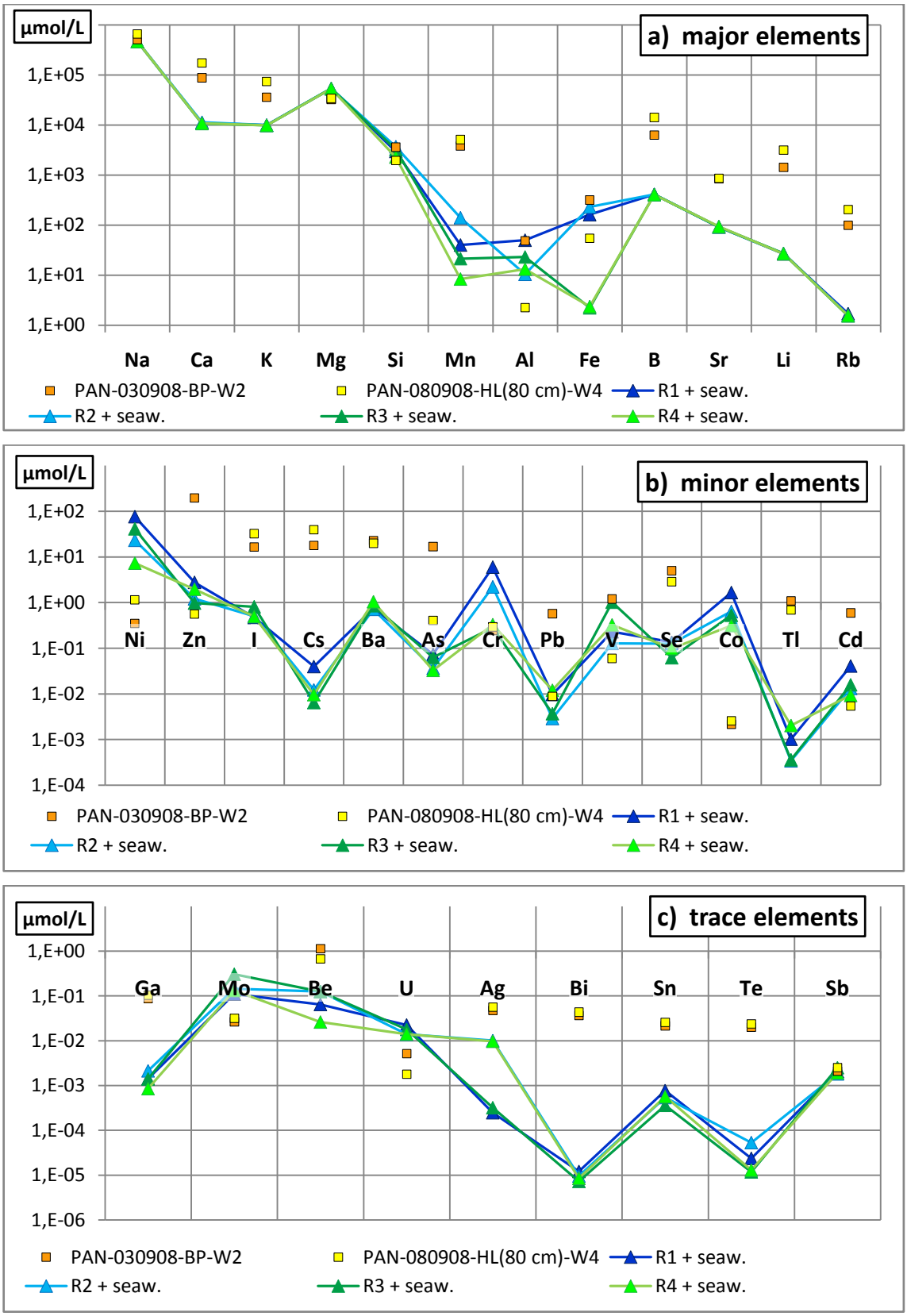

Figure 20: Comparison of the experimentally performed leaching samples and the Panarea reference samples, separated after (a) major, (b) minor and (c) trace elements. To the experimental concentrations a standard seawater composition (from BROWN et al [1995]) has been added. The concentrations are given in µmol/L on a logarithmic scale. Note: the connecting line between the samples does not indicate a correlation between the single elements, but should clarify the data points belonging to one sample

For the minor elements (Figure 20.b), the addition of seawater has only a slight influence on the total concentration due to an amount of only µg/L in seawater (Appendix 3) and the experimental concentrations for each element are more diverse. Similar to the major elements, there is a significant lack of concentration in the experimental samples for most of the minor elements. Different appearance in contrast is exhibited by the elements Ni, Cr, V, and Co, whose concentrations are similar to or even exceed the concentrations of the Panarea samples. This expresses the additional elemental input of the system alloys during experimental treatment.

Another distinction has to be made between the reference sample from Black Point and Hot Lake, which show extreme differences for the elements Zn, As, Pb, V and Cd (and also Al in Figure 20.a), in the way of a much higher concentration always found in the sample from Black Point. It occurs for Zn, As, Pb and Cd that the experimental samples matches quite well the lower concentrations of Hot Lake, but are still in strong discrepancy to the Black Point fluid. For Al and V, the experimental concentrations lie between those of Hot Lake and Black Point.

The comparison of the trace elements (Figure 20.c) shows a similar appearance like the minor elements in the way of a slightly influencing contribution by the seawater addition and a significant lack of concentration in the experimental samples. Only for Mo and U, the experimental concentration exceeds those in the Panarea fluids, which is explainable by the fact, that Mo and U have been depleted in the hydrothermal fluids from Panarea compared to standard seawater (see Figure 17). Thus, the additions of seawater-concentrations to the experimental ones must lead to these exceeded concentrations. Mo is moreover a constituent of the applied alloys and can be extracted from the system.

Regarding this comparative graphs in Figure 20, further aspects have to be taken into account. In general, for most of the elements there exists a moderate to huge concentration deficiency in the experimental samples, compared to the natural hydrothermal fluids from Panarea. That means that additional processes or different conditions than those simulated in the autoclave must have affected the Panarea samples. Such aspects could be higher temperatures in the region of fluid generation and water-rock interaction, a more acidic pH, the ratio between water and rock material as well as phase separation during ascend of the fluids to the seafloor. They are all dedicated to fluid generation in hydrothermal systems and are described in detail in the following section (4.10.3).

Hypothesising now, these processes would result in higher concentrations such that the lacking concentrations were approximated to the naturals, but maintaining the relation between all elements, this would lead to an overestimation of those elements, that are now already in agreement with the natural amounts (Na, Mg, Si, Al, (Fe); compare Figure 20 (elements clearly originating from the system alloys have been disregarded)).

But these hypothesised overestimations are explainable by processes occurring in natural hydrothermal systems which would result in a (relative) loss of these elements (except of Fe, because the too high concentrations are most likely cause by leaching of the system alloys).

Mg is quantitatively removed from seawater during hydrothermal water-rock interaction, which will be described in the following section (4.10.3).

Concerning the major cations Na, K, Ca, their concentration in solution of high-temperature systems is influenced by temperature-dependent ion exchange reaction between co-existing alkali feldspars according to the reaction

$$\text{Na-feldspar} + K^{+}_{(aq)} \rightarrow \text{K-feldspar} + Na^{+}_{(aq)}$$ [NICHOLSON 1993].

Using the approach of the so called “geothermometers”, the ratio of Na/K concentration can be applied as indicator for the temperature that has been prevalent during the respective Na/K adjustment. Thereby, the lower the ratio, the higher the temperature [CAN 2002], which means, that the amount of K leached from the rock is much higher in relation to Na leaching. A similar behaviour is found for the ratio of Na/Ca in the temperature range of 200-400°C [MOTTL & HOLLAND 1978]. Consequently it can be recorded, that by mean of high-temperature water-rock reactions within a geothermal system, the concentrations of Ca and K are enriched relative to Na, explaining why the hypothesised overestimation of the experimental samples does not occur in natural systems.

The solubility of any silica mineral (SiO_2) in solution is highly dependent on temperature: at low temperatures in the way of a better solubility with increasing temperature, but at higher temperatures firstly quartz is going to precipitate due to supersaturation (e.g. the maximum solubility of quartz at 340°C is 27.5 mmol/kg) [MOTTL & HOLLAND 1978; NICHOLSON 1993].

The behaviour of these major elements under hydrothermal conditions can be seen as an example for the complexity of high-temperature water-rock interactions, that may be determine by temperature-, pressure- and also salinity-dependent dissolution equilibria.

4.10.3 Hydrothermal water-rock-interactions – the leaching of rock material

The characteristic processes, going on in a typical hydrothermal system for example at mid-oceanic ridges or related to subduction zones, are investigated by many scientists, both in-situ and experimentally [e.g. DANDO et al. 1999; HERZIG & HANNINGTON 2006; SEYFRIED & BISCHOFF 1981; SEYFRIED et al. 1991].

A volcanically active region evolves at the seafloor through heating by an underlying magma chamber or magma intrusion that arose from the mantel to the lower crust. Seawater is thought to penetrate deeply into this reaction zone through fractures and fissures, and thereby is converted into a metal-bearing hydrothermal fluid by intensive heating and water- rock exchanging reactions [HERZIG & HANNINGTON 2006; NICHOLSON 1993]. The major changes in chemical and physical conditions of these fluids include increasing temperature, decreasing pH and decreasing E_h [HERZIG & HANNINGTON 2006].

With rising temperatures the seawater becomes more and more dissociated into H^+ and OH^-. Concomitantly, the Mg^{2+}-ions, dissolved in the circulating seawater combine with these emerging OH^--ions forming $Mg(OH)_2$. During water-rock interaction, this mineral phase is further incorporated into alteration products such as smectite ($T \leq 200°C$) and smectite-chlorite ($T \geq 200°C$) [SEYFRIED JR & MOTTL 1982] which leads to a quantitative removal of both, Mg^{2+} and OH^-. The result is an excess of H^+ and thus a massive drop in pH value from 7.8 (normal seawater at 2 °C) to as low as pH 3 in minimum [HERZIG & HANNINGTON 2006; SEYFRIED & BISCHOFF 1977]. An initial buffering of this pH-depression is provided by exchange-reactions between silicates of the host rock and the hydrothermal fluid, at which H^+ is consumed in exchange for Ca^{2+} and K^+ that are released into solution [NICHOLSON 1993]. At higher temperatures (>150°C) Ca^{2+}-ions together with SO_4^{2-}-ions precipitate as anhydrite, contributing to both, further decrease of pH as well as quantitative removal of seawater sulphate [SEYFRIED & BISCHOFF 1977]. Reductive redox conditions are generated mainly by the oxidation of Fe^{2+} to Fe^{3+} in basalts as well as reaction of igneous pyrrhotite (FeS) in secondary pyrite (FeS_2) [HERZIG & HANNINGTON 2006].

In summary, by these processes the seawater turns into a hot acidic and hence highly reactive hydrothermal fluid, being capable of intensively leaching metals from the rock basement.

The result of such hydrothermal water-rock-interaction in general is enrichment in Ca, K, Na and many minor and trace elements (such as Al, Li, Rb, Ba, Fe, Mn, Cu, Zn, Si...

[HERZIG & HANNINGTON 2006; MILLERO 2006]) together with a depletion in Mg and SO_4. The element composition that adjusts in the hydrothermal fluid is initially controlled by water-rock interactions and thus is dependent on the mineral assemblage in the rock basement. When ascending towards the seafloor, the fluid composition is further modified as a result of cooling, mixing with fresh seawater or eventually phase separation processes.
The two reference samples from the Panarea hydrothermal system are considered to have undergone the processes described above, showing characteristic depletion of magnesium and sulphate, enrichment of many minor and trace elements (Figure 17; Appendix 2) together with a low pH and reducing (HL) or partly reducing (BP) redox conditions (Table 4).

Lots of experiments have been carried out on hydrothermal water-rock interactions, where magmatic rock material was reacted with seawater under a broad range of elevated temperature and pressure conditions [e.g. BISCHOFF & ROSENBAUER 1996; ELLIS & MAHON 1964; MOTTL & HOLLAND 1978; MOTTL et al. 1979; SEYFRIED JR et al. 1998; SEYFRIED & BISCHOFF 1977]. By these experiments, the main hydrothermal reactions could be induced and "typical" hydrothermal fluids were gained, that well agreed with natural hydrothermal samples. During experimental simulation of hydrothermal conditions, further details of the mechanisms of hydrothermal water-rock interactions turned out, like for example the importance of the water-to-rock ratio, which means the flux of water in relation to the amount of rock that is encountered and altered [SEYFRIED & BISCHOFF 1981].

If the **water-rock ratio** is low (≤ 10), the system is chemically dominated by the rock, which is expressed initially by a rapid loss in OH^- due to incorporation of magnesium-hydroxide into the alteration phase of the rock [SEYFRIED & BISCHOFF 1977]. Under these hot and acidic conditions, effective dissolution from the rock takes place. Subsequently, however, the pH rise again, when Mg removal has completed but further input of OH^- is provided by silicate hydrolysis. As a consequence of the rising pH re-precipitation of the previously leached metals into the alteration phase is induced.
Under high water-rock ratios (≥ 50), the water dominates the system, providing an excess of available Mg, such that the rock can completely turn over into alteration phase, assimilating as much $Mg(OH)_2$ as needed [SEYFRIED & BISCHOFF 1977]. By this, quasi-equilibrium adjusts between the Mg reservoir and the alteration phase, maintaining a

slightly acidic pH and thus driving continued metal dissolution from surrounding rocks, which leads to highly mineralised hydrothermal fluids.
The Panarea hydrothermal system is characterized by both a high water-rock ratio and high rate of water circulating at depth [ITALIANO & NUCCIO 1991].

The heated water tends to ascend towards the seafloor due to buoyancy caused by thermal expansion. Depending on the temperature and pressure conditions inside the reaction zone of a hydrothermal system, the ascending fluids may reach boiling point due to reduced hydrostatic pressure. On boiling, gases including water vapour and other volatile species partition into the vapour phase and can roam independently of the residual liquid phase [NICHOLSON 1993]. The remaining water phase receives proportional increase in concentration of dissolved constituents. This process is called **phase separation** and results in the formation of a low-saline vapour phase and a residual high-saline liquid phase (brine). Hence, phase separation is a further important process beside water-rock interaction that determines the composition of a hydrothermal fluid. Phase separation is more likely to occur under high ascending flow rates, where adiabatic cooling of the fluid can be considered, whereas under slow movement, the fluid may have sufficient time to lose heat by conduction to cooler the host rock [NICHOLSON 1993]. Cooling then owes to the process of evaporation and separation of the volatile species.
Phase separation is accepted to be the primary mechanism of causing large variations (> ±10%) of chloride content in seafloor hydrothermal systems compared to ambient seawater [VON DAMM et al. 1997]. This is due to only a slight contribution of Cl resulting from water-rock interactions, whereas the major input is provided by the seawater content. Hence higher Cl-concentrations in relation to seawater must be a result of concentration processes like phase separation.
For the reason that Cl means the major complexing anion in hydrothermal fluids [HERZIG & HANNINGTON 2006], phase separation is observed to lead to significant increase in dissolved trace metals in solution due to the formation of metal-chloride complexes [BISCHOFF & ROSENBAUER 1987].
The Panarea reference samples from Black Point and Hot Lake show strong enrichment in chloride of 118% (BP) and 46% (HL) compared to normal seawater [SIELAND 2009] and consequently are suggested to have undergone phase separation during ascension from the reaction zone to the seafloor. Moreover, the high circulation rates of seawater though the

system that is declared by Italiano & Nuccio [1991] leads to the assumption that phase separation is likely to take place at Panarea.

When contrasting the rock leaching experiments that have been carried out for this thesis with the natural reference samples from Panarea (section 4.10.2), several aspects concerning hydrothermal processes have to be taken into account:

First of all, the leaching experiments have been accomplished with only deionised water instead of **seawater** due to the risk of severe damage on the equipment caused by chloride-induced corrosion (compare section 4.5). Deionised water denotes a lack of magnesium in solution, comparable with the situation under rock-dominated conditions. Hence, the extreme drop in pH caused by precipitation of $Mg(OH)_2$-silicates occurring in natural systems is impeded although the applied water-to-rock ratio of 37.5 is moderate indicating rather water dominated conditions.

Under the experimental conditions, the **pH** is initially determined by the previous aeration with CO_2, adjusting at about pH 4.4 (section 4.10.1). During the leaching process, the dissolution of silicate minerals frees OH^--ions that slightly raise the pH to maximal pH 5.48 (Table 5). For the reason that – in contrast to seawater – neither magnesium nor sulphur (as sulphate) is provided by the leaching fluid, these elements only originate from the rock material and are not supersaturated and precipitated as consequence of water-rock interaction as it would be typical for hydrothermal systems. The sulphur emanating from the rock contributes to the solution composition in form of reduces sulphur (S^{2-}) [HERZIG & HANNINGTON 2006].

The **temperature** in natural hydrothermal systems is thought to have a major impact on the leaching capacity of entering seawater [NICHOLSON 1993; SEEWALD & SEYFRIED 1990; SEYFRIED & BISCHOFF 1979], mostly due to its provoke of dissociation and concomitant loss of OH^- into alteration minerals as discussed previously, but also by accelerating endothermic dissolution reactions like dissolution of silicates, sulphides and oxides [MERKEL & PLANER-FRIEDRICH 2002].

It is presumed that the experimental leaching would have been more intensive and effective under higher temperatures of ~300-400°C instead of the applied 150°C. However, this may be particular effective for systems containing seawater as fluid for water-rock interaction.

Moreover it is considered to be likely, that natural thermal waters, evolving at high temperatures (> 250°C) could be generated under moderate temperatures (e.g. 150°C), if

only the reaction time for water-rock interaction is exceeded sufficiently such that all volcanic rock can make over to alteration minerals or that equilibrium is established between rock, leaching fluid and alteration phase [ELLIS & MAHON 1964]. Such assumption is only valid for solubility equilibriums that are independently of temperature.

Aside from the need of seawater to react with the rock in simulating submarine hydrothermal water-rock interaction, the experimental samples with a **reaction time** of 24h are far from being in steady state conditions. Those are declared to may take some thousands of hours reaction duration [BISCHOFF & DICKSON 1975; GHIARA et al. 1993; MOTTL & HOLLAND 1978]. Both aspects (no seawater for buffering the low pH together with short reaction time), lead to a relatively ineffective leaching under experimental conditions compared to those that are supposed to elapse in the natural system (as discussed previously in this section). Nevertheless, when hypothesising extremely fast flow rates inside the hydrothermal reaction zone of Panarea (like it is suggested by ITALIANO & NUCCIO [1991]), the elemental composition could comprise only small portions of elements that are leached from the bedrock.
Further concentration would then arise only from the assumed phase separation process during ascent. Using the geochemical modelling program PHREEQC [PARKHURST & APPELO 1999], it was tried to simulate process like phase separation and seawater mixing (see section 4.11) in different approaches.

4.11 Modelling

Because the experimental conditions differ significantly from those suggested for the Panarea hydrothermal system, only representing the compositional proportion that is provided by rock leaching under moderated conditions, it was tried to simulate the process of phase separation through which the fluid composition is more concentrated.
Different scenarios have been conceived for the behaviour of the hydrothermal fluids during its ascend from the region of generation to the point of release at the seafloor:

- In the first scenario **(A)**, the experimental sample looses a portion of water while undergoing phase separation, representing only the contribution to the final composition that is released from the rock.

- The second scenario **(B)** also includes evaporation of the experimental sample, but supplemental a remix of the phase separated brine with fresh seawater is simulated. The proportions of remix are defined as 30% brine and 70% seawater, comparable to a dilution of seawater that is suggested also for the natural samples from Hot Lake and Black Point [SIELAND 2009].

- Scenario **(C)** tries to consider the fact, that in the experimental water-rock interaction no seawater is included. Under natural conditions the seawater as leaching fluid would also undergo phase separation and the contained elements are concentrated in the same way than the rock-leached ones. Hence, in the simulation the experimental sample is mixed with seawater to varying percentages (30%, 50%, 60% and 80% sample respectively) previously to the evaporation. After phase separation, the brine is remixed with seawater similarly to scenario B.

For the modelling, the geochemical computer program PHREEQC was used, developed by PARKHURST & APPELO [1999] together with the database ldll.dat, that is provided together with the computer code.
In a preceding step to all three scenarios, the solution was virtually aerated with CO_2 by equilibrating the solution under a partial pressure of 1 bar CO_2 (see Input-file in the digital Appendix D.1). The resulting concentration of inorganic carbon represents the amount that might be present in the initial experiment solution and thus is added to the starting solution of the second modelling step (evaporation).
Using the keyword “charge” in association with the chloride content, the amount of entered cations is equalise by adding the necessary amount of chloride-anions such that charge balance between all anions and cations is established. The aerated and electrically neutral solution was then evaporated by withdrawing a distinct amount of water molecules such that all dissolved constituent were concentrated in the remaining fluid portion. Subsequently, this concentrate was mixed with itself in the way that the amount of previously withdrawn water is exactly replaced by concentrate. For the different approaches, each are evaporated to the varying degrees of 75%, 90% and 99% respectively. In the simulation cases where the phase separation is followed by remix with seawater, the solution is subsequent mixed with a 70%-proportion of seawater. The composition of a standard seawater was taken and modified from BROWN et al [1995].

The simulation of phase separation was exemplarily accomplished using the experimental sample *R2_mean_(VII-XII)* as starting solution. The respective input-files are given in digital Appendix D.

Results of the modelling:

For evaluating the results of the modelling, the generated element concentrations were related to the respective amount in normal seawater (Appendix 3) and for an objective appraisal the **residues** (that means the absolute differences between the modelled enrichments and those of the real samples from Panarea) have been calculated. All residues were summed up to achieve a value for the total error and thus a quality of the simulation. Thereby, the concentrations of Co, Cr and Ni have been excluded, because they are suggested to be highly overestimated in most scenarios, due to their additional input resulting from the alloys (compare Figure 20 and Figure 21). Furthermore, the elements B, Cs, I, Li and Rb are strongly underestimated due to a probable crustal input (as discussed in the following) and are therefore likewise excluded from calculating the quality of simulation.

The total error was compared between all simulation scenarios separated into results for Black Point and Hot Lake, in order to find the minimal error that represents the computations that on an overall scale best fit the two Panarea samples. These total errors of all simulations are listed in Appendix 5.

For Black Point, a 99%-evaporation in scenario (C_80-20) which considers an 80-to-20 composition of experimental sample and seawater previous to the phase separation shows the minimal error. But also the results of 90% evaporation in scenario (A) and (B), as well as 99% evaporation of all (C)-combinations (compare Appendix 5) have nearly the same values of error, showing only 2-5% discrepancy to the minimal value. For Hot Lake, scenario (B) with 99% evaporation has the minimal error, but comparable to Black Point-modelling, there exist similar values of error with only 1-4% discrepancy for scenario (A) and (C) in other evaporations (compare Appendix 5).

Exemplarily for all simulations, the results of scenario (C_80-20) are presented in Figure 21 and discussed in the following. The results of all other simulations inclusive the diagrams are given in the digital Appendix D.4 and D.5.

It seems obvious, that it is impossible to use such a simple simulation approach for reproduce the complex behaviour and interacting processes that take place in the natural

hydrothermal system of Panarea. But in a general overview and disregarding the detailed concentration differences, the modelled concentrations do quite well represent those of the reference samples from Hot Lake and Black Point.

Considerable overestimations do occur for C, Co, Cr, Cu, and Ni, as well as Fe and Si (when 99% evaporation) (Figure 21) whereas all these concentrations are explainable by known sources of error that have been ignored in the course of the modelling assumption.

Carbon is added in form of CO_2 until equilibrium at 1 bar CO_2-partial pressure. Although it can be assumed, that also the samples from Panarea are saturated with CO_2 at (due to assimilation of magmatic gases which consist mainly of CO_2 [SCHMINCKE 2000]), they lose most of their CO_2- content during the phase separation process, where all volatile constituents are lost to the vapour phase [NICHOLSON 1993]. Cobalt, chromium, nickel, iron and also copper are all constituents of the system alloys (see sections 4.2 and 4.5) and thus are leached additionally to the amounts from the rock material. By a further concentration on evaporating 99% of the water from solution such high overestimations of these elements are generated.

Silicon is likely to precipitate as quartz at high temperatures or on cooling during ascent (as discussed in the previous section). The maximum solubility of quartz at 340 °C is reported as 27.5 mmol/kg [NICHOLSON 1993], which is clearly exceeded by the modelled concentration of the 99% evaporation scenario (90 mmol/kg, see Appendix D.5.5) but not by the 90%-evaporation scenario (9 mmol/kg). Hence the overestimation of Si means only a simulation mistake, not occurring in natural geothermal systems.

It should be mentioned that, depending on the modelling scenario and the degree of evaporation, a few mineral phases are oversaturated in the final solution (positive saturation index SI) and hence are likely to would precipitate from solution while changing the fluid composition. Mineral precipitation may also affect the relative abundance of different elements. However, for the reason of higher temperature and acidity in the natural Panarea fluids, type and degree of precipitated minerals are most probably different to the modelled ones. The specific saturation indices of the different scenarios can be taken from the output-files in the digital Appendix D.

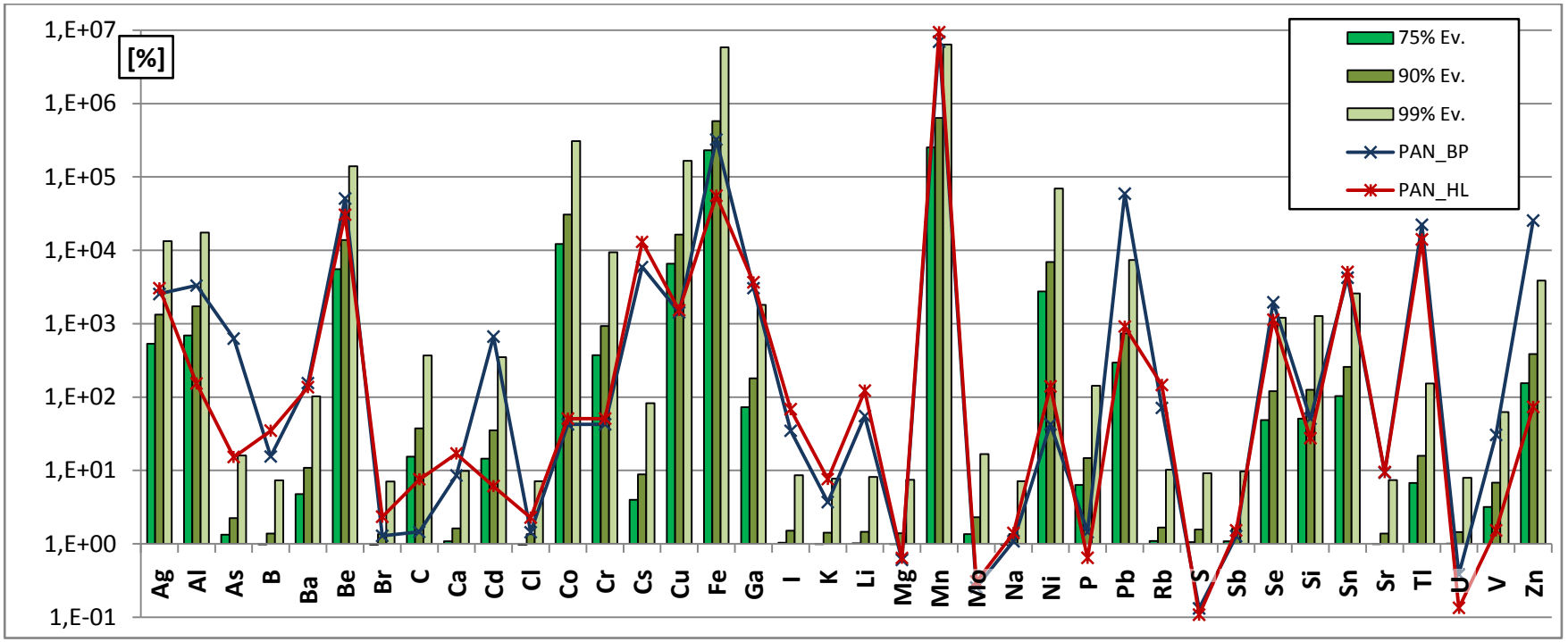

Figure 21: Results of the modelling scenario (C_80-20): Enrichment (%) of modelled and measured concentrations in relation to standard seawater (taken and modified after BROWN et al, [1995]).

For the reason that no seawater that provide an excess of magnesium and sulphate has been included in the experiments, the typical hydrothermal seawater-rock interaction where magnesium and sulphate are depleted in comparison to seawater could not take place inside the autoclaves. Therefore, the amount of Mg and S found in the experiment samples denotes a supplemental input to the remixes with seawater which can be seen from the slightly enriched concentrations in Figure 21.

Underestimated are the elements (As), B, Cs, (Ga), I, Li, Rb and Tl. For some of these elements, the sub-seafloor processes may explain their discrepancies to the experimental and modelled data. Most of these elements (As, B, Cs, Li and Rb) belong to the so called "conservative" or "mobile" group, referring to their behaviour of remaining in solution a as comparatively unreactive species [BERNDT & SEYFRIED 1990; NICHOLSON 1993].

The concentration of these elements in the unaltered rock material is very small [BERNDT & SEYFRIED 1990; CHANNER et al. 1997]. For the reason, that the simulated phase separation was not able to approximate these concentrations to the Panarea concentrations although for all other elements it was possible, some additional inputs or processes are supposed to have entered or rather modified the reference fluids.

In experimental alteration of volcanic rocks under hydrothermal conditions it was found that **boron** and **lithium** are intensively leached from the rock into solution at temperatures ≥ 375°C [SEYFRIED JR et al. 1984]. Thereby, B concentration is only limited by its concentration in the solid phase and the prevailing water-rock ratio respectively. In the contrary, the alteration of oceanic crust at low temperatures (≤ 150°C) is known as a sink for B and Li due to incorporation into a mainly smectite alteration phase [SEYFRIED JR et al. 1984; VILS et al. 2009; ZHANG et al. 1998] but also clay minerals, particularly illite [ARNORSSON & ANDRESDOTTIR 1995; VILS et al. 2009].

In this context, the modelled concentration deficiencies can be explained by the different hydrothermal conditions that have controlled the experimental and natural samples: under an experimental temperature of 150°C the incorporation of B and Li into the altered rock material has probably been the dominating process and only marginal amounts leached into solution. WHITE [1957] also postulated that Li together with other alkalis are added to a hydrothermal system in form of alkali-halides that have been transported in a dense vapour phase directly from a residual magma. For B, an additional supply is also provided by degassing of a magma intrusion during consolidation [ARNORSSON & ANDRESDOTTIR 1995].

Enrichment of **iodine** (by factors of up to 5000) is related to organic matter in marine sediments that, when degraded, release I into pore waters [LU et al. 2008]. It is suggested, that during subduction these I-rich pore waters are transported from the subducting sediments along a fracture network [LU et al. 2008] and may enter hydrothermal bulk fluids.

The concentration of the trace alkalis **rubidium** and **caesium** in hydrothermal fluids are almost entirely derived from the rock basement (basalt) [PALMER & EDMOND 1989]. The leaching of these elements show a similar appearance than it is observed for Li and B: at high temperatures (~ 300°C), both elements are intensively leached from the rock with an experimentally determined efficiency of 80% of the total amount contained in basalt, whereas the low temperatures, these elements are incorporated into alteration phases [BERGER et al. 1988; SEYFRIED JR et al. 1998].

Under extreme phase separation, however, the ratios of Li, Br, Rb, and Cs become fractionated between vapour, brine and halite, whereupon Li and Br preferentially partition into the low-salinity vapour phase but Rb and Cs remain in the coexisting brine [FOUSTOUKOS & SEYFRIED 2007b], The fact that all these elements are enriched in the Panarea fluids, supports the hypothesise of a remix of brine and vapour during further ascent.

The effect of temperature on trace element distribution or dissolution intensity is depicted here exemplarily for some selected elements because they have been underestimated in the modelling of phase separation and seawater remix. However, it should be clearly revealed that the temperature - as already mentioned - is an important factor influencing equilibrium distribution between rock, fluid and secondary minerals for many elements.

In general it can be summarised that the process of phase separation means a dramatic change concerning fluid chemistry and the relative abundance of elements.

For example on boiling, carbon dioxide (and other volatile acids) are lost from the liquid phase which cause an increase in pH, an increase in silica solubility and an initial fall of calcite solubility [NICHOLSON 1993].

Moreover, during phase separation a considerable amount of (trace) metals and SiO_2 are partitioned into the vapour phase, constituting an effective transport medium for these elements [BISCHOFF & ROSENBAUER 1987]. Together with the supposed extensive formation of metal-chloride-complex in the liquid phase during phase separation, both

aspects lead to much higher solubilities of metals (compared to fluids of ordinary seawater composition) and consequently to a considerable undersaturation of metal sulphides in solution [HERZIG & HANNINGTON 2006].
Using the chosen modelling approach, such processes mentioned above are not included in calculating the final fluid composition.

Looking again at the modelling results it can be adhered, that there exists a discrepancy between the elemental amounts coming from seawater and from the rock material. Dependant on whether the amount of seawater or rock contribution is enhanced in the simulation through stronger evaporation or higher seawater-mixing, the one or other is each potentiated in the resulting solution. For example in scenario (A) where no seawater is included, elements such as bromine, chloride, sodium and strontium (which are mainly contributed by seawater) are significantly underestimated (digital Appendix D, Table D.4.3), whereas in scenario (C_30-70), where finally only 9% of the experiment sample contributes to the solution, the concentrations of the mentioned elements are well in agreement with the natural ones (digital Appendix D, Table D.5.2). For the best overall approximation, several simulations achieved nearly the same minimal error as already mentioned. It seems obvious, that none of the scenarios applied for the modelling approaches is able to exactly represent the natural hydrothermal samples due to the complexity of mechanisms that interact on fluid generation and modification. Hence, the modelling results depict only indications for ongoing processes rather than proofs and certitude.
Nevertheless, the simulations clearly depicts the complexity of hydrothermal processes that determine fluid compositions and supplied indications for on the one hand phase separation, taking place beneath the seafloor and otherwise a further input of elements from magmatic components.

5 Conclusions

The influence of water-rock interactions under geothermal conditions on the chemical composition of hydrothermal fluids has been investigated. Thereby, rock samples from the natural geothermal system of Panarea have been reacted under normal and elevated temperature and pressure conditions.

The application of three different experimental **reaction durations** (24, 48 and 84 hours) did not show a clear trend in the way of higher leaching amounts with a longer reaction time, which would have been expectable due to slow reaction kinetics of some mineral phases. In experimental rock leaching performed by other scientists, reaction times of up to several thousands of hours have been applied to provide equilibration between rock, leaching fluid and alteration phase. Thus, the time differences have been interpreted under the applied conditions to be too short for causing noticeable different extraction amounts.

The **autoclave leaching experiments** under 150 °C temperature and 250 bars pressure have been performed on four different rock materials, sampled at Panarea. The resulting concentrations in the leaching fluids appear to be quite similar for all of the four rock samples, showing concentrations in the range of 1 – 1000 µmol/L for the major elements and lesser lower concentrations (down to 0.01 nmol/L) for minor and trace elements. The similarity may be an indication that the four rock materials, which do indeed originate from different rock types, have an overall similar composition of minerals.

Experiments in the overhead rotator have been performed with both, deionized water and

0.5 M NaCl-solution in order to initially evaluate the effect of salinity on rock leaching. Of cause this approach means a strong simplification that is not comparable to the natural systems, but reasoned by the risk of severe corrosion damage induced by high chloride concentrations, autoclave leaching with NaCl-solution could not be performed.

Evaluating the chemical composition of the resulting fluids, no clear distinction between the dissolution capacity of NaCl-solution and deionised water under the applied conditions could be ascertained. Although chloride is known as a major complexing agent for aqueous species [HERZIG & HANNINGTON 2006], their stability and reaction kinetic under normal temperatures is probably too low for causing a considerable effect on leaching intensification.

Blanks have been accomplished with most of the experiment runs to determine the amount of elements that is added to solution by leaching of the system. It turned out, that - especially during the autoclave treatment - **severe contamination** is caused by metals (like Cr, Cd, Fe, Mn, Zn, Ni...) that are extracted from the system alloys during **corrosive attack**. The characteristic of the corrosion was determined to be of decreasing intensity throughout the course of autoclave experiments for the reason of a protective metal-oxide layer, forming as a kind of corrosion product.

However, the main source of corrosive contamination is thought to be the pockets of metal-wire mesh encasing the rock material during the experiment. By the interlacement of the metal wire, a quantity of small corners, angles and wholes for initial and intensive corrosion is provided.

The previous ambition to simply subtract the blank concentrations from those in the sample failed due to resulting in slight till massive negative values for many typical alloy metals. The cause was identified to be a more intensive corrosion under experimental conditions without rock material. From this it can be considered that the presence of rock material alleviatively affects the corrosion process. Consequently, it was not possible to eliminate the corrosive contamination through blind subtraction or somehow differently.

Total digestions denoted a quite similar compositional character of all four rock samples and may be an indication for a common magmatic origin.

The **extraction efficiency** of the rock leaching experiments is calculated by comparing the experimentally gained element amounts (related to 1 g rock material) to the respective amount being actually present in 1 g rock (determined by the total digestions). This calculation offered that under the applied temperature and pressure conditions only a very low efficiency between 0.1 – 10% for the autoclave samples and even lower for the rotation experiments could be reached. Higher efficiencies are only gained by elements (Mn, Ni, Zn, Cr, Co and Cd) where an additional supply from corrosion processes is assumed. However, the overall pattern of element concentrations show a similar behaviour between all three types of experiments (autoclave, rotation with and without NaCl), leading to the conclusion, that the same dissolution reactions take place under normal and elevated temperatures, but only with different intensities.

Such slight extractions can probably be attributed to the comparably low temperature and low pressure, high pH and short reaction time, which are all known as parameters that strongly effect water-rock interactions.

A **cluster analysis** applied on the data of leaching experiments and total digestions identified 5 clusters with significant dissimilarities between the groups of total digestions, rotation samples with NaCl-solution and the bulk of both, autoclave and rotation samples with deionized water respectively. In a previous run, also all total digestions have been grouped separately on their own. These results represent quite well the different types of experimental samples performed for this thesis and indicate that each type of samples owns its characteristic elemental signature that is leached from the rock material.

Hydrothermal water samples from all different sampling sites at Panarea have been collected and analysed with respect to their physico-chemical parameters. However, as it was found out by SIELAND [2009] that for most diving sites the samples have been highly diluted with seawater, only two reference samples have been chosen for comparison. These samples belong to the investigation sites Black Point and Hot Lake and are found to have the lowest dilution. These reference samples show typical hydrothermal characters, including acidic pH values, reduced and partly reduced redox conditions respectively as well as high enrichment (with respect to seawater) of major, minor and trace elements. Depletion occurs for Mg and sulphate due to incorporation into alteration minerals.

The samples produced under experimental hydrothermal conditions have been compared to these reference samples from Panarea, disregarding all sources of contamination. Thereby, the missing features concerning the experimental approach (most of all the lack of seawater as leaching solution which is responsible for the characteristic drop in pH but also likely too low temperatures) become seriously apparent. Hence, there occurs a significant discrepancy in most element concentrations between the experimental and the real samples.

Nevertheless, it was found that the water-rock interactions under experimental conditions resulted in an element pattern, that is (in an overall view) comparable with those of the Panarea samples. It is therefore considered that a higher level of all leached elements could be achieved by applying seawater as leaching fluid under high temperatures.

Besides a more intensive leaching of the exposed rock material in the Panarea hydrothermal system, fluid composition may also affected by **phase separation**. With the extremely high concentrations of Cl^- that were measured in the natural fluids, clues exists that they have undergone phase separation during ascent. This process can be responsible for dramatic changes in fluid chemistry due to the massive loss of water vapour and other volatile components and contemporaneous strong concentration in the remaining liquid

brine. Moreover, phase separation causes fractionation between elemental relations by partitioning species either in the vapour or in the liquid phase.

A simplified approach was conceived for **modelling** the impact of phase separation on the experimentally derived fluids. Thereby water was removed from the solution like normal evaporation or in the present case boiling. Subsequent, the concentrated brine was remixed with unmodified seawater of standard composition. The resulting fluids were then compared to the reference samples by calculating their respective enrichment relative to standard seawater. Using the calculated absolute residues between modelled and real concentration as criterion, for Black Point fluids a scenario of 80:20 fluid-seawater mixing previously to a 99%-evaporation and followed by remix with 70% seawater showed the best approximation whereas for Hot Lake fluids a scenario with only 99% evaporation and subsequent remix with 70% seawater was best fitted.

These modelled fluids well reproduce some major peaks of enrichment like for Mn, Zn, Be, Fe, and Ag as well as some minor peaks like Br, K, Sb and Sr. Nevertheless, some concentrations are severely overestimated (Co, Cr, Cu, Ni) which is attributed to the corrosive input under autoclave treatment, or also underestimated (I, Li, B, Cs, Rb, Tl) and an additional process or even another source than leaching from rock is assumed to contribute these elements into the Panarea fluids. An affecting characteristic is for example the temperature dependency of Li, B, Rb and Cs for being either leached from rock (at high temperatures) or incorporated into alteration minerals (at low temperatures). An additional supply may be provided by subduction related fluids, entering the hydrothermal fluids.

Conclusively it can be adhered, that water-rock interaction is a major factor in determining the chemistry of hydrothermal fluids, but its intensity determined by reaction rate and equilibrium solubility of mineral dissolution is highly dependent on parameters like temperature, pH, redox conditions and salinity.

Performing hydrothermal experiments, these parameters as well as the water-to-rock ratio have to be adjusted adequately for gaining suitable results, especially as they may influence each other and the mineral solubility in reverse manner.

The aim of discovering the determining processes of the hydrothermal fluid generation at Panarea – especially with respect to the obvious differences occurring between the investigation sites Black Point and Hot Lake – could not be fulfilled satisfyingly for the reason of insufficient equipment. But instead, indications for processes like phase separation, remix and magmatic input could be identified under distinct assumptions.

Recommendations for future hydrothermal experiments are:

- most importantly equipment that provides the possibility of applying seawater-composed leaching fluids under the desired elevated temperature and pressure conditions as this means an important factor for hydrothermal chemism to be induced.

- the practicability of higher temperatures than 150 °C for a better approximation to high-temperature geothermal systems.

- if necessary, an enclosure for the rock material should be utilized that consists of inert material like e.g. Teflon. Thus, contamination of the experiment fluids by corrosively extracted metals from the equipment is avoided.

- also the autoclave vessels itself should preferably consist of inert material (special equipment for hydrothermal experiments contain a reaction cell and pressure-closing apparatus of gold-titanium combinations). Moreover, their online-sampling during the running experiment exhibits great advantages.

These mentioned aspects should seriously be followed in order to achieve suitable results and reliable detail information about the really complex mechanisms that go on during water-rock interaction in geothermal systems and that determine the chemical composition of hydrothermal fluids.

6 References

AIUPPA, A., DONGARRA, G., CAPASSO, G. and ALLARD, P. (2000). "Trace elements in the thermal groundwaters of Vulcano Island (Sicily)." Journal of Volcanology and Geothermal Research **98**(1-4): 189-207.

ALLEN, DOUGLAS E. and SEYFRIED, W. E. (2003). "Compositional controls on vent fluids from ultramafic-hosted hydrothermal systems at mid-ocean ridges: An experimental study at 400°C, 500 bars." Geochimica et Cosmochimica Acta **67**(8): 1531-1542.

ANZIDEI, M., ESPOSITO, A., BORTOLUZZI, G. and DE GIOSA, F. (2005). "The high resolution bathymetric map of the exhalative area of Panarea (Aeolian Islands, Italy)." Annals of Geophysics **48**(6): 899-921.

ARNORSSON, S. and ANDRESDOTTIR, A. (1995). "Processes Controlling the Distribution of Boron and Chlorine in Natural-Waters in Iceland." Geochimica Et Cosmochimica Acta **59**(20): 4125-4146.

BECKE, RONNY (2009). Mineralogische & Geochemische Untersuchung von submarinen, vulkanogen-hydrothermalen Mineralpräzipitaten im back-arc-basin des Tyrrhenischen Meeres am Beispiel von Panarea, Äolischer Inselbogen, Italien. Fakultät für Physik und Geowissenschaften, Institut für Geophysik und Geologie. Leipzig, Universität Leipzig. **diploma**.

BENEDIX, ROLAND (2008a). Chemie der Baumetalle. Bauchemie, Vieweg & Teubner Wiesbaden.

BENEDIX, ROLAND (2008b). Redoxreaktionen — Grundlagen der Elektrochemie. Bauchemie, Vieweg & Teubner Wiesbaden**:** 206-230.

BERGER, GILLES, SCHOTT, JACQUES and GUY, CHRISTOPHE (1988). "Behavior of Li, Rb and Cs during basalt glass and olivine dissolution and chlorite, smectite and zeolite precipitation from seawater: Experimental investigations and modelization between 50° and 300°C." Chemical Geology **71**(4): 297-312.

BERNDT, M. E. and SEYFRIED, W. E. (1990). "Boron, bromine, and other trace elements as clues to the fate of chlorine in mid-ocean ridge vent fluids." Geochimica Et Cosmochimica Acta **54**: 2235-2245.

BISCHOFF, J. L. and SEYFRIED, W. E. (1978). "Hydrothermal chemistry of seawater from 25 degrees to 350 degrees C." Am J Sci **278**(6): 838-860.

BISCHOFF, JAMES L. and DICKSON, FRANK W. (1975). "Seawater-basalt interaction at 200°C and 500 bars: Implications for origin of sea-floor heavy-metal deposits and regulation of seawater chemistry." Earth and Planetary Science Letters **25**(3): 385-397.

BISCHOFF, JAMES L. and ROSENBAUER, ROBERT J. (1984). "The critical point and two-phase boundary of seawater, 200-500°C." Earth and Planetary Science Letters **68**(1): 172-180.

BISCHOFF, JAMES L. and ROSENBAUER, ROBERT J. (1987). "Phase separation in seafloor geothermal systems; an experimental study of the effects on metal transport." Am J Sci **287**(10): 953-978.

BISCHOFF, JAMES L. and ROSENBAUER, ROBERT J. (1996). "The alteration of rhyolite in CO2 charged water at 200 and 350°C: The unreactivity of CO2 at higher temperature." Geochimica et Cosmochimica Acta **60**(20): 3859-3867.

BONASIA, V., LUONGO, G. and MONTAGNA, S. (1973). "A land gravity survey of the Aeolian islands." Bulletin of Volcanology **37**(1): 134-146.

BOUCIER, WILLIAM L. and BARNES, HUBERT L. (1987). Rocking Autoclaves for Hydrothermal Experiments I - Fixed-Volume Systems. Hydrothermal experimental techniques. ULMER, GENE CARLETON; BARNES, HUBERT LLOYD, John Wiley & Sons, New York, NY, United States (USA)**:** 189-215.

BRIEHL, HORST (2008). Korrosion von Metallen. Chemie der Werkstoffe, B.G. Teubner Verlag Wiesbaden**:** 107-118.

BROWN, E., COLLING, A., PARK, D., PHILLIPS, J., ROTHERY, D. and WRIGHT, J. (1995). Seawater: Its Composition, Properties And Behaviour. Kidlington, Pergamon.

BROWN, JOAN, COLLING, ANGELA, PARK, DAVE, PHILLIPS, JOHN, ROTHERY, DAVE and WRIGHT, JOHN (1989). Seawater: its composition, properties and behaviour. Walton Hall, Milton, The Open University.

CALANCHI, N., PECCERILLO, A., TRANNE, C. A., LUCCHINI, F., ROSSI, P. L., KEMPTON, P., BARBIERI, M. and WU, T. W. (2002). "Petrology and geochemistry of volcanic rocks from the island of Panarea: implications for mantle evolution beneath the Aeolian island arc (southern Tyrrhenian sea)." Journal of Volcanology and Geothermal Research **115**(3-4): 367-395.

CAN, IBRAHIM (2002). "A new improved Na/K geothermometer by artificial neural networks." Geothermics **31**(6): 751-760.

CAPASSO, G., CARAPEZZA, M., FEDERICO, C., INGUAGGIATO, S. and RIZZO, A. (2005). "Geochemical monitoring of the 2002–2003 eruption at Stromboli volcano (Italy): precursory changes in the carbon and helium isotopic composition of fumarole gases and thermal waters." Bulletin of Volcanology **68**(2): 118-134.

CARACAUSI, A., DITTA, M., ITALIANO, F., LONGO, M., NUCCIO, P. M. and PAONITA, A. (2005a). "Massive submarine gas output during the volcanic unrest off Panarea Island (Aeolian arc, Italy): Inferences for explosive conditions." Geochemical Journal **39**(5): 459-467.

CARACAUSI, A., DITTA, M., ITALIANO, F., LONGO, M., NUCCIO, P. M., PAONITA, A. and RIZZO, A. (2005b). "Changes in fluid geochemistry and physico-chemical

conditions of geothermal systems caused by magmatic input: The recent abrupt outgassing off the island of Panarea (Aeolian Islands, Italy)." Geochimica et Cosmochimica Acta **69**(12): 3045-3059.

CHANNER, D. M. D., DERONDE, C. E. J. and SPOONER, E. T. C. (1997). "The Cl--Br--I-composition of similar to 3.23 Ga modified seawater: implications for the geological evolution of ocean halide chemistry." Earth and Planetary Science Letters **150**(3-4): 325-335.

CHEN, KOUPING, JIAO, JIU J., HUANG, JIANMIN and HUANG, RUNQIU (2007). "Multivariate statistical evaluation of trace elements in groundwater in a coastal area in Shenzhen, China." Environmental Pollution **147**(3): 771-780.

CHIODINI, GIOVANNI, CALIRO, STEFANO, CARAMANNA, GIORGIO, GRANIERI, DOMENICO, MINOPOLI, CARMINE, MORETTI, ROBERTO, PEROTTA, LAVINIA and VENTURA, GUIDO (2006). "Geochemistry of the Submarine Gaseous Emissions of Panarea (Aeolian Islands, Southern Italy): Magmatic vs. Hydrothermal Origin and Implications for Volcanic Surveillance." Pure and Applied Geophysics.

DANDO, P. R., STUBEN, D. and VARNAVAS, S. P. (1999). "Hydrothermalism in the Mediterranean Sea." Progress in Oceanography **44**(1-3): 333-367.

DEKOV, VESSELIN M. and SAVELLI, CARLO (2004). "Hydrothermal activity in the SE Tyrrhenian Sea: an overview of 30 years of research." Marine Geology **204**(1-2): 161-185.

E.V., DIN DEUTSCHES INSTITUT FÜR NORMUNG, DIN EN 10088-1 Nichtrostende Stähle Teil 1: Verzeichnis der nichtrostenden Stähle; Deutsche Fassung EN 10088-1:2005 (2005)

DIN EN ISO 9453: Weichlote – Chemische Zusammensetzung und Lieferformen (ISO 9453:2006); Deutsche Fassung EN ISO 9453:2006 (2006)

DOLFI, DANIELA, DE RITA, DONATELLA, CIMARELLI, CORRADO, MOLLO, SILVIO, SOLIGO, MICHELE and FABBRI, MARINA (2007). "Dome growth rates, eruption frequency and assessment of volcanic hazard: Insights from new U/Th dating of the Panarea and Basiluzzo dome lavas and pyroclastics, Aeolian Islands, Italy." Quaternary International **162-163**: 182-194.

DOMENICO, PATRICK A. and SCHWARTZ, FRANKLIN W. (1998). Physical and Chemical Hhydrogeology. New York, Weinheim, John Wiley & Sons.

DUAN, ZHENHAO and SUN, RUI (2003). "An improved model calculating CO2 solubility in pure water and aqueous NaCl solutions from 273 to 533 K and from 0 to 2000 bar." Chemical Geology **193**(3-4): 257-271.

ELLIS, A. J. and MAHON, W. A. J. (1964). "Natural Hydrothermal Systems and Experimental Hot-Water-Rock Interactions." Geochimica Et Cosmochimica Acta **28**(Aug): 1323-1357.

ELLIS, A. J. and MAHON, W. A. J. (1967). "Natural Hydrothermal Systems and Experimental Hot Water/Rock Interactions (Part 2)." Geochimica Et Cosmochimica Acta **31**(4): 519-&.

ESPOSITO, ALESSANDRA, GIORDANO, GUIDO and ANZIDEI, MARCO (2006). "The 2002-2003 submarine gas eruption at Panarea volcano (Aeolian Islands, Italy): Volcanology of the seafloor and implications for the hazard scenario." Marine Geology **227**(1-2): 119-134.

FAVALLIM, M., KARATSON, D., MAZZUOLI, R., PARESCHI, M. T. and VENTURA, G. (2005). "Volcanic geomorphology and tectonics of the Aeolian archipelago (Southern Italy) based on integrated DEM data." Bulletin of Volcanology **68**(2): 157-170.

FLIETHMANN, J. , SCHLERKMANN, H. and SCHWENK, W. (1992). "Autoklaven-Untersuchungen der Spannungsrißkorrosion von Fe-Cr-Ni-Legierungen in NaCl / CO2 / H2S-Medien." Materials and Corrosion/Werkstoffe und Korrosion **43**(10): 467-474.

FOUSTOUKOS, D. I. and SEYFRIED, W. E. (2007a). "Fluid phase separation processes in submarine hydrothermal systems." Fluid-Fluid Interactions **65**: 213-239.

FOUSTOUKOS, D. I. and SEYFRIED, W. E. (2007b). "Trace element partitioning between vapor, brine and halite under extreme phase separation conditions." Geochimica Et Cosmochimica Acta **71**(8): 2056-2071.

FRANCALANCI, L., TAYLOR, S. R., MCCULLOCH, M. T. and WOODHEAD, J. D. (1993). "Geochemical and Isotopic Variations in the Calc-Alkaline Rocks of Aeolian Arc, Southern Tyrrhenian Sea, Italy - Constraints on Magma Genesis." Contributions to Mineralogy and Petrology **113**(3): 300-313.

GABBIANELLI, G., GILLOT, P. Y., LANZAFAME, G., ROMAGNOLI, C. and ROSSI, P. L. (1990). "Tectonic and volcanic evolution of Panarea (Aeolian Islands, Italy)." Marine Geology **92**(3-4): 313-326.

GAMBERI, FABIANO, MARANI, MICHAEL and SAVELLI, CARLO (1997). "Tectonic, volcanic and hydrothermal features of a submarine portion of the Aeolian arc (Tyrrhenian Sea)." Marine Geology **140**(1-2): 167-181.

GHIARA, M. R., FRANCO, E., PETTI, C., STANZIONE, D. and VALENTINO, G. M. (1993). "Hydrothermal interaction between basaltic glass, deionized water and seawater." Chemical Geology **104**(1-4): 125-138.

GUGLIANDOLO, C., ITALIANO, F. and MAUGERI, T. L. (2006). "The submarine hydrothermal system of Panarea (Southern Italy): biogeochemical processes at the thermal fluids-sea bottom interface." Annals of Geophysics **49**(2-3): 783-792.

HANDL, ANDREAS (2002). Multivaritate Analysenmethoden - Theorie und Praxis multivariater Verfahren unter besonderer Berücksichtigung von S-PLUS. Berlin Heidelberg, Springer Verlag.

HENNET, RÉMY J. C., CRERAR, DAVID A. and SCHWARTZ, JEFFREY (1988). "The effect of carbon dioxide partial pressure on metal transport in low-temperature hydrothermal systems." Chemical Geology **69**(3-4): 321-330.

HERZIG, P. and HANNINGTON, M. (2006). Input from the Deep: Hot Vents and Cold Seeps. Marine Geochemistry. SCHULZ, HORST D. and ZABEL, MATTHIAS. Berlin Heidelberg, Springer Verlag Berlin Heidelberg.

HÖLTING, BERNWARD and COLDEWEY, WILHELM G. (2005). Hydrogeologie - Einführung in die Allgemeine und Angewandte Hydrogeologie. München, Elsevir GmbH, Spektrum Akademischer Verlag.

ILSCHNER, B. and SINGER, R.F. (2005). Korrosion und Korrosionsschutz. Werkstoffwissenschaften und Fertigungstechnik, Springer-Verlag Berlin Heidelberg**:** 135-161.

ITALIANO, F. and NUCCIO, P. M. (1991). "Geochemical investigations of submarine volcanic exhalations to the east of Panarea, Aeolian Islands, Italy." Journal of Volcanology and Geothermal Research **46**(1-2): 125-141.

JAMES, RACHAEL H., ALLEN, DOUG E. and SEYFRIED, W. E. (2003). "An experimental study of alteration of oceanic crust and terrigenous sediments at moderate temperatures (51 to 350°C): insights as to chemical processes in near-shore ridge-flank hydrothermal systems." Geochimica et Cosmochimica Acta **67**(4): 681-691.

LU, ZUNLI, TOMARU, HITOSHI and FEHN, UDO (2008). "Iodine ages of pore waters at Hydrate Ridge (ODP Leg 204), Cascadia Margin: Implications for sources of methane in gas hydrates." Earth and Planetary Science Letters **267**(3-4): 654-665.

LUCCHI, F., TRANNE, C. A., CALANCHI, N., ROSSI, P. L. and KELLER, J. (2007a). "The stratigraphic role of marine deposits in the geological evolution of the Panarea volcano (Aeolian Islands, Italy)." Journal of the Geological Society **164**: 983-996.

LUCCHI, F., TRANNE, C., CALANCHI, N. and ROSSI, P. (2007b). "Late Quaternary deformation history of the volcanic edifice of Panarea, Aeolian Arc, Italy." Bulletin of Volcanology **69**(3): 239-257.

MARAMAI, A., GRAZIANI, L., ALESSIO, G., BURRATO, P., COLINI, L., CUCCI, L., NAPPI, R., NARDI, A. and VILARDO, G. (2005a). "Near- and far-field survey report of the 30 December 2002 Stromboli (Southern Italy) tsunami." Marine Geology **215**(1-2): 93-106.

MARAMAI, A., GRAZIANI, L. and TINTI, S. (2005b). "Tsunamis in the Aeolian islands (southern Italy): a review." Marine Geology **215**(1-2): 11-21.

MARKL, GREGOR (2004). Minerale und Gesteine. München, Elsevir, Spektrum Akademischer Verlag.

MERKEL, B.J. and PLANER-FRIEDRICH, B. (2002). Grundwasserchemie - Praxisorientierter Leitfaden zur numerischern Modellierung von Beschaffenheit, Kontamination und

Sanierung aquatischer Systeme. Berlin Heidelberg New York, Springer-Verlag Berlin Heidelberg.

MILLERO, FRANK J. (2006). Chemical Oceanographie. Boca Ranton, Taylor & Francis Group.

MOORE, E. L., ULMER, G. C. and GRANDSTAFF, D. E. (1985). "Hydrothermal interaction of Columbia Plateau basalt from the Umtanum flow (Washington, U.S.A.) with its coexisting groundwater." Chemical Geology **49**(1-3): 53-71.

MOTTL, MICHAEL J. and HOLLAND, HEINRICH D. (1978). "Chemical exchange during hydrothermal alteration of basalt by seawater--I. Experimental results for major and minor components of seawater." Geochimica et Cosmochimica Acta **42**(8): 1103-1115.

MOTTL, MICHAEL J., HOLLAND, HEINRICH D. and CORR, ROSAMUND F. (1979). "Chemical exchange during hydrothermal alteration of basalt by seawater--II. Experimental results for Fe, Mn, and sulfur species." Geochimica Et Cosmochimica Acta **43**(6): 869-884.

NICHOLSON, KEITH (1993). Geothermal Fluids - Chemistry and Exploration Techniques. Berlin Heidelberg New York, Springer-Verlag.

NICOLICS, J. (2005). Elektrochemische Grundlagen. Werkstoffe für die Elektrotechnik. FASCHING, GERHARD, Springer Verlag Wien NewYork**:** 586-619.

PAIS, ISTVÁN and J. BENTON JONES, JR. (1997). The Handbook of Trace Elements.

PALMER, M. R. and EDMOND, J. M. (1989). "Cesium and rubidium in submarine hydrothermal fluids: Evidence for recycling of alkali elements." Earth and Planetary Science Letters **95**(1-2): 8-14.

PANZA, G. F., PECCERILLO, A., AOUDIA, A. and FARINA, B. (2007). "Geophysical and petrological modelling of the structure and composition of the crust and upper mantle in complex geodynamic settings: The Tyrrhenian Sea and surroundings." Earth-Science Reviews **80**(1-2): 1-46.

PARKHURST, D.L. and APPELO, C.A.J. (1999). User's guide to PHREEQC (Version 2) - A computer program for speciation, batch-reaction, one-dimensional transport and inverse geochemical calculations. Water-Resources Investigations Report 99-4259. Denver, Colorado, U.S. Geological Survey, Department of the Interior.

PECCERILLO, ANGELO (2005). The Aeolian arc. Plio-Quaternary Volcanism in Italy - Petrology, Geochemistry, Geodynamics. Berlin Heidelberg, Springer 173-213.

PICHLER, T. (2005). "Stable and radiogenic isotopes as tracers for the origin, mixing and subsurface history of fluids in submarine shallow-water hydrothermal systems." Journal of Volcanology and Geothermal Research **139**(3-4): 211-226.

REESE, E. and GRABKE, H. J. (1993). "Einfluß von Natriumchlorid auf die Oxidation von hochlegierten Chrom- und Chrom-Nickel-Stählen." Materials and Corrosion/Werkstoffe und Korrosion **44**(2): 41-47.

RIEDEL, ERWIN (2008). Allgemeine und Anorganische Chemie. Berlin, New York, Walter de Gruyter, Berlin.

ROOS, EBERHARD and MAILE, KARL (2005). Korrosion. Werkstoffkunde für Ingenieure, Springer-Verlag Berlin Heidelberg**:** 337-366.

SAVELLI, C., MARANI, M. and GAMBERI, F. (1999). "Geochemistry of metalliferous, hydrothermal deposits in the Aeolian arc (Tyrrhenian Sea)." Journal of Volcanology and Geothermal Research **88**(4): 305-323.

SCHMINCKE, HANS-ULRICH (2000). Vulkanismus. Darmstadt, Wissenschaftliche Buchgesellschaft.

SCHULZ, HORST D. and ZABEL, MATTHIAS (2006). Marine Geochemistry. Berlin Heidelberg, Springer Verlag Berlin Heidelberg.

SEDWICK, P. and STÜBEN, D. (1996). "Chemistry of shallow submarine warm springs in an arc-volcanic setting: Vulcano Island, Aeolian Archipelago, Italy." Marine Chemistry **53**(1-2): 147-161.

SEEWALD, JEFFREY S. and SEYFRIED, W. E. (1990). "The effect of temperature on metal mobility in subseafloor hydrothermal systems: constraints from basalt alteration experiments." Earth and Planetary Science Letters **101**(2-4): 388-403.

SEYFRIED JR, W. E., CHEN, XIAN and CHAN, LUI-HEUNG (1998). "Trace Element Mobility and Lithium Isotope Exchange During Hydrothermal Alteration of Seafloor Weathered Basalt: An Experimental Study at 350°C, 500 Bars." Geochimica Et Cosmochimica Acta **62**(6): 949-960.

SEYFRIED JR, W. E., JANECKY, D. R. and MOTTL, M. J. (1984). "Alteration of the oceanic crust: Implications for geochemical cycles of lithium and boron." Geochimica Et Cosmochimica Acta **48**(3): 557-569.

SEYFRIED JR, WILLIAM E. and MOTTL, MICHAEL J. (1982). "Hydrothermal alteration of basalt by seawater under seawater-dominated conditions." Geochimica Et Cosmochimica Acta **46**(6): 985-1002.

SEYFRIED, W. E. and BISCHOFF, J. L. (1979). "Low temperature basalt alteration by sea water: an experimental study at 70°C and 150°C." Geochimica Et Cosmochimica Acta **43**(12): 1937-1947.

SEYFRIED, W. E. and BISCHOFF, J. L. (1981). "Experimental seawater-basalt interaction at 300°C, 500 bars, chemical exchange, secondary mineral formation and implications for the transport of heavy metals." Geochimica Et Cosmochimica Acta **45**(2): 135-147.

SEYFRIED, W. E., DING, K. and BERNDT, M. E. (1991). "Phase-Equilibria Constraints on the Chemistry of Hot-Spring Fluids at Midocean Ridges." Geochimica Et Cosmochimica Acta **55**(12): 3559-3580.

SEYFRIED, W. E., GORDON, P. C. and DICKSON, F. W. (1979). "A new reaction cell for hydrothermal solution equipment." American Mineralogist **64**(5-6): 646-649.

SEYFRIED, WILLIAM and BISCHOFF, JAMES L. (1977). "Hydrothermal transport of heavy metals by seawater: The role of seawater/basalt ratio." Earth and Planetary Science Letters **34**(1): 71-77.

SEYFRIED, WILLIAM E, JR; , JANECKY, DAVID R; and BERNDT, MICHAEL E (1987). Rocking autoclaves for hydrothermal experiments II - The flexible reaction-cell system. Hydrothermal experimental techniques. ULMER, GENE CARLETON; BARNES, HUBERT LLOYD, John Wiley & Sons, New York, NY, United States (USA)**:** 216-239.

SIELAND, ROBERT (2009). Chemical and isotopic analyses of fluid samples from Panarea, Aeolian Islands, Italy. Department of Geology, Chair for Hydrogeology. Freiberg, Technische Universität Bergakademie Freiberg. **diploma**.

SPYCHER, NICOLAS and PRUESS, KARSTEN "A Phase-Partitioning Model for CO2–Brine Mixtures at Elevated Temperatures and Pressures: Application to CO2-Enhanced Geothermal Systems." Transport in Porous Media.

STEINBRÜCKNER, DANIEL (2009). Quantification of submarine degassing of Panarea Volcano in the Aeolian archipelago, Italy. Department of Geology, Chair for Hydrogeology. Freiberg, Technische Universität Bergakademie Freiberg. **diploma**.

STOYAN, DIETRICH, STOYAN, HELGA and JANSEN, UWE (1997). Umweltstatistik: statistische Verarbeitung und Analyse von Umweltdaten. Stuttgart, Leipzig, Teubner Verlag.

TAKENOUCHI, SUKUNE and KENNEDY, GEORGE C. (1964). "The binary system H2O-CO2 at high temperatures and pressures." Am J Sci **262**(9): 1055-1074.

TASSI, FRANCO, CAPACCIONI, BRUNO, CARAMANNA, GIORGIO, CINTI, DANIELE, MONTEGROSSI, GIORDANO, PIZZINO, LUCA, QUATTROCCHI, FEDORA and VASELLI, ORLANDO (2009). "Low-pH waters discharging from submarine vents at Panarea Island (Aeolian Islands, southern Italy) after the 2002 gas blast: Origin of hydrothermal fluids and implications for volcanic surveillance." Applied Geochemistry **24**(2): 246-254.

TINTI, S., MANUCCI, A., PAGNONI, G., ARMIGLIATO, A. and ZANIBONI, R. (2005). "The 30 December 2002 landslide-induced tsunamis in Stromboli: sequence of the events reconstructed from the eyewitness accounts." Natural Hazards and Earth System Sciences **5**(6): 763-775.

UEDA, A., KATO, K., OHSUMI, T., YAJIMA, T., ITO, H., KAIEDA, H., METCALFE, R. and TAKASE, H. (2005). "Experimental studies of CO2-rock interaction at elevated

temperatures under hydrothermal conditions." Geochemical Journal **39**(5): 417-425.

VILS, FLURIN, TONARINI, SONIA, KALT, ANGELIKA and SEITZ, HANS-MICHAEL (2009). "Boron, lithium and strontium isotopes as tracers of seawater-serpentinite interaction at Mid-Atlantic ridge, ODP Leg 209." Earth and Planetary Science Letters **286**(3-4): 414-425.

VON DAMM, K. L., BUTTERMORE, L. G., OOSTING, S. E., BRAY, A. M., FORNARI, D. J., LILLEY, M. D. and SHANKS, W. C. (1997). "Direct observation of the evolution of a seafloor 'black smoker' from vapor to brine." Earth and Planetary Science Letters **149**(1-4): 101-111.

WHITE, DONALD E. (1957). "Thermal Waters Of Volcanic Origin." Geological Society of America Bulletin **68**(12): 1637-1658.

WIMMENAUER, WOLFHARD (1985). Petrographie der magmatischen und metamorphen Gesteine. Stuttgart, Ferdinand Emke Verlag.

WISTAU (2007). (unbublished) Scientific Diving Excursion on Panarea 2007 - Final reports of participants, Department of Geology, Section for Hydrogeology - TU Bergakademie Freiberg.

WISTAU (2008). (unpublished) Scientific Diving Excursion on Panarea 2008 - Final reports of participants, Department of Geology, Section for Hydrogeology - TU Bergakademie Freiberg.

ZHANG, L. B., CHAN, L. H. and GIESKES, J. M. (1998). "Lithium isotope geochemistry of pore waters from Ocean Drilling Program Sites 918 and 919, Irminger Basin." Geochimica Et Cosmochimica Acta **62**(14): 2437-2450.

Appendix

Appendix 1: Dendrogramm presenting the results of the Cluster Analysis A (the appropriate input data are given in the digital Appendix C, Table C.1)..... 108

Appendix 2: Element concentrations in the Panarea reference samples of Black Point (BP) and Hot Lake (HL), in standard seawater as well as the calculated percentage enrichment of the Panarea samples in relation to seawater 109

Appendix 3: Average abundance of elements in seawater [taken from BROWN et al. 1995] 110

Appendix 4: Concentration-dependency of electrode potentials - refering to the Nernst equation [calculation taken from Briehl 2008]. 111

Appendix 5: Total errors of the different modeling scenarios, calculated by summarizing the absolute residues between modeled and natural enrichment in relation to seawater. Total errors were separately calculated for Black Point (BP) and Hot Lake (HL). The respective minimal error for each scenario is marked in light grey and the overall lowest error for each investigation site is marked in darker grey. 112

Appendix 6: Chemical composition of the stainless steels that constitute the autoclave vessels and the metal wire of the sample pockets [taken from DIN EN 10088-1 2005]..... 112

Appendix 7: Chemical composition of a selection of solder alloys [taken from DIN EN ISO 9453 2006]..... 113

Appendix 8: Results of the experiments accomplished in the overhead rotator, with both, deionised water and NaCl- solution, applied on each of the two rock materials R1 and R2..... 114

Appendix 9: Results of the experiments accomplished in the overhead rotator, with both, deionised water and NaCl-solution applied, on each of the two rock materials R3 and R4..... 114

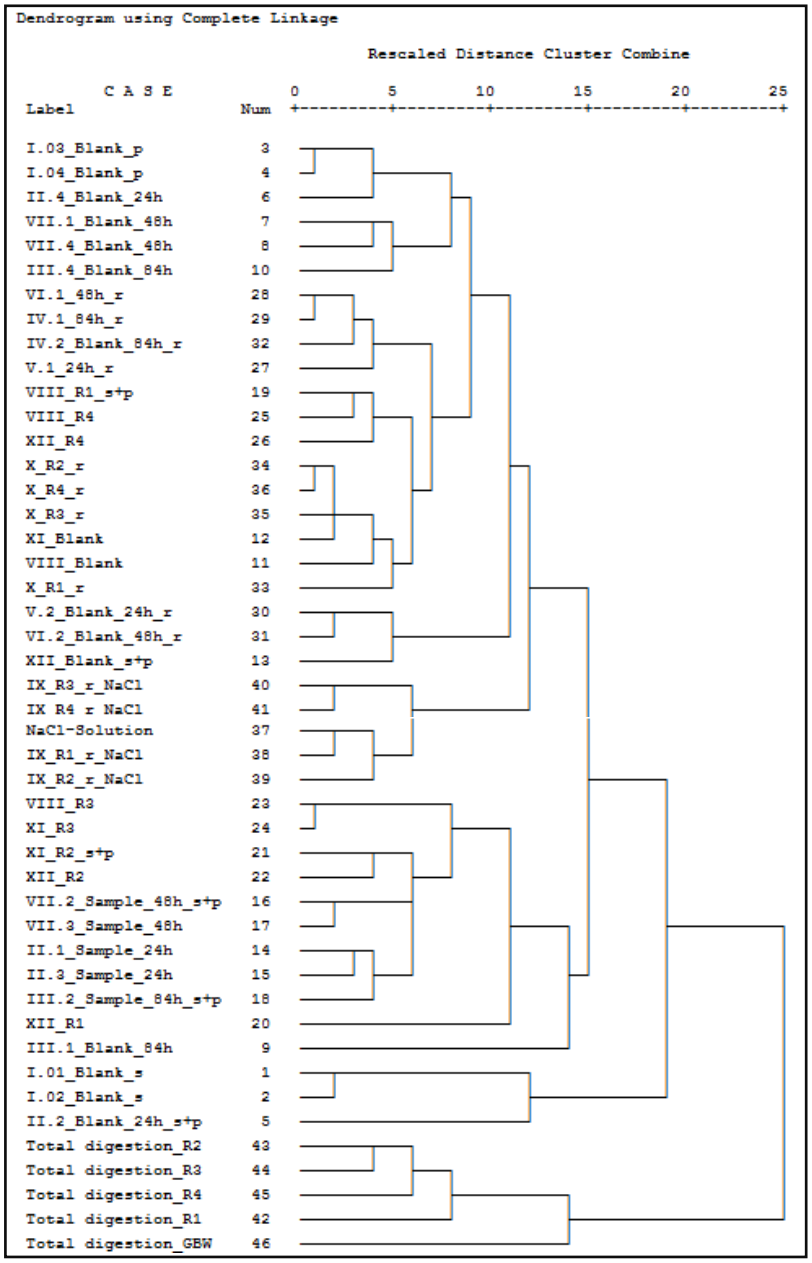

Appendix 1: Dendrogramm presenting the results of the Cluster Analysis A (the appropriate input data are given in the digital Appendix C, Table C.1)

Appendix 2: Element concentrations in the Panarea reference samples of Black Point (BP) and Hot Lake (HL), in standard seawater as well as the calculated percentage enrichment of the Panarea samples in relation to seawater

Element	Panarea reference samples		Seawater (from Brown et al, 1995) [µmol/L]	Enrichment relative to Seawater [%]	
	PAN-030908-BP-W2 [µmol/L]	PAN-080908-HL(80 cm)-W4 [µmol/L]		Black Point	Hot Lake
Na	5.08E+05	6.56E+05	4.68E+05	8.45E+00	4.01E+01
Ca	8.80E+04	1.74E+05	1.03E+04	7.56E+02	1.60E+03
K	3.60E+04	7.40E+04	9.72E+03	2.70E+02	6.62E+02
Mg	3.23E+04	3.40E+04	5.31E+04	-3.92E+01	-3.60E+01
Si	3.63E+03	1.95E+03	7.12E+01	5.00E+03	2.65E+03
Mn	3.83E+03	5.13E+03	5.46E-04	7.02E+08	9.39E+08
Al	4.91E+01	2.26E+00	1.48E-02	3.31E+05	1.52E+04
Fe	3.20E+02	5.46E+01	9.85E-04	3.25E+07	5.55E+06
B	6.32E+03	1.42E+04	4.07E+02	1.45E+03	3.38E+03
Sr	8.54E+02	8.65E+02	9.13E+01	8.35E+02	8.47E+02
Li	1.43E+03	3.16E+03	2.59E+01	5.43E+03	1.21E+04
Rb	1.00E+02	2.05E+02	1.40E+00	7.04E+03	1.45E+04
Cu	2.25E+00	2.40E+00	1.57E-03	1.43E+05	1.52E+05
Ni	3.48E-01	1.14E+00	8.18E-03	4.15E+03	1.39E+04
Zn	1.95E+02	5.60E-01	7.65E-03	2.55E+06	7.22E+03
I	1.65E+01	3.22E+01	4.73E-01	3.39E+03	6.71E+03
Cs	1.78E+01	3.91E+01	3.01E-03	5.93E+05	1.30E+06
Ba	2.27E+01	1.98E+01	1.46E-01	1.55E+04	1.35E+04
Br	1.08E+03	1.96E+03	8.39E+02	2.89E+01	1.33E+02
As	1.68E+01	4.07E-01	2.67E-02	6.29E+04	1.43E+03
Cr	2.45E-01	2.93E-01	5.77E-03	4.15E+03	4.98E+03
Pb	5.71E-01	8.83E-03	9.65E-06	5.92E+06	9.14E+04
V	1.20E+00	5.99E-02	3.93E-02	2.96E+03	5.25E+01
Se	4.97E+00	2.86E+00	2.53E-03	1.96E+05	1.13E+05
Co	2.16E-03	2.59E-03	5.09E-05	4.15E+03	4.98E+03
Tl	1.10E+00	6.86E-01	4.89E-05	2.24E+06	1.40E+06
Cd	5.94E-01	5.43E-03	8.90E-04	6.67E+04	5.10E+02
Ga	8.78E-02	1.05E-01	2.87E-05	3.06E+05	3.66E+05
Mo	2.66E-02	3.18E-02	1.04E-01	-7.45E+01	-6.95E+01
Be	1.13E+00	6.77E-01	2.22E-05	5.10E+06	3.05E+06
U	5.14E-03	1.79E-03	1.34E-02	-6.18E+01	-8.67E+01
Ag	4.73E-02	5.65E-02	1.85E-05	2.55E+05	3.05E+05
Bi	3.66E-02	4.38E-02	9.57E-08	3.82E+07	4.57E+07
Sn	2.15E-02	2.57E-02	5.06E-06	4.25E+05	5.08E+05
Te	2.00E-02	2.39E-02	7.84E-08	2.55E+07	3.05E+07
Sb	2.09E-03	2.51E-03	1.64E-03	2.75E+01	5.25E+01

Appendix 3: Average abundance of elements in seawater [taken from BROWN et al. 1995]

Symbol	concentration [mg/l]	molar mass [g/mol]	concentration [mmol/l]	Symbol	concentration [mg/l]	molar mass [g/mol]	concentration [mmol/l]
Ag	2.00E-06	107.87	1.85E-08	**N**	11.50	14.007	0.82
Al	4.00E-04	26.98	1.48E-05	**Na**	10770.00	22.99	468.46
Ar	0.43	39.95	1.08E-02	**Nb**	1.00E-05	92.91	1.08E-07
As	2.00E-03	74.92	2.67E-05	**Nd**	3.00E-06	144.24	2.08E-08
Au	2.00E-08	196.97	1.02E-10	**Ne**	1.20E-04	20.18	5.95E-06
B	4.40	10.81	4.07E-01	**Ni**	4.80E-04	58.7	8.18E-06
Ba	2.00E-02	137.33	1.46E-04	**O**	6.00	15.999	3.75E-01
Be	2.00E-07	9.01	2.22E-08	**P**	6.00E-02	30.97	1.94E-03
Bi	2.00E-08	208.98	9.57E-11	**Pa**	5.00E-11	231.04	2.16E-13
Br	67.00	79.9	0.84	**Pb**	2.00E-06	207.2	9.65E-09
C	28.00	12.01	2.33	**Pd**	5.00E-08	106.4	4.70E-10
Ca	412.00	40.08	10.28	**Po**	5.00E-16	209	2.39E-18
Cd	1.00E-04	112.41	8.90E-07	**Pr**	6.00E-07	140.91	4.26E-09
Ce	2.00E-06	140.12	1.43E-08	**Ra**	7.00E-11	226	3.10E-13
Cl	19500.00	35.45	550.07	**Rb**	0.12	85.47	1.40E-03
Co	3.00E-06	58.93	5.09E-08	**Re**	4.00E-06	186.21	2.15E-08
Cr	3.00E-04	51.996	5.77E-06	**Rn**	6.00E-16	222	2.70E-18
Cs	4.00E-04	132.91	3.01E-06	**S**	905.00	32.06	28.23
Cu	1.00E-04	63.55	1.57E-06	**Sb**	2.00E-04	121.75	1.64E-06
Dy	9.00E-07	162.5	5.54E-09	**Sc**	6.00E-07	44.96	1.33E-08
Er	8.00E-07	167.26	4.78E-09	**Se**	2.00E-04	78.96	2.53E-06
Eu	2.00E-07	151.96	1.32E-09	**Si**	2.00	28.09	7.12E-02
F	1.30	18.998	6.84E-02	**Sm**	6.00E-07	150.35	3.99E-09
Fe	5.50E-05	55.85	9.85E-07	**Sn**	6.00E-07	118.69	5.06E-09
Ga	2.00E-06	69.72	2.87E-08	**Sr**	8.00	87.62	9.13E-02
Gd	7.00E-07	157.25	4.45E-09	**Ta**	2.00E-06	180.95	1.11E-08
Ge	5.00E-06	72.59	6.89E-08	**Tb**	1.00E-07	158.92	6.29E-10
He	6.80E-06	1.008	6.75E-06	**Te**	1.00E-08	127.6	7.84E-11
Hf	7.00E-05	178.49	3.92E-07	**Th**	1.00E-05	232.04	4.31E-08
Hg	1.00E-06	200.59	4.99E-09	**Ti**	1.00E-03	47.9	2.09E-05
Ho	3.00E-07	164.93	1.82E-09	**Tl**	1.00E-05	204.37	4.89E-08
I	6.00E-02	126.9	4.73E-04	**Tm**	2.00E-07	168.93	1.18E-09
In	2.00E-07	114.82	1.74E-09	**U**	3.20E-03	238.03	1.34E-05
K	380.00	39.1	9.72	**V**	2.00E-03	50.94	3.93E-05
Kr	2.00E-04	83.8	2.39E-06	**W**	1.00E-04	183.85	5.44E-07
La	3.00E-06	138.91	2.16E-08	**Xe**	5.00E-05	131.3	3.81E-07
Li	0.18	6.94	2.59E-02	**Y**	1.00E-06	88.91	1.12E-08
Lu	2.00E-07	174.97	1.14E-09	**Yb**	8.00E-07	173.04	4.62E-09
Mg	1290.00	24.31	53.06	**Zn**	5.00E-04	65.38	7.65E-06
Mn	3.00E-05	54.94	5.46E-07	**Zr**	3.00E-05	91.22	3.29E-07
Mo	1.00E-02	95.94	1.04E-04				

Appendix 4: Concentration-dependency of electrode potentials - refering to the Nernst equation [calculation taken from Briehl 2008].

Using the Nernst equation, the electrode potentials *E* (that means the equilibrium reduction potential) of a metal half cell under different than standard conditions can be calculated. Thereby, the Nernst equation describes the dependency of the electrode potential on the concentration (exactly the activity) of both related ions.

Nernst Equation:

$$E = E^o + \frac{R * T}{z * F}\, ln\, \frac{[ox]}{[red]} \quad (1)$$

With:

E^0 = standard electrode potential
R = universal gas constant,
T = absolute temperature
z = number of electrons transferred in cell reaction
[ox] = activity of the oxidised redox species
[red]= activity of the reduced redox species
F = Faraday constant

Exemplarily, the correlation between electrode potential and the concentration of an electrolyte in a metal half-cell is shown for the tin-half-cell (Zn / Zn^{2+}). The Nernst equation for this system (including substitution of the constants and modification to decadal logarithm, is as follows:

$$E(Zn/Zn^{2+}) = E^0(Zn/Zn^{2+}) + \frac{0.059\,V}{2}\, lg\, \frac{[Zn^{2+}]}{[Zn]} \quad (2)$$

For solids, the activity is defined to equal 1, which means that [Zn] = 1 and leads to a direct dependency of electrode potential on the prevalent concentration of the ions in solution (equation 3):

$$E(Zn/Zn^{2+}) = E^0(Zn/Zn^{2+}) + \frac{0.059\,V}{2}\, lg\, [Zn^{2+}] \quad (3)$$

This equation demonstrates:

> **The lower the concentration of the electrolyte, the more negative is the electrode potential and hence, the higher is the reductive power of the metal.**

As example, the electrode potential of the Tin-half-cell is calculated for Zn^{2+}-concentrations of i) 1 mol/L, ii) 0.01 mol/L and iii) 0.0001 mol/L

i)	$\mathbf{E} = -\mathbf{0.76\ V} + \frac{\mathbf{0.059\ V}}{\mathbf{2}} \mathbf{lg}\ 1$	E = -0.76
ii)	$\mathbf{E} = -\mathbf{0.76\ V} + \frac{\mathbf{0.059\ V}}{\mathbf{2}} \mathbf{lg}\ 10^{-2}$	E = -0.76 – 0.059 = 0.819 V
iii)	$\mathbf{E} = -\mathbf{0.76\ V} + \frac{\mathbf{0.059\ V}}{\mathbf{2}} \mathbf{lg}\ 10^{-4}$	E = -0.76 – 0.118 = 0.878 V

As predicted: the result shows Zn to be a stronger reducing agent, when its concentration in solution is lower.

Appendix 5: Total errors of the different modeling scenarios, calculated by summarizing the absolute residues between modeled and natural enrichment in relation to seawater. Total errors were separately calculated for Black Point (BP) and Hot Lake (HL). The respective minimal error for each scenario is marked in light grey and the overall lowest error for each investigation site is marked in darker grey.

	Residues BP				Residues HL			
		Res (BP-75)	Res (BP-90)	Res (BP-99)		Res (HL-75)	Res (HL-90)	Res (HL-99)
R2_Evaporation (A)	∑ residues	6.77E+06	**6.65E+06**	4.75E+07	∑ residues	9.30E+06	9.23E+06	4.54E+07
R2_Evaporation_Remix (B)	∑ residues	6.91E+06	6.80E+06	8.39E+06	∑ residues	9.37E+06	9.33E+06	**9.03E+06**
sample + seawater (30-70)_Evaporation_Remix (C_30-70)	∑ residues	7.34E+06	7.06E+06	**6.76E+06**	∑ residues	9.39E+06	9.37E+06	9.29E+06
sample + seawater (50-50)_Evaporation_Remix (C_50-50)	∑ residues	7.23E+06	6.86E+06	6.84E+06	∑ residues	9.40E+06	9.40E+06	9.43E+06
sample + seawater (60-40)_Evaporation_Remix (C_60-40)	∑ residues	7.15E+06	6.83E+06	6.66E+06	∑ residues	9.38E+06	9.35E+06	9.24E+06
sample + seawater (80-20)_Evaporation_Remix (C_80-20)	∑ residues	7.03E+06	6.81E+06	**6.50E+06**	∑ residues	9.37E+06	9.34E+06	**9.09E+06**
similarity			94.97%	97.73%			96.12%	99.35%

Calculation with all elements excluding alloy-Input (Co, Cr, Ni) and crustal input (B, Cs, I, Li, Rb)

Appendix 6: Chemical composition of the stainless steels that constitute the autoclave vessels and the metal wire of the sample pockets [taken from DIN EN 10088-1 2005]

	Material Number	per cent by weight										
		C	Si	Mn	P	S	N	Cr	Cu	Mo	Nb	Ni
Autoclave alloy [A]	1.4542	≤ 0.07	≤ 0.7	≤ 1.50	≤ 0.04	≤ 0.015	—	15.0 - 17.0	3.0 - 5.0	≤ 0.60	5xC - 0.45	3.0 - 5.0
Wire pocket alloy [B]	1.4401	≤ 0.07	≤ 1.0	≤ 2.0	≤ 0.045	≤ 0.015	≤ 0.11	16.5 - 18.5	—	2.0 - 2.5	—	10.0 - 13.0

[A] martensitic corrosion restistant steel
[B] austenitic corrosion resistant steel

Appendix 7: Chemical composition of a selection of solder alloys [taken from DIN EN ISO 9453 2006]

Group	alloy number	short label after ISO 3677	per cent by weight													
			Sn	Pb	Sb	Bi	Cd	Cu	Au	In	Ag	Al	As	Fe	Ni	Zn
Tin-Lead-Alloys Solidus temperature 183 °C	101	S-Sn63Pb37	62.5 - 63.5	residue	0.2	0.1	0.002	0.08	0.05	0.1	0.1	0.001	0.03	0.02	0.01	0.001
	102	S-Sn63Pb37E	62.5 - 63.5	residue	0.05	0.05	0.002	0.08	0.05	0.1	0.1	0.001	0.03	0.02	0.01	0.001
	103	S-Sn60Pb40	59.5 - 60.5	residue	0.2	0.1	0.002	0.08	0.05	0.1	0.1	0.001	0.03	0.02	0.01	0.001
	104	S-Sn60Pb40E	59.5 - 60.5	residue	0.05	0.05	0.002	0.08	0.05	0.1	0.1	0.001	0.03	0.02	0.01	0.001
Lead-Tin-Alloys Solidus temperature 183 °C	111	S-Pb50Sn50	49.5 - 50.5	residue	0.2	0.1	0.002	0.08	0.05	0.1	0.1	0.001	0.03	0.02	0.01	0.001
	112	S-Pb50Sn50E	49.5 - 50.5	residue	0.05	0.05	0.002	0.08	0.05	0.1	0.1	0.001	0.03	0.02	0.01	0.001
	113	S-Pb55Sn45	44.5 - 45.5	residue	0.5	0.25	0.005	0.08	0.05	0.1	0.1	0.001	0.03	0.02	0.01	0.001
	114	S-Pb60Sn40	39.5 - 40.5	residue	0.5	0.25	0.005	0.08	0.05	0.1	0.1	0.001	0.03	0.02	0.01	0.001
	115	S-Pb65Sn35	34.5 - 35.5	residue	0.5	0.25	0.005	0.08	0.05	0.1	0.1	0.001	0.03	0.02	0.01	0.001
	116	S-Pb70Sn30	29.5 - 30.5	residue	0.5	0.25	0.005	0.08	0.05	0.1	0.1	0.001	0.03	0.02	0.01	0.001
	117	S-Pb80Sn20	19.5 - 20.5	residue	0.5	0.25	0.005	0.08	0.05	0.1	0.1	0.001	0.03	0.02	0.01	0.001
Lead-Tin-Alloys Solidus temperature < 183 °C	121	S-Pb85Sn15	14.5 - 15.5	residue	0.5	0.25	0.005	0.08	0.05	0.1	0.1	0.001	0.03	0.02	0.01	0.001
	122	S-Pb90Sn10	9.5 - 10.5	residue	0.5	0.25	0.005	0.08	0.05	0.1	0.1	0.001	0.03	0.02	0.01	0.001
	123	S-Pb95Sn5	4.5 - 5.5	residue	0.5	0.1	0.005	0.08	0.05	0.1	0.1	0.001	0.03	0.02	0.01	0.001
	124	S-Pb98Sn2	1.8 - 2.2	residue	0.12	0.1	0.002	0.08	0.05	0.1	0.1	0.001	0.03	0.02	0.01	0.001

further alloys contain higher amounts of antimony, silver, copper, cadmium, bismuth, and indium in varying combinations

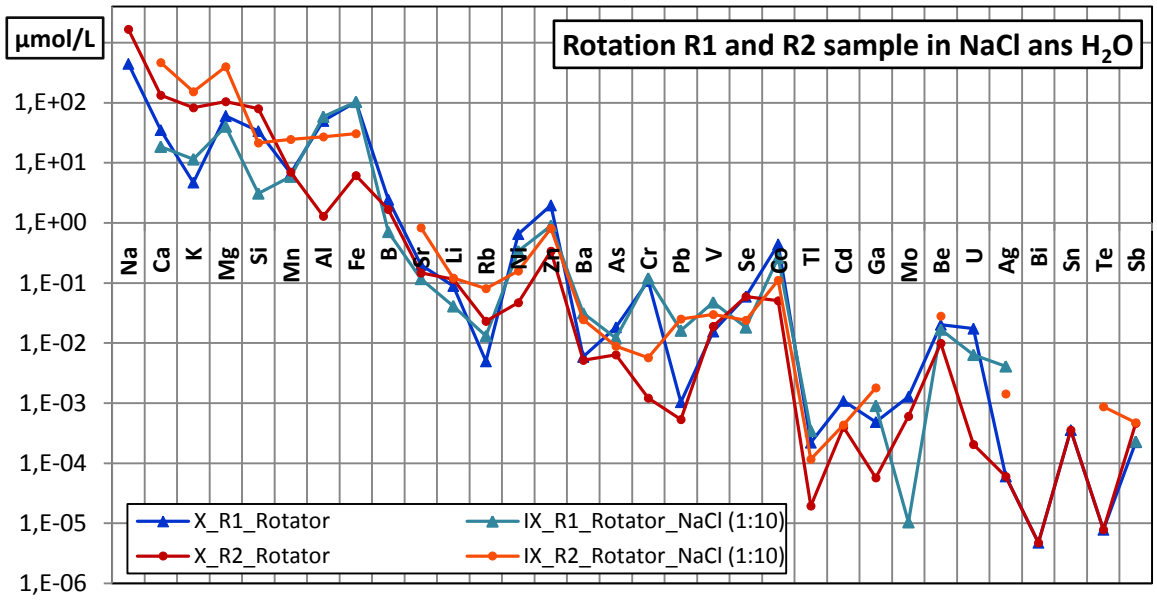

Appendix 8: Results of the experiments accomplished in the overhead rotator, with both, deionised water and NaCl-solution, applied on each of the two rock materials R1 and R2.

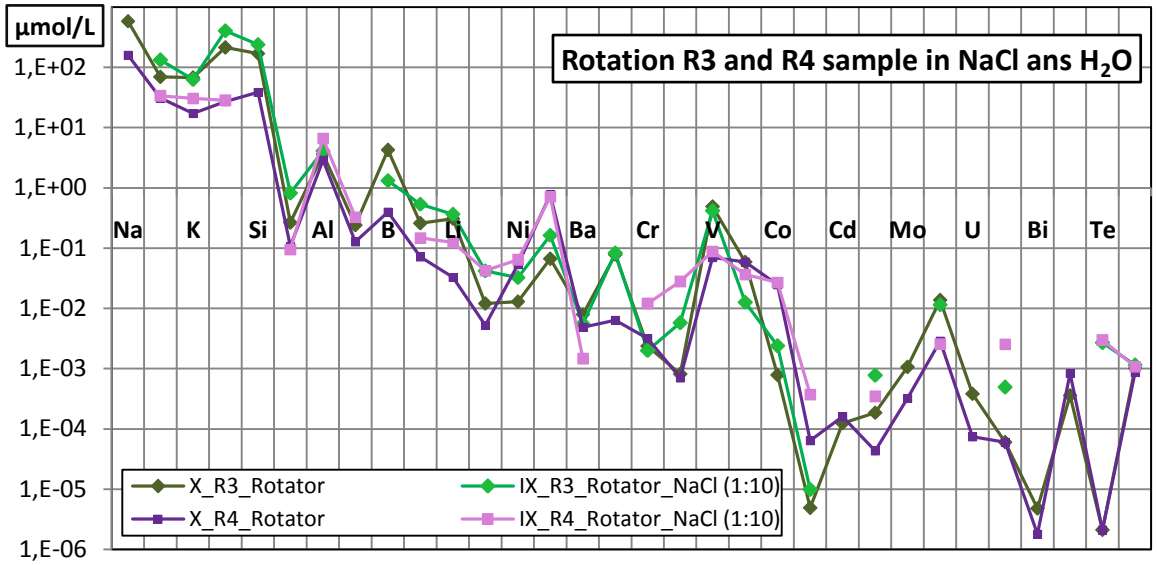

Appendix 9: Results of the experiments accomplished in the overhead rotator, with both, deionised water and NaCl-solution applied, on each of the two rock materials R3 and R4.

Content of Digital Appendix

Digital Appendix A:	**Experimental Data of Pre-tests, Time Series and Blanks**
Digital Appendix B:	**Experimental Data of Rock Leaching Experiments and the Total Digestions, Detection limits ICP-MS**
Digital Appendix C:	**Input-Data for Cluster Analyses A and B, Output-Files of Cluster Analyses A and B as well as Kruskal-Wallis-Test, Evaluation of the Cluster Analyses A and B**
Digital Appendix D:	**Modelling: PHREEQC-Input-Files for the three scenarios, PHREEQC-Input-Files of the three scenarios, Evaluation of the Modelling Results including Diagrams**
Digital Appendix E:	**Original Data of ICP-MS-measurements**
Digital Appendix F:	**Chemical Data of the Panarea Water Samples**